POLITECNICO DI MILANO

Facoltà di Ingegneria Industriale
Dipartimento di Energetica

Corso di Laurea Magistrale in Ingegneria Energetica

Analysis and optimization of an industrial-scale pre-combustion CO_2 capture unit of an IGCC power plant

Relatore: Prof. Giampaolo MANZOLINI

Correlatore: Prof. Dr. Piero COLONNA

Correlatore: Dipl.-Ing. Carsten TRAPP

Tesi di Laurea di:

Timon THOMASER Matr. 783083

Anno Accademico 2012-2013

Acknowledgements

First of all, I would like to sincerely thank my daily supervisor Carsten Trapp for his outstanding support in the development of this thesis. My sincere thanks also to my supervisor Prof. Dr. Piero Colonna, Kay Damen, Eric van Dijk, and Lukas Valenz who guided the work in the right direction.

I am grateful to my supervisor at the home university, Giampaolo Manzolini, for his support in the correction of the thesis and his patience.

My sincere thanks to my girlfriend Cristel Valzer who supported me when I saw no way out and helped me whenever possible.

Finally, I want to thank my family for their love and financial support throughout the entire university studies.

Bressanone (Italy) Timon Thomaser
November 28, 2013

“Habe nun, ach! Philosophie,
Juristerei und Medizin,
Und leider auch Theologie
Durchaus studiert, mit heißem Bemühn.
Da steh ich nun, ich armer Tor!
Und bin so klug als wie zuvor;”

— *Johann Wolfgang von Goethe, Faust I*

Table of Contents

List of Figures

List of Tables

Abstract

The incorporation of a carbon dioxide (CO_2) capture unit into an Integrated Gasification Combined Cycle (IGCC) power plant is a promising technology to achieve a significant reduction of CO_2 emissions in the near future and to limit the climate change. This work presents an analysis and optimization of a pre-combustion CO_2 capture unit of an IGCC power plant in a process simulator environment. The focus is on the capture unit, which comprises an integrated CO_2 and H_2S removal unit, a sweet water-gas shift (WGS) unit, and a five-stage intercooled CO_2 compression. The main objective of the work is to reduce the energy penalty related to the introduction of the CO_2 capture unit into the IGCC power plant.

Different operating temperatures in the absorption section are compared showing that it is thermodynamically and economically more convenient to operate at low temperatures. Subsequently, a thermodynamic optimization of the operating parameters of the capture unit is performed. The optimization is performed within the range 75 to 91% of CO_2 capture rate. The analysis shows that the power consumption increases with the CO_2 capture rate, while the specific energy consumption (per captured amount of CO_2) has a minimum within the analyzed range of capture rates. Different operating conditions for fresh and partially deactivated WGS catalysts are compared. For the latter case, the inlet temperature of the WGS reactors has to be increased and causes a rise of the power consumption at high capture rates. At lower capture rates, no significant impact on the power consumption was observed due to the deactivated catalysts. For fresh catalysts, a reference case with a minimum steam/CO ratio of 2.65 mol/mol and a reactor inlet temperature of 340°C is defined; but a study performed by Nuon estimated that the minimum steam/CO ratio can be reduced to 1.5 mol/mol and the minimum inlet temperature of the reactors can be reduced to 315°C. It is calculated that the specific energy requirement per captured amount of CO_2 can be reduced up to 10%, when operating at these more severe conditions for the WGS reactors. Finally, the performance of the H_2S absorption section is evaluated with and without CO_2 capture. This is of interest, because the H_2S absorption section has to be sized to guarantee an effective operation also when no CO_2 is captured. In this way, the IGCC power plant can be operated without CO_2 capture if the CO_2 market price does not pay-back the additional cost connected to the CO_2 capture. The main difference to the case with CO_2 capture is that the solvent at the inlet

of the H_2S absorber is not preloaded with CO_2. This increases the necessary solvent mass flow and the power consumption of the capture unit. Nevertheless, it is demonstrated that the sizing of the H_2S absorption section also depends on the chosen inlet temperature to the H_2S absorber and the maximum sulphur content in the syngas at the outlet of the sulphur removal section.

Keywords: IGCC, CCS, pre-combustion CO_2 capture, optimization, DEPG, HTS catalysts

Sommario

Secondo l'International Energy Agency (IEA), carbon capture and storage (CCS) é una soluzione promettente per ridurre le emissioni di anidride carbonica (CO_2) nei prossimi decenni. Oggetto di questo lavoro é lo studio di una delle tecnologie CCS che prevede la cattura di anidride carbonica in un impianto di produzione di energia elettrica IGCC (Integrated Gasification Combined Cycle). La tesi si colloca all'interno di un progetto che studia la cattura pre-combustione di anidride carbonica di un impianto IGCC ed é stata sviluppata in collaborazione con la Delft University of Technology, il fornitore di energia elettrica olandese Nuon e l'Energy Research Centre of the Netherlands. L'obiettivo principale dell'analisi svolta é la riduzione del consumo di energia elettrica nella sezione dell'impianto dedicata alla cattura dell'anidride carbonica. L'impianto di cattura é stato simulato in Aspen Plus e comprende una sezione per la rimozione di CO_2 e di H_2S, una sezione di sweet water-gas shift (WGS) e una sezione di compressione della CO_2. Il presente lavoro si focalizza su tre analisi.

Nella prima parte si confronta la fattibilità tecnico-economica relativa a diverse temperature operative della sezione di absorbimento della CO_2 e dell'H_2S. Sarà dimostrato che in una prima approssimazione é più vantaggioso operare a temperature più basse. Nella seconda parte, é effettuata un'ottimizzazione termodinamica delle condizioni operative dell'intero impianto di cattura. L'ottimizzazione é stata eseguita in un range di efficienza di cattura dell'anidride carbonica tra il 75% e il 91%. L'analisi effettuata mostra che il consumo di potenza elettrica dell'impianto di cattura é strettamente crescente con l'efficienza di cattura, mentre il consumo specifico (per massa di CO_2 catturata) presenta un minimo. Inoltre vengono confrontati differenti vincoli per le condizioni operative dei reattori di shift. Una prima analisi simula catalizzatori di shift parzialmente deattivati, per i quali le temperature d'ingresso dei reattori di shift devono essere aumentate. Questo causa un incremento del consumo di potenza elettrica dell'impianto di cattura per alte efficienze di cattura, mentre per efficienze di cattura più basse il consumo elettrico non ne risulta influenzato significativamente. Una seconda analisi simula le condizioni operative di catalizzatori nuovi. Per quest'ultima si confrontano le prestazioni dovute a un minimo rapporto di steam/CO di 2.65 mol/mol e una temperatura d'ingresso nei reattori di 340°C con condizioni operative più estreme. Infatti, uno studio eseguito da Nuon ha dimostrato che le temperature d'ingresso nei reattori pos-

sono essere abbassate a 315°C e i minimi rapporti di vapore/CO possono essere ridotti a 1.5 mol/mol. Sarà evidenziato che operare i reattori di shift a questi nuovi limiti può portare a una riduzione del consumo di energia elettrica della sezione di cattura del 10%. Nella terza e ultima parte sono state studiate le prestazioni della sezione di rimozione dell'acido solfidrico in assenza di cattura di CO_2. Quest'analisi serve per la progettazione adeguata della sezione di rimozione dell'H2S. Infatti, questa deve rimanere operativa anche quando l'impianto IGCC opera senza cattura di CO_2, nel caso in cui il prezzo di mercato della CO_2 non giustifichi i costi aggiuntivi connessi alla cattura del carbone. La differenza principale tra il caso con e senza cattura di CO_2 é che quando vi é cattura, il solvente all'ingresso della colonna di absorbimento dell'H_2S é pre-caricato con anidride carbonica. Questo riduce la portata massica di solvente e favorisce la riduzione di consumo di energia elettrica dell'impianto di cattura. Nonostante ciò, sarà evidenziato che il consumo di energia elettrica e il dimensionamento dell'impianto di cattura dipende anche dalla temperatura d'ingresso della colonna di absorbimento dell'H_2S e dal massimo contenuto di zolfo consentito nel syngas all'uscita della sezione di rimozione dello zolfo.

Parole chiave: IGCC, CCS, cattura pre-combustione di anidride carbonica, ottimizzazione, DEPG, catalizzatori HTS

Chapter 1

Introduction

1-1 Relevance of CCS

'Climate change is happening' [1] states the United States Environmental Protection Agency. The global mean temperature is already 0.8°C above pre-industrial levels and is expected to rise further [2]. The cause is anthropogenic emissions of CO_2 and other Greenhouse Gases (GHG) which increase the average global temperature. At the United Nations Climate Change Conferences in 2009 and 2010 it was agreed that this increase should be kept under 2°C compared to the start of the industrial era [3]. Although no binding agreement was signed, the International Energy Agency (IEA) analyzed this objective in the 'World Energy Outlook 2012' [4]. Three different scenarios which predict the energy trends until 2035 were developed:

- Current Policies Scenario (CPS)
- New Policies Scenario (NPS)
- 450 Scenario (450)

The CPS illustrates the impact of the current energy policies on the world energy outlook, which means that only the governmental policies enacted or adopted by mid-2012 are applied unchanged. The IEA predicted that this scenario leads to a long-term temperature increase of 5.3°C compared to pre-industrial temperatures and implies drastic effects on the climate.

In fact, there is a broad political consensus that more effort needs to be put into new energy policies. This idea is summarized in the NPS, which assumes that '[e]xisting energy policies are maintained and recently announced commitments and plans, including those yet to be formally adopted, are implemented in a cautious manner' [4]. Despite the efforts, there is a 50% probability that the global temperature increases of 3.6°C, which is above the objective of 2°C. Thus the IEA developed the 450 scenario which assumes that '[p]olicies are adopted that put the world on a pathway that is consistent with having around a 50% chance of limiting the global increase in average temperature to 2°C in the long term, compared with

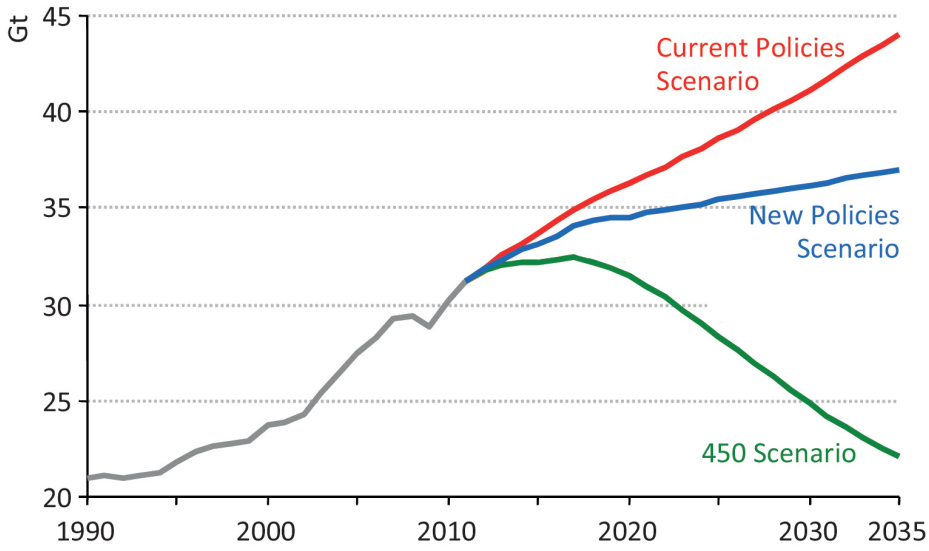

Figure 1-1: Global-energy-related CO_2 emissions for different scenarios, adapted from [4]

pre-industrial levels' [4]. The name of this scenario has origin in the fact that a 450 ppm CO_2-equivalent long-term concentration of greenhouse gases in the atmosphere leads to a 2°C temperature increase.

In 2011 around 60% of the total anthropogenic CO_2-equivalent emissions were energy-related. Therefore, the energy sector has a key influence. The global energy-related CO_2 emissions for the different scenarios are shown in Figure 1-1. From this figure it can be inferred that the CPS and NPS incline towards a consistent increase in the CO_2 emissions. The increase is mainly attributable to Non-OECD countries, because they are expected to undergo a large increase of the population and economy, which influences directly the total primary energy consumption. Furthermore, this increase is related to a consistently high coal demand (coal emits much more CO_2 than other fuels) of these regions, which is expected to increase from 3,411 Mtoe (Million Tonnes of Oil Equivalent) in 2010 to 4845 Mtoe and 6,311 Mtoe in 2035 for the NPS and CPS, respectively [4]. To limit the long-term temperature increase to only 2°C above pre-industrial levels the much more severe 450 Scenario is necessary (a 50% likelihood of success was estimated). In this scenario the CO_2 emission level has a peak of 32.4 Gt before 2020 which declines to 22.1 Gt in 2035. The steps which have to be taken to achieve the 450 scenario compared to the NPS are illustrated in Figure 1-2 (a reduction of 15Gt CO_2 emissions is necessary). The most important mitigation measures by 2035 are: end-use efficiency, electricity savings, renewable energy sources, nuclear power and carbon capture and storage (CCS). Electricity savings is expected to have the biggest impact on the reduction of the carbon dioxide emissions. Next to them the renewable energy sources are becoming a significant source of mitigation. Scientists agree that renewables are one the few sustainable long-term energy production sources, but it is technically not possible and economically not sustainable to switch in the near-term to a fully renewable-energy production. Thus, their influence on the global energy mix in the next decades is important, but limited. Carbon capture and storage plays therefore an crucial role and will become the third most important abatement measure. The IEA expects in the 450 scenario that 17% of the total CO_2 abatement by 2035 should be achieved by CCS, in total terms this is equal to 2.5 Gt

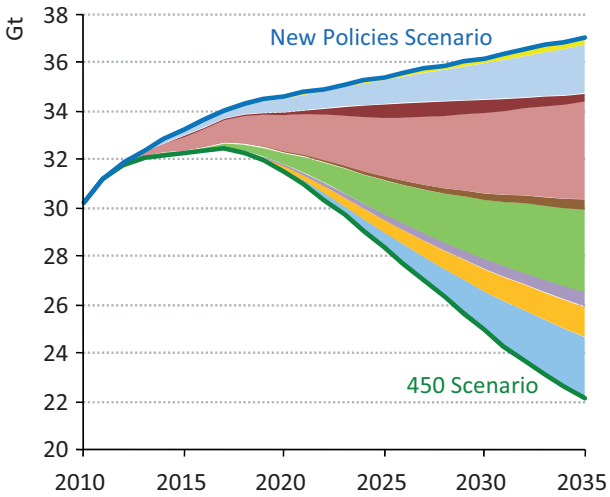

CO_2 abatement	2020	2035
Activity	2%	2%
End-use efficiency	18%	13%
Power plant efficiency	3%	2%
Electricity savings	50%	27%
Fuel and technology switching in end-uses	2%	3%
Renewables	15%	23%
Biofuels	2%	4%
Nuclear	5%	8%
CCS	4%	17%
Total (Gt CO_2)	**3.1**	**15.0**

Figure 1-2: Global-energy-related CO_2 emissions abatement in the 450 Scenario relative to the New Policies Scenario [4]

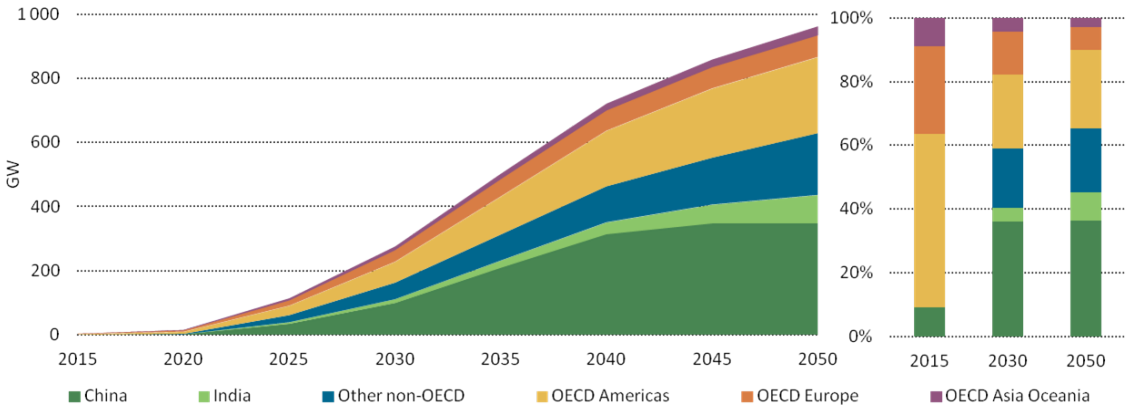

Figure 1-3: Power generation with CCS by region [5]

CO_2 emissions. The share of CO_2 emissions abatement reached from CCS will increase significantly after 2020, because many coal-fired power stations constructed to 2020 are going to be retrofitted with carbon capture and storage when the CO_2 market price is going to increase.

Figure 1-3 shows that CCS will also play a crucial role in the lowest-cost greenhouse gas mitigation portfolio after 2035. This graphic was published in the 'Energy Technology Perspective 2012' from the IEA under the hypothesis of an energy policy that ensures a 80% chance of limiting the global temperature increase to 2°C [5]. In 2050 960 GW of the total power generation will be equipped with CCS. The majority will be located in China (over one third) and other non-OECD countries. The reason is that by that time probably the majority of CO_2 emissions are given by non-OECD countries and therefore they have to contribute significantly to the global aim of limiting the temperature increase. In the near term instead, most CCS will be installed in OECD countries, mainly in the United States.

The data from the IEA shows that to limit the average global temperature increase, carbon capture and storage will become an important mitigation measure. A temporary solution

is indeed necessary till a complete transition to renewable energy sources is possible or new innovative power-production technologies like nuclear fusion become feasible. The strength of CCS is that proven, reliable and cheap technologies can be utilized and only minor changes to the already existing plants are required. On the other hand one day fossil fuels are going to run out and therefore CCS is no long-term solution to limit the climate change. Furthermore, the usage of fossil fuels like crude oil and gas could lead to conflicts and wars, because they are concentrated in few countries of the world, and most of them are politically unstable. Coal is less critical in this context, because it is more equally distributed over the world. Moreover, it is going to run out later than oil and gas (around 53% of all fossil-fuel reserves are coal). The disadvantage of coal is that its combustion emits 68% more CO_2 than natural gas and 42% more CO_2 than oil for the same energy output. Nevertheless, the research on CCS in a long-term view is mostly concentrated on the combustion of coal. In the near-term post-combustion CO_2 capture from natural gas-fired power plants seems to be the most attractive option [6].

CO_2 capture technology is already commercially available, even if some important steps have still to be taken [7]. In fact, the storage in geological formations has to be studied accurately, a sufficient value for CO_2 has to be created, a legal and regulatory framework must be developed and suitable geological formations for a secure and environmentally sustainable storage have to be found. An analysis of these challenges, even if quite important for the implementation of CCS, are beyond the scope of this work. Another challenge of CCS is that the introduction of the sequestration section to power plants ends up in significant additional costs and a considerable energy efficiency penalty. The objective of this work is to minimize this energy penalty for a pre-combustion CO_2 -capture unit in an Integrated Gasification Combined Cycle (IGCC) power plant.

1-2 Overview of CCS technologies

Carbon capture and storage consists in capturing, transporting and storing carbon dioxide (Figure 1-4). CO_2 produced from power generation, cement production, steel mills and other large point sources does not anymore enter the atmosphere, but it is withdrawn before. All three stages of the process (CO_2 capture, CO_2 transport and CO_2 storage) are technically feasible and have already been used commercially for several decades in other industries [7].

1-2-1 CO_2 capture

For the removal of CO_2 different technologies are currently available or under development. In a short-term view particular attention should be paid to CO_2 capture from power plants, which account for almost 50% of the total CO_2 emissions from fossil fuel combustion [8]. Therefore, this introduction will focus on the following three CO_2 capture methods suitable for power plants:

- Post-combustion - CO_2 is removed from the flue gas after the combustion
- Pre-combustion - CO_2 is removed from the synthetic gas (syngas) obtained through gasification before its combustion

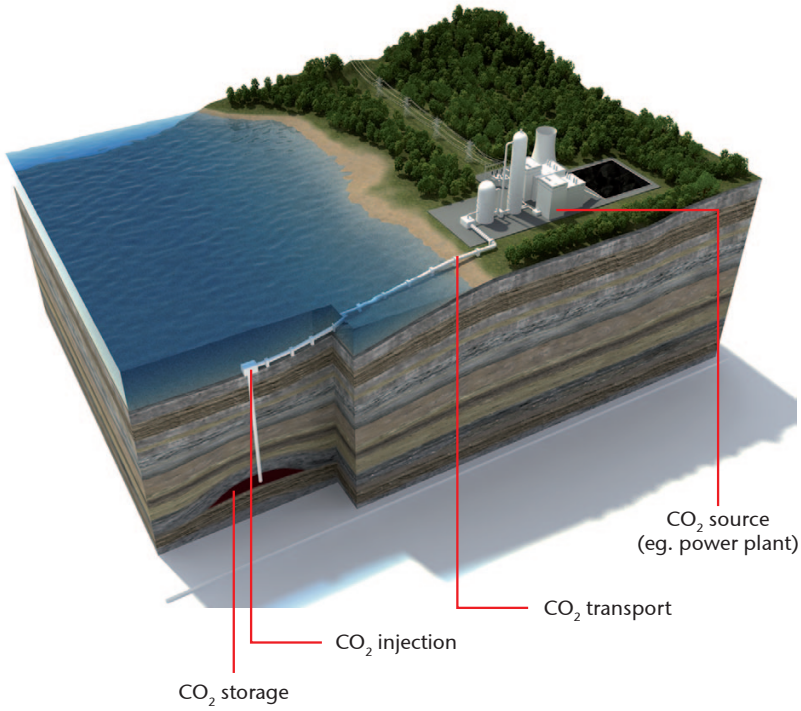

Figure 1-4: The CCS process [7]

- Oxy-combustion - CO_2 can easily be removed from the flue gas by condensation, as the fuel is combusted using pure oxygen instead of air

The advantages and disadvantages of each technology are summarized in Table 1-1.

Independent of the applied capture process, the removal of CO_2 requires a significant amount of energy. Subsequently, the efficiency of the power plant decreases. The efficiency loss is in a range of 6 to 11% depending on the technology and the type of fuel used [9]. For coal fired power plants the energy penalty is higher than for gas fired power plants, because a higher amount of CO_2 has to be captured per unit of electricity produced. A detailed analysis of the three capture methods is presented in the following paragraphs.

Pre-combustion As shown in Figure 1-5 the primary fuel, usually coal or biomass, is gasified to a syngas, which contains mainly H_2, CO_2 and CO. Steam is added and in apposite reactors the CO is converted into CO_2 and H_2. Finally, the CO_2 is separated from the rest of the syngas, compressed and stored. The syngas is then used as a fuel in a combustion process. For pre-combustion CO_2 capture the current development focuses on IGCC power plants, which use carbon as primary fuel and the most efficient thermodynamic cycle for power production, the combined cycle. Different technologies are available for the CO_2 separation. They can be distinguished by the technology of separation. The most mature is separation based on physical absorption with solvents as Selexol, Rectisol, Purisol and Fluor Solvent. Chemical solvents as MDEA are considered for pre-combustion CO_2 sequestration when the partial pressure of carbon dioxide is very low. Other separation technologies under development are adsorption, membrane separation and cryogenic separation.

Table 1-1: Advantages and disadvantages of capture options, adapted from [8]

Capture option	Advantages	Disadvantages
Pre-combustion	Lower energy requirements for CO_2 capture and compression	Temperature and efficiency issues associated with hydrogen-rich gas turbine fuel
Post-combustion	commercially deployed technology at the required scale in other industrial sectors	High parasitic power requirement for solvent regeneration
	Opportunity for retrofit to existing plant	High capital and operating costs for current absorption systems
Oxy-combustion	Mature air separation technologies available	Significant plant impact makes retrofit less attractive

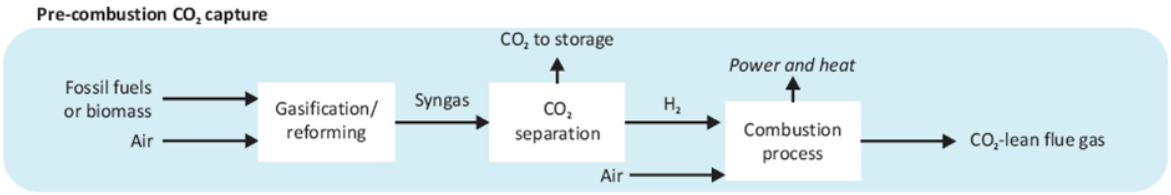

Figure 1-5: Pre-combustion process flowsheet [5]

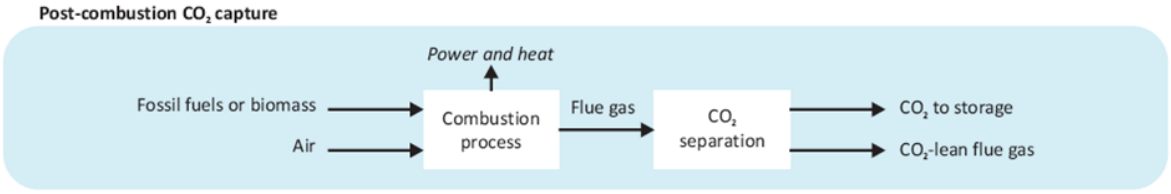

Figure 1-6: Post-combustion process flowsheet [5]

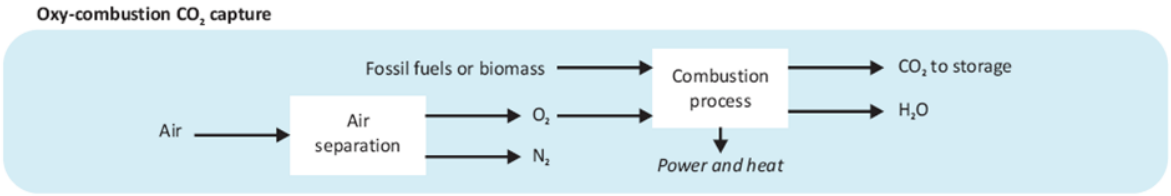

Figure 1-7: Oxy-combustion process flowsheet [5]

An important technological challenge of pre-combustion CO_2 capture has still to be cleared by R&D. It is related to the combustion of hydrogen-rich syngas as fuel in the gas turbine. The hydrogen has a higher explosion risk, the adiabatic flame temperature increases and the higher heat transfer with the turbine blades leads to critical blade temperatures.

Post-combustion Post-combustion capture describes the removal of CO_2 from the flue gas treatment (Figure 1-6) and can be considered as an extension of the flue gas treatment. It consists in the removal of CO_2 from the exhaust gases of the combustion process. Among the different techniques used for post-combustion capture, such as absorption, adsorption, membrane separation and cryogenic separation the use of chemical solvents like ethanolamine (MEA) is the most mature treatment technology [9]. The chemical solvent is particularly adapted to absorb CO_2 with a concentration of 4-14% by volume from the flue gas [9]. The disadvantage is that chemical solvents require a lot of energy in regeneration (to break the chemical link between CO_2 and the solvent), which results in a high energy penalty for the power plant. On the other hand, post combustion has already been used in the 1980s in the United States in order to produce CO_2 for Enhanced Oil Recovery and is therefore a fully developed technology [10].

Oxy-combustion Oxy-combustion is based on the concept that fossil fuels when combusted with pure oxygen and recycled flue gases produce a flue gas containing only CO_2 and water, and not a considerable amount of N_2 as in air combustion. Therefore, for oxy-combustion the CO_2 can easily be separated by condensation of steam. Typically, the oxygen is obtained by separation from air by cryogenic distillation. This process is shown in Figure 1-7; note that the oxygen is not 100% pure, as some Ar and N_2 are separated together with O_2. Other researchers proposed that the pure oxygen may be delivered as a solid oxide. The CO_2 concentration in the separated carbon dioxide stream is 95% mole based or higher and is therefore competitive with pre- and post-combustion capture. However, oxy-combustion is the least studied capture technology. Pilot and large-scale plants are at an advanced stage, but the IEA expects that the potential for further development is big [9].

1-2-2 CO_2 transport

After sequestration, the CO_2 has to be transported to adequate storage sites. Ships, trucks and trains are viable options and have already been used in demonstration projects. They represent a possible short-term measure, especially for regions with low storage capabilities. The long-term and main option for CO_2 transport are pipelines. Pipelines have higher investment costs, but the IEA expects that the mean total costs are significantly lower than for other transport technologies. Furthermore, in the United States and Canada a 6,200 km long CO_2 pipeline has been operating for over four decades. The CO_2 was transported to oil production fields and injected for Enhanced Oil Recovery [10, 7, 11]. In the next year CO_2 transportation is expected to evolve rapidly. The International Energy Agency estimated in 2009 the evolution of the CO_2 transport sector for a scenario, which sets year 2050 as the target for reducing the global-energy related CO_2 emissions to half compared to the ones of 2005. The results of the analysis show that in 2050 the total length of the CO_2 pipeline network is estimated from 200,000 km to 360,000 km, with a necessary total investment of $ 0.55 trillion to $ 1 trillion. However, health and safety regulations are still missing and techniques for leak remediation and managing of different CO_2 stream impurities must be improved. A potential pipeline leakage can cause respiratory diseases and other fatal health risks. CO_2 cannot explode or take fire when it is transported in a supercritical state, but it is heavier than air and in case of a leakage it is accumulated in low-lying areas. In the presence of H_2S and SO_2 the health risk even increases [12]. Furthermore, the impurities alter the thermodynamic behaviour of the CO_2 and could pose a threat to the integrity of the transmission system and cause other health, safety and environmental problems [11].

1-2-3 CO_2 storage

Various storage options have been proposed. Oceans are prime candidates. Their carbon inventory is 50 times greater than the one of the atmosphere. Although the surface of the oceans exchanges CO_2 with the atmosphere, if CO_2 is injected in higher depth a rapid release can be avoided (the critical pressure depth is 800 m under the sea level) [8]. Therefore, ocean storage was expected to have a large potential, but because of a severe environmental opposition it so no longer considered feasible.

Another storage opportunity is mineral storage. CO_2 reacts with minerals such as iron, calcium or silicates of magnesium to form stable carbonates. A so called chemical trapping occurs, because chemical reactions are the basis of this technology. The chemical reaction would consume about 2 tons of silicate mineral per ton of CO_2. Therefore, large-scale mining would be necessary if mineral storage would become a main storage site; but there are also other ideas for small-scale applications. For instance, mineral storage in wastes from incinerators, steel and cement industries [8].
Injecting carbon dioxide directly into underground geological formations is the idea of the geological storage. There are three different options for geological storage: saline formations, oil and gas reservoirs and deep coal seams [7]. Saline formations are the most promising long-term option, because they have the greatest storage quantities and are geographically more accessible. Oil and gas reservoirs on the other hand have already been utilized in the oil and gas sector on a commercial scale and the technology is ready. Furthermore, this technology brings the advantage of enhancing hydrocarbon recovery (Enhanced Oil Recovery) and could

also reduce the risks of oil and gas reservoirs [8].
CO_2 storage exploration is a pressing priority, because suitable storage sites need to be located and further knowledge on costs and security is necessary if CCS should represent a main mitigation measure in the global energy mix. The uncertainty is reflected in the expected cost of storing CO_2, which is estimated around $ 0.6 to $ 4.5 per tonne of CO_2 stored [7].

1-3 Integrated Gasification Combined Cycle

In order to achieve a significant reduction of CO_2 emissions in the near future, CCS should be applied to various large point sources of carbon dioxide [5]. The world's largest CO_2 emitters are power plants. Therefore, the IEA expects that the highest deployment of CCS until 2050 will be in the power sector [5]. One of the applications of CCS in the power sector is the incorporation of capture units into IGCC power plants. An IGCC power plant gasifies carbon based fuels into a syngas, cleans the latter one from impurities and burns it in a gas turbine. The exhaust gases are then routed to the Heat Recovery Steam Generator (HRSG). The generated vapor is then fed to a steam turbine to produce energy.

The advantage of IGCC systems is that the combustion process is cleaner than for traditional carbon based systems. The GHG-emissions are lower. In fact, the gas turbines demand deep gas cleaning, and therefore impurities are removed before routing the syngas to the gas turbine [13]. If the plant is coupled to a capture system, also the CO_2 emission can be significantly reduced. Different capture technologies can be applied. This work will focus on the integration of a pre-combustion CO_2 capture unit into an IGCC power plant.

Figure 1-8 presents a detailed process description of a possible IGCC plant configuration with a pre-combustion CO_2 capture unit. Coal, after an appropriate preparation depending on the type of gasifier, is fed to the gasifier together with pure oxygen from the air separation unit (note that also other carbon based fuels as biomass could be used). A synthetic gas containing mainly H_2 and CO is produced at high temperature and pressure. The high temperatures lead to a high sensible heat content, but most of it is recovered producing steam which is send to the steam turbine. The syngas then enters cyclones & filters and the water scrubber, where the HCl and the remaining fly ash is removed. In the next step, called COS Hydrolysis, COS is converted to H_2S (note that also HCN reacts to NH_3). This is necessary in order to recover most of the sulphur in the downstream H_2S removal section. The sulphur at the outlet is sent to the Claus plant, where pure sulphur is produced as a by-product. Following this, the fuel gas is transferred to the sweet shift reactors, where the so called water-gas shift (WGS) reaction takes place. The reactors convert most of the carbon monoxide to carbon dioxide and hydrogen. After this, a washing column removes the carbon dioxide from the gasified fuel. The CO_2 is recovered and compressed in an intercooled multistage compressor. The clean fuel, which contains mainly H_2, is mixed with nitrogen and/or water and fed to the gas turbine. The exhaust gases from the turbine are cooled down in the HRSG to evaporate water for the steam turbine. Both gas and steam turbine, produce electricity.

This process is a simplification of the real process and is only one of the many possible configurations, which depend, e.g., on the type of gasifier and the degree of process integration.

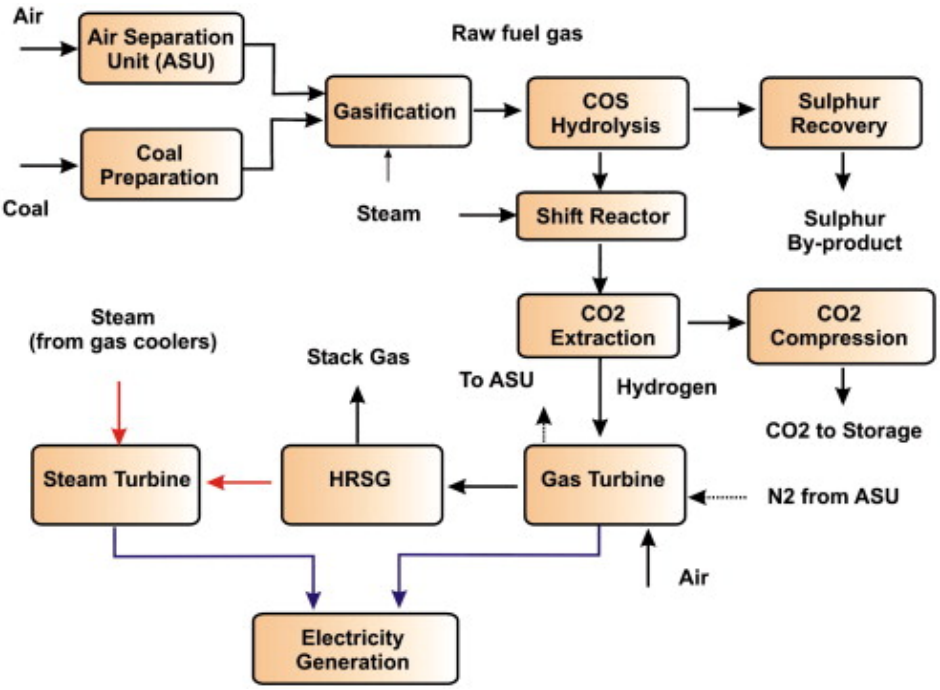

Figure 1-8: Block flow diagram of IGCC plant with CO_2 capture, adapted from [13]

Another distinction between the different processes is the location of the shifting section. If the shifting section is located before the H_2S removal section one deals with a 'sour shift', otherwise with a 'sweet shift'. Sweet shift reactors are less expensive as the catalyst is not required to be sulphur resistant. In contrast, the attractiveness of sour shift is given from higher process efficiencies. However, the choice depends also on the degree of CO conversion, the durability of the catalyst and the possibility to by-pass the shifting and CO_2 absorption section. An accurate description of the process and the different configurations is beyond the scope of this work. Useful information can be found on the website of the U.S. Energy Department [14].

1-4 Literature review (recent process design and optimization studies)

This literature review focuses on IGCC power plants with pre-combustion CO_2 capture units. Several studies have been performed. An extensive techno-economic analysis of different IGCC configurations was done by Huang et al. [13] in 2008. The authors compared the Shell dry feed and General Electric (GE) wet feed entrained flow gasifier with and without CO_2 capture, for both a sweet and sour shift configuration. The GE IGCC power plant was slightly less expensive and produced more electricity. Nonetheless, the much lower efficiency led to a higher breakeven electricity selling price (the hypothetical electricity price for which the net present value would be zero). For both gasifier types, the sour shift configuration had higher efficiencies and lower electricity generation costs than the sweet shift option. The overall efficiency losses, due to the introduction of the capture unit, were between 8 and 11%.

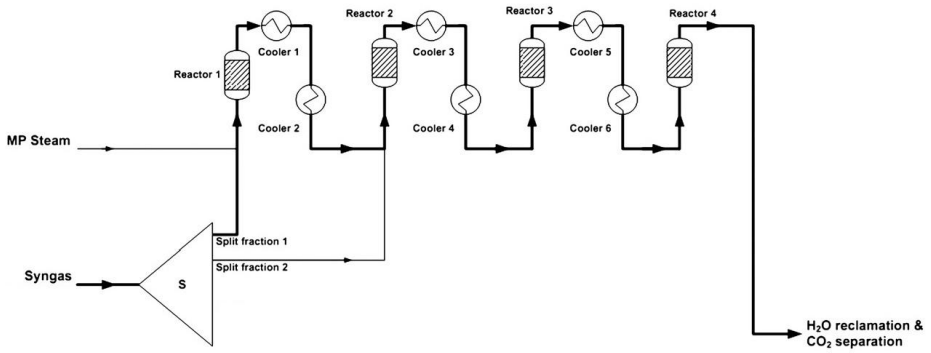

Figure 1-9: Optimized novel WGS configuration studied from Martelli et al., adapted from [15]

The efficiency loss represents the major drawback of the integration of a capture unit into IGCC power plants. Therefore, the success of CCS technologies will depend among others on the ability to reduce this energy penalty. How to reduce this energy penalty was investigated by Kunze, Riedl and Spliethoff in 2011 [16]. The paper shows that the gas turbine, the gasifier and the capture unit (shifting, H_2S removal and CO_2 removal section) cause the highest exergy losses in the IGCC plant. Thus, the improvement and optimization of these units could lead to high efficiency gains. Therefore various studies focused on the capture unit, especially on the shifting section.

Martelli et al. studied novel WGS configurations, which require less steam for the same degree of CO conversion. This increases the plant efficiency [15]. They proposed a new configuration for approximately 93% of overall carbon capture, which uses a steam injection before the first reactor and a single syngas quench between the first and second reactor (see Figure 1-9). It was shown that the new configuration reduces significantly the levelized cost of energy. This was already expected from Carbo et al. in 2009. In fact, Carbo already expected that the gain in efficiency of novel WGS configuration would overcompensate the higher capital expenses. The capital costs are higher than in traditional configurations, because of the bigger catalyst volume and the higher number of reactors used [17]. In addition, Carbo proved that the attractiveness of these novel configurations is independent from the choice between sour and sweet shift, and the choice between slurry- and dry-fed gasification. In this study it was also observed that there is an optimum CO_2 capture ratio between 80 and 90%, calculated as the specific lost work per captured amount of CO_2.

A more extensive optimization of a sour shift capture unit of an IGCC plant with precombustion CO_2 capture was performed in 2010 [18]. In the absorption section (H_2S removal and CO_2 removal unit) the physical solvent Selexol was used to absorb H_2S and CO_2. In order to regenerate the two gases from the solvent, a flash vessel in the CO_2 absorption section and a stripper in the H_2S absorption section were used. The authors, Bhattacharyya, Turton and Zitney performed an optimization including design decisions and operating conditions. The trade-off between CO conversion (in the shifting section) and CO_2 recovery (in the CO_2 absorption section) to achieve a fixed overall capture rate of 90% was analyzed. An optimization of the pressures of the flash vessels in the absorption section was also included. The results show that with the optimization of the above described variables, a considerable gain in the

Figure 1-10: Nuon Magnum power plant in Eemshaven, Netherlands [20]

net plant efficiency and the power output is achievable.

A few pre-combustion IGCC capture pilot plant are in operation for experimentation and acquisition of operating experience. One of these is the CO_2 capture pilot plant which has been build at the site of the Buggenum IGCC power station (253 MW_e) [19]. The pilot plant uses uses approximately 0.8% of the total syngas stream of the power plant. The capture unit is based on a pre-combustion sweet-shift capture technology, which uses dimethyl-ether of poly-ethylene-glycol (DEPG) as physical solvent in the absorption section. The decision between sweet and sour shift fell on sweet shift, as sweet shift is more adequate to by-pass the CO_2 capture unit if the CO_2 market price does not justify the additional cost of CCS. This could become relevant for an eventual fluctuating carbon price in the future. The drawback of sweet shift is that the efficiency loss is higher. Therefore, most research work till now focused on sour shift and less literature is available on sweet shift.

1-5 Research questions

This work deals with the analysis and optimization of the pre-combustion CO_2 capture unit which should be integrated into the IGCC power plant Nuon Magnum in Eemshaven (see Figure 1-10). The capture unit includes a shifting, CO_2 removal, H_2S removal and CO_2 compression section. With respect to most other research works, the present work focuses on a sweet shift capture unit and is based on experimental results. In fact, results from test runs at the pilot plant in Buggenum (see section 1-4) and the obtained operating experience is used throughout the model development and analysis. The primary objective is to reduce the energy penalty related to the introduction of CO_2 capture to an IGCC power plant. The following research questions have been addressed in this project and are treated in the thesis:

- Comparison of the thermodynamic and economic convenience between chilling (down to 4°C) and cooling (down to 35°C) the solvent in the absorption section

- Development of a suitable optimization framework for the optimization of the capture unit, and analysis of the influence of the minimum steam/CO ratio and the minimum inlet temperature of the WGS reactors on the energy consumption of the capture unit
- Impact on the performance of the sulphur absorption section in case the CO_2 absorption section is by-passed (no capture)

The outcome of previous studies has been used as a starting point, e.g., the design of the shifting section (see Chapter 2) recalls the novel WGS configuration proposed by Martelli [15]. A detailed sensitivity analysis and optimization of the operating variables of the capture unit was performed. Configuration changes are not taken into consideration. However, different column heights and different solvent cooling systems for the absorption section were investigated.

Chapter 2

Process description

In 2005, Nuon, a Dutch utility company, started the development of a multi-fuel Integrated Gasification Combined Cycle (IGCC) power plant, the so-called Nuon Magnum, in Eemshaven, the Netherlands [21]. They decided to build a pre-combustion IGCC pilot plant at the site of the Buggenum power station (see Sec. 1-4) with the aim to use the knowledge for the scaled-up Magnum power plant. The Magnum IGCC power plant was planned to be built in two phases. First, a natural gas combined-cycle power plant would be realized, and afterwards it would be converted into an IGCC power plant with an integrated capture unit. The first phase was launched in 2007 and was concluded in 2012, while phase two was postponed, due to the rise in raw material costs and in general the unanticipated magnitude of the investment [22]. In any case, it was decided to proceed with detailed studies about the design of a large-scale IGCC power plant integrating CO_2 capture technology. The plant consists of three combined cycles with a net power output of 438 MW each, for a total electrical output of approximately 1,300 MW [22]. For each gas turbine a separate capture unit is planned, which treats more than 70 kg/s of syngas coming from a dry-feed gasifier by means of a sweet-shift and bulk CO_2 removal. Almost 80 kg/s of CO_2 should be captured for each capture unit, which is equivalent to an overall capture rate of approximately 85%.

In this work a fixed design for the capture unit is used. This has already been developed previously. The planned capture unit is made of the following four main sections: H_2S removal, water-gas shift, CO_2 removal and CO_2 compression. Figure 2-1 shows the integration of the sections. The syngas from the downstream gasifier is fed to the H_2S Absorber. The physical solvent DEPG extracts the hydrogen sulfide (H_2S) from the main stream. After that the solvent is regenerated in a desorber, and the H_2S is sent to a Claus plant where pure sulphur is produced as a by-product. The poisonous, corrosive, flammable and explosive hydrogen sulfide has to be removed from the syngas upstream the shifting unit in order to protect the catalyst of the shift-reactors. By adding Reaction Water to the Unshifted Syngas the desired steam/CO ratio for the water-gas shift is obtained. The operating temperature of the reactors is around 300°C to 500°C and thus the syngas has to be heated after the H_2S absorption, which takes place at low temperature. In the shifting section most of the CO is converted

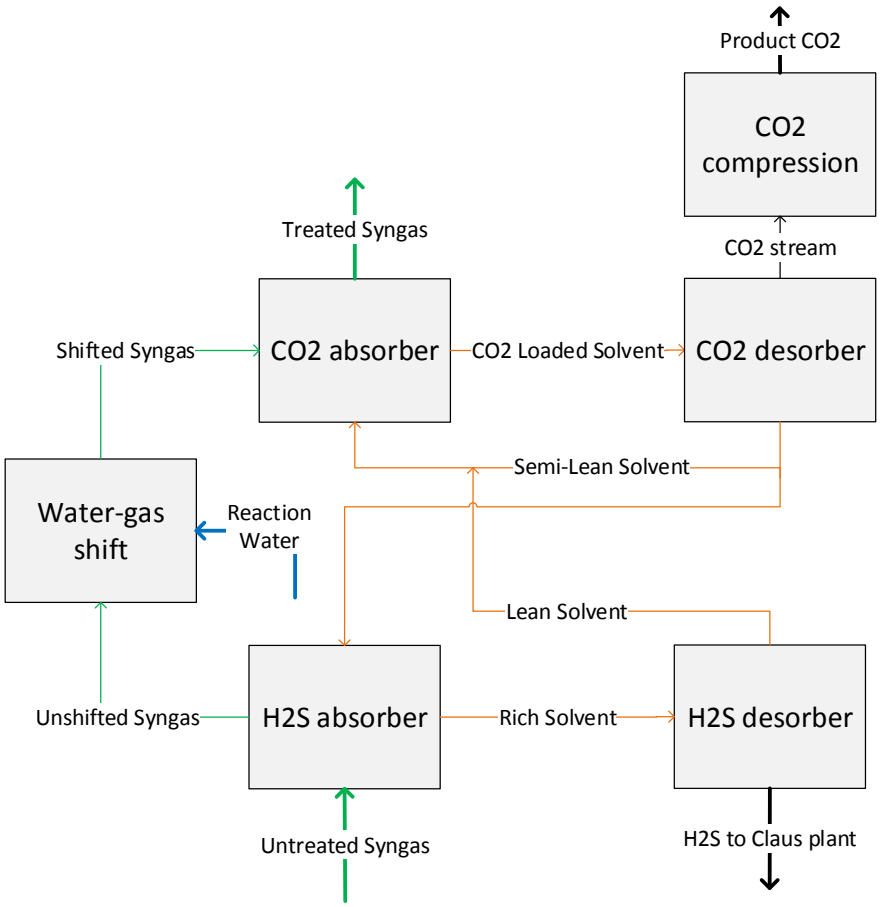

Figure 2-1: Layout of the studied capture unit

into CO_2 in order to facilitate the carbon dioxide absorption process in the downstream CO_2 Absorber column. Like in the H_2S Absorber, DEPG is used to remove the CO_2 from the main process stream. Afterwards the CO_2 is recovered by means of a three stage-flash, which in Figure 2-1 is for simplicity indicated as the CO_2 desorber. Almost pure CO_2 exits the CO_2 desorption unit and is sent to the storage site after a multi-stage intercooled compression. The syngas at the outlet of the CO_2 Absorber is fed to the combined cycle. The particularity of this design is that the two absorption sections are integrated into each other. In other words, the same solvent passes first through the CO_2 Absorber and then through the H_2S Absorber. A detailed description of the individual sections follows in the next paragraphs.

2-1 Water-Gas Shift Section

The purpose of the CO shifting section is an efficient conversion from carbon monoxide to carbon dioxide. Figure 2-2 shows a simplified process flow diagram of the water-gas shift section. The Unshifted Syngas coming from the upstream Sulphur Absorber is fed to the Syngas Booster Compressor. The compressor has to overcome the pressure drop of the capture

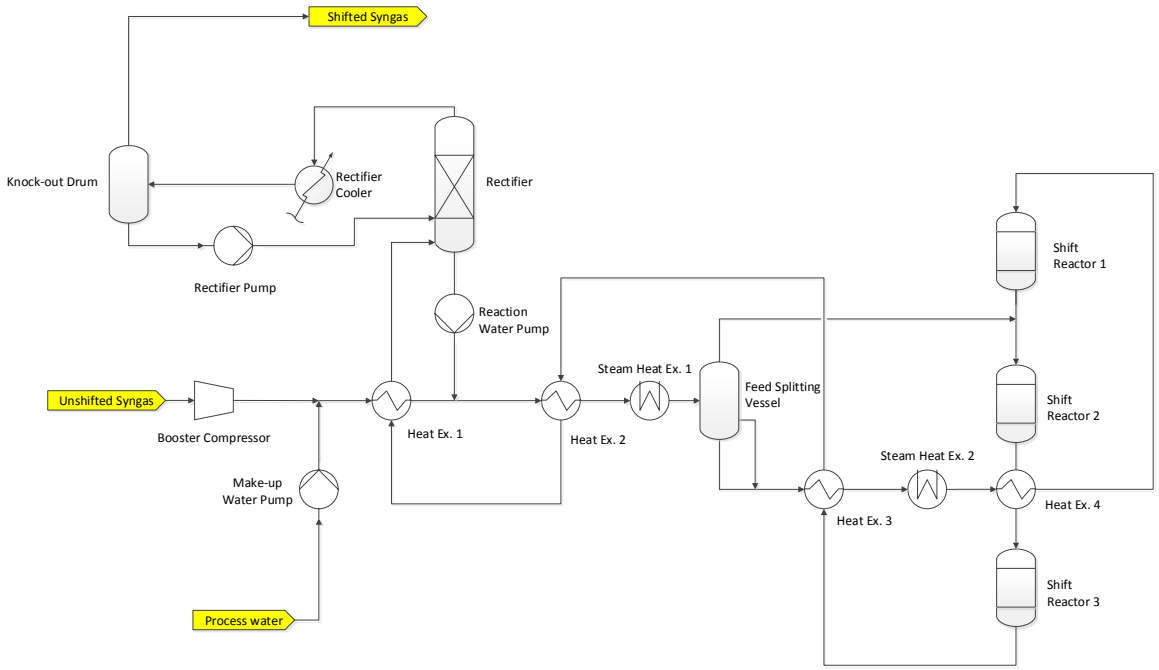

Figure 2-2: Simplified process flow diagram of the shifting section, based on CB&I Lummus design

unit, because a minimum pressure at the inlet of the Combined Cycle is required. It is located upstream the CO_2 absorption section, because higher pressures favour the absorption process. Furthermore, a study which was performed by CB&I Lummus before this project, but within the same larger research project focused on CCS, shows that locating the compressor upstream the shifting section is more beneficial than locating it downstream. The energy consumption of the entire shifting section is reduced. This is partly caused by a lower energy consumption of the compressor, due to lower pressure ratios for the same pressure increase and lower volumetric flow rates. The rest is caused by less required steam for the Steam Heat Exchangers. In fact, for higher condensing pressures more heat can be regenerated from the vapor effluent of the reactors. Therefore, less steam is needed for the feed preheat [21]. An alternative to the Syngas Booster Compressor is to use a higher gasifier pressure. Although this option can also guarantee a minimum inlet pressure to the combined cycle without using any compressor, it was not studied during the research project, because a detailed input from the gasifier licensor was missing.

The compressed syngas is then mixed with make-up water at the same pressure. How much make-up water is necessary is mainly determined by the water consumption in the water-gas shift reactors. Reaction water coming from the Rectifier is then added to the outlet stream of the mixer. The aim is to a achieve a sufficient steam/CO ratio for the WGS reactors. A series of heat exchangers heat up and partially evaporate the combined feed by recovering the sensible and latent heat from the reactor effluent. To achieve the requested shift reaction temperature, additional heat has to be provided by intermediate pressure steam (IP steam) coming from the gasifier syngas cooler and used in the two steam heat exchangers. Between the heat exchanger train a Feed Splitting Vessel is located. It separates the reactor feed in two

streams. The liquid bottom and a part of the vapor are send to the first shift reactor, while the demisted overhead vapor by-passes the first reactor and quenches the first reactor effluent. This design is similar to the optimal design of the shifting section proposed by Martelli et al., mentioned in Sec. 1-4. In contrast to Martelli's configuration the steam is used in the Steam Heat Exchangers (not mixed to the syngas) and three instead of four shift reactors are used. The shift reactors operate in series and are filled with an apposite catalyst. The following exothermic, equilibrium controlled reaction takes place:

$$CO + H_2O \rightleftharpoons H_2 + CO_2 \tag{2-1}$$

The thermodynamic reaction equilibrium is favored at low temperatures, where it proceeds to the right. On the other hand low temperatures adversely affect the reaction velocity. Indeed, the Arrhenius equation suggests that the reaction rate and velocity increases with temperature. Consequently, the inlet temperature to the reactors is a trade-off between the reactor size and the operating costs. If the inlet temperature is low, the reaction is slow and the reactor dimensions have to increase causing higher investment costs. For high inlet temperature the reaction is faster. The reactors can be smaller, but the thermodynamic equilibrium of the reaction is disadvantaged. Therefore, the steam/CO has to be pushed higher in order to obtain the same CO conversion. This leads to a higher energy consumption causing higher operating costs. The trade-off between the reaction equilibrium and the reaction velocity influences also the shifting section configuration. In fact, the shifting section is often divided into two parts: a high temperature stage for an initial fast conversion, due to high reaction velocities, and a downstream low temperature stage. In the second stage the reaction velocity is low, but the equilibrium is favoured and deeper conversions can be achieved [17].
Another factor which influences the WGS reaction is the steam/CO ratio. The higher the steam/CO ratio, the more the reaction proceeds to the right and more CO is converted to CO_2. Therefore, steam is always added in excess, so that the overall steam/CO ratio is above stoichiometric ratios. This drives the equilibrium of the shift reaction further to the right, limits the temperature increase in the reactors and protects the catalyst from undesired iron carbide formation. On the other hand too high steam/CO ratios influence negatively the energy consumption. Accordingly, also the steam/CO ratio has to be chosen accurately to perform an optimal shift reaction in terms of energy consumption; but the optimal choice depends, e.g., also on maximum adiabatic temperature rise in the WGS reactors. Throughout the reactors the temperature always increases, because the water-gas shift reaction is exothermic ($\Delta H^{\circ}_{298} = -41.1 kJ/mol$). This temperature increase has to be controlled, because there is a limit on the highest outlet temperature of the reactors (about 520°C) in order to avoid irreversible deactivation of the catalyst by sintering [23]. A higher steam/CO ratio reduces the adiabatic temperature increase. Nevertheless, the WGS reactors have to be intercooled in order to avoid sintering and to favour the equilibrium of the WGS reaction. The first reactor effluent is cooled by the quench stream coming from the Feed Splitting Vessel. The hot effluent of the second and third reactor is instead cooled in the heat exchanger train. The cooled shifted syngas is then sent to the Condensate Recovery Section.
In the Condensate Recovery Section as much water as possible should be recovered from the shifted syngas. In this way, the make-up water stream can be limited and less heat is wasted. Some of the excess vapor from the shift reactor effluent has already been partially condensed in the heat exchanger train. The Rectifier favours further the condensation and strips off the condensed water. The rectifier bottom (mainly water) is sent back to the syngas upstream the

reactors. The overhead stream is sent to the Rectifier Cooler, where most of the remaining water in the H_2 rich syngas is condensed and thereafter separated in the Knock-out Drum and fed to the Rectifier. The Shifted Syngas at the top of the Knock-out Drum is sent to the CO_2 Absorber.

2-2 Absorption Section

The absorption section is a dual-stage DEPG unit. It removes H_2S and CO_2 from the syngas by selective absorption with a DEPG-type commercial blend, composed of polyethylene glycol dimethylethers (glymes). The absorber and desorber columns are packed with structured packing. The aim of this section is to separate the syngas into a hydrogen rich gas, a CO_2 stream and an acid gas stream. In this work two different configurations are analyzed: an ambient temperature configuration (ATC) (also called unchilled configuration) which uses only water coolers to cool down the solvent, and a below-ambient temperature configuration (BATC) (also called chilled configuration) which makes use of chillers in order to cool down the solvent to lower temperatures. The two configurations will be explained in the following two subsections.

2-2-1 Ambient temperature configuration (ATC)

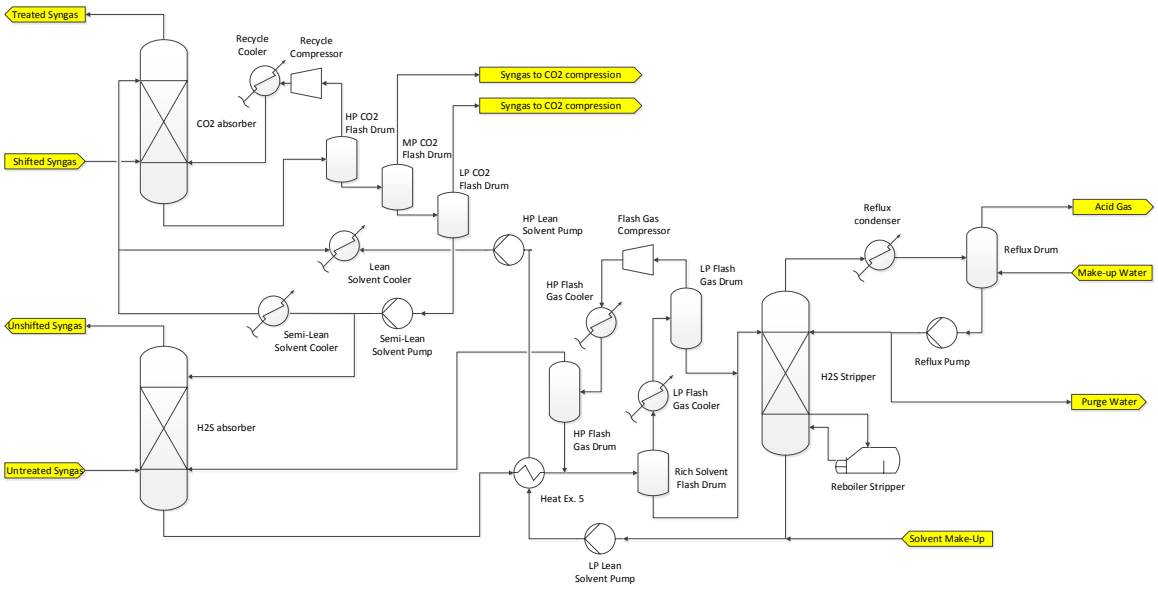

Figure 2-3: Simplified process flow diagram of the absorption section (ambient temperature configuration)

Figure 2-3 shows a simplified process flow diagram for the ambient temperature configuration. The untreated syngas coming from the gasifier passes through the H_2S Absorber, where most of the hydrogen sulfide is removed. The off-gas from the H_2S Absorber leaves the absorption unit as Unshifted Syngas and is fed to the shifting section. The H_2S is absorbed into the Semi-Lean Solvent coming from the CO_2 absorption section. The Rich Solvent exchanges

heat with the Lean Solvent from the bottom of the Regenerator (also called H_2S Stripper). Thereafter, the Rich Solvent is routed to the Rich Solvent Flash Drum. This drum is necessary to control the fraction of hydrogen sulfide in the acid gas stream. The off-gas from the top is cooled in the LP Flash Gas Cooler. The condensed liquid at the outlet of the cooler is directly routed to the Regenerator, while the gas stream is compressed. The compression increases the temperature, and therefore another cooler is located downstream the Flash Gas Compressor. Once again liquids are removed and then the flash gas is recycled back to the H_2S Absorber.
The bottom stream from the Rich Solvent Flash Drum is mixed with the liquid outlet stream from the LP Flash Gas Cooler and is fed to the H_2S Stripper. This column operates at high temperature and low pressure, because at these conditions the desorption is favoured. At the bottom of the Stripper a Reboiler partially evaporates the water in the solvent. The steam rises up and strips countercurrently the Rich Solvent falling down from the top. H_2S passes from the solvent to the vapor. Consequently, the steam at the top of the column is rich in H_2S. In order to recover the hydrogen sulfide, the steam is condensed in a Reflux Condenser. A simple Reflux Drum then separates the condensed liquid from the vapor phase. The latter one is called Acid Gas stream and is sent to the Claus plant. At the bottom of the Reflux drum a Make-up water stream is added for purification issues. To compensate the Make-up water the same amount of water has to be removed with the Reflux stream. Furthermore, some water is co-absorbed together with CO_2 and H_2S in the absorber columns and has to be extracted in order to maintain a fixed water content in the solvent. The two withdrawn water streams together form the Purge Water stream. Finally, the rest of the Reflux stream is sent back to the regenerator column.
The Lean Solvent at the bottom of the H_2S Stripper is mixed with make-up solvent and after the Heat Ex. 1 and an apposite pressure increase the solvent is sent back to the CO_2 Absorber. In the CO_2 Absorber carbon dioxide is removed from the Shifted Syngas and passes into the solvent. The Treated Syngas is sent to the combined cycle, while the liquid solvent at the bottom is routed to the CO_2 Flash Drums. In contrast to the H_2S Stripper, the CO_2 is recovered by simple depressurization in three flash drums. No stripping column and no temperature increase is necessary, since the desorption of the carbon dioxide is much easier and a less deep removal is required. The first flash drum recovers H_2 and CO. These burnable components have a high heating value and are sent back to the absorber after compression and cooling. The loaded solvent at the bottom outlet of the flash drum is sent to the MP and LP CO_2 Flash Drum. Almost pure CO_2 gas is recovered from the off gases of the flash drums and sent to the CO_2 compression section. The solvent at the bottom outlet of the last flash drum is sent to the Semi-Lean Solvent Pump. A minor fraction of the pressurized Semi-Lean Solvent is sent to the H_2S Absorber, while the rest is cooled and fed again to the CO_2 Absorber.

2-2-2 Below ambient temperature configuration (BATC)

The attractiveness of a below-ambient temperature configuration is that the absorption process is favoured at low temperatures. Hence, chilling the solvent instead of only cooling it is advantageous for the absorber columns. In a first approximation, the phenomenon is explained by the laws which are followed by a physical absorption process, namely:

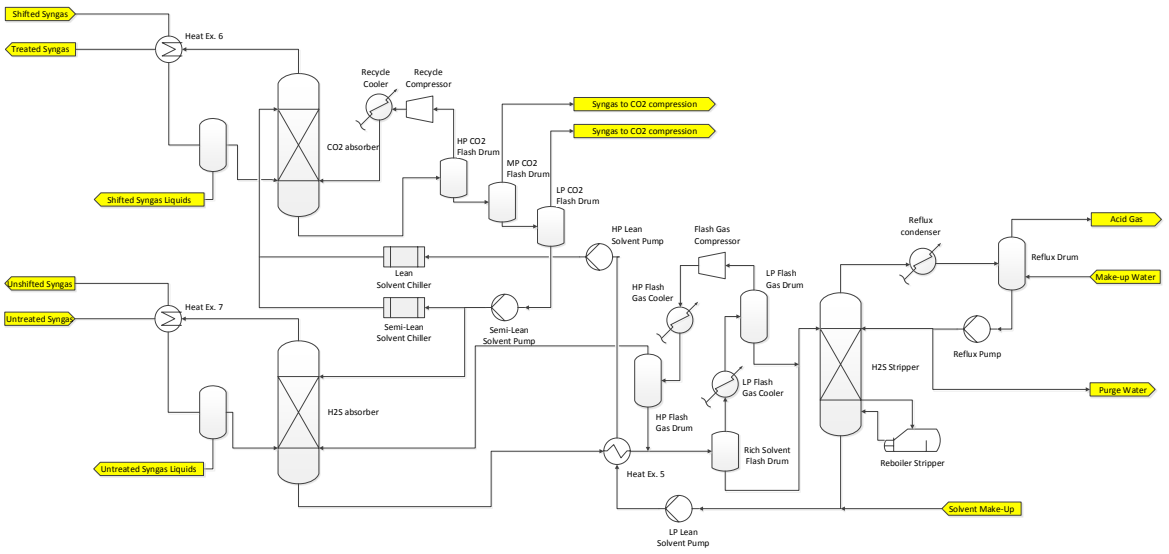

Figure 2-4: Simplified process flow diagram of the absorption section (below-ambient temperature configuration)

$$y_i = H_i \cdot x_i \tag{2-2}$$

The equation governs the distribution of a single component between the vapor and the liquid phase once equilibrium is reached. The mole fraction in the vapor phase of the component i is the product of the equilibrium constant H_i and the mole fraction of the component i in the liquid phase. The equilibrium constant H_i depends on the pressure, temperature and composition. For highly diluted solutions the equilibrium constant follows the Henry's law, while for less diluted solutions, as in the CO_2 and the H_2S absorbers, the Raoult's law is the better approximation of reality. Under the hypothesis of an ideal solution and an ideal gas for the Raoult's law the equilibrium constant H_i can be written as:

$$H_i = P_i^{vap}(T)/P \tag{2-3}$$

Combining the two equations the mole fraction in the vapor phase of the component i can be expressed as:

$$y_i = P_i^{vap}(T) \cdot x_i/P \tag{2-4}$$

The equation Eq. (2-4) [24] shows how the mole fraction of CO_2 and H_2S in the syngas can be reduced in the absorber columns. The vapor pressure should be as low as possible, while the total pressure as high as possible. Since the vapor pressure increases with the temperature, higher total pressures and lower temperatures favour the absorption process. Note that the above equations should give a general explanation of the influence of the temperature and pressure on the absorption process. In fact, note that the mixtures present in the CO_2 and H_2S absorber are no ideal solutions and gases.

Compared to the ambient temperature configurations only minor configuration changes are made (see Figure 2-4). The main difference is that the Lean Solvent Cooler and the Semi-Lean Solvent Cooler are replaced by chillers. The outlet temperatures of the syngas from the two absorbers are significantly reduced. This suggests the use of heat exchangers between the incoming and outgoing syngas stream from the absorbers. The syngas downstream the absorbers is heated up. This is advantageous for both the shifting section and the combined cycle. The syngas upstream the absorber is instead cooled. Then the condensed liquid, mainly water, is knocked out while the rest of the syngas is fed to the bottom of the CO_2 Absorber column. The operating temperature of the absorber is hereby reduced and the absorption process is favoured. Therefore, a lower solvent mass flow is necessary to assure the same CO_2 recovery (see section 2-5). An accurate comparison between the ambient and below-ambient temperature configuration will be made in this work in order to point out the more optimal configuration.

2-3 CO_2 Compression Section

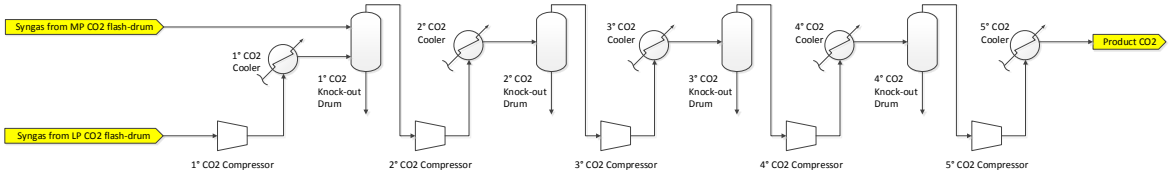

Figure 2-5: Simplified process flow diagram of the compression section, based on CB&I Lummus

The CO_2 compression section is made of a five-stage intercooled compressor with discharge Knock-out Drums. The aim of this section is to supply the almost pure CO_2 stream at an adequate pressure and temperature to the pipeline which transports the carbon dioxide to a storage site.
Figure 2-5 shows a simplified process flow diagram of the compression section. The CO_2 stream separated from the medium pressure (MP) and low pressure (LP) CO_2 Flash Drum enters the CO_2 compression section. The low pressure stream is compressed in the first CO_2 Compressor and intercooled in the following CO_2 Cooler. The outlet pressure is equal to the pressure of the medium pressure stream and so the two streams can be mixed in the first Knock-out Drum. The condensed liquid is removed in order to protect the following compressors and to obtain a purer CO_2 stream. The overhead stream is fed to the second CO_2 Compressor which is followed by the second CO_2 Cooler and the second CO_2 Knock-out Drum. The same combination of components is repeated also for the last three stages of the compression section. The only exception is the outlet of the last stage. The difference is that here no Knock-out Drum is used after the CO_2 Cooler, since no condensed water is present at the outlet of the compression section. In fact, the temperature and pressure at the outlet of the last compressor are above the critical point conditions. The CO_2 becomes supercritical and a compression will not produce any liquid. For a better understanding of the transition from the liquid to the supercritical phase, consult the PT diagram in Figure 2-6. This indicates the CO_2 phases.

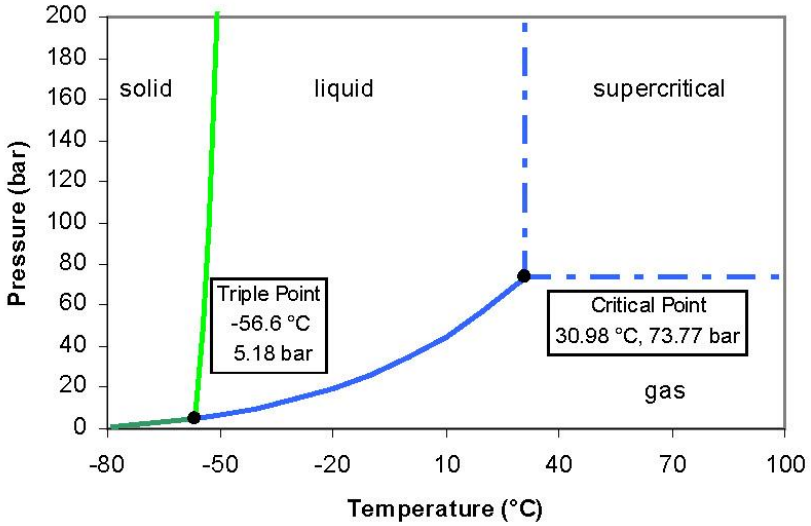

Figure 2-6: CO_2 phase diagram, adapted from [11]

This configuration is a simplification of the actual design. The condensed liquid is normally sent back to the CO_2 absorption section; but the mass flows of these knock-out streams are very small and have a limited impact on the performance of the absorption section. For simplicity these tear streams were left out. Furthermore, no drier was considered in the compression section. In an actual compression section a drier is used to extract the remaining water from the CO_2 stream before the fluid is compressed and becomes supercritical.

2-4 CO_2 Capture Unit Process Flow Diagram

The process flow diagrams of the entire capture unit for the ambient and below-ambient temperature configuration are represented in Figure 2-7 and Figure 2-8, respectively.

2-5 Definitions

In this section some important definitions to measure the efficiency of the capture unit are given.
The efficiency of the water-gas shift section is called CO conversion efficiency. It represents a measure of the fraction of CO converted in the shift reactors:

$$\eta_{CO} = \frac{\dot{m}_{CO\_Unshifted} - \dot{m}_{CO\_Shifted}}{\dot{m}_{CO\_Unshifted}} \tag{2-5}$$

The Shifted Syngas at the outlet of the WGS section is then fed to the absorption section and compression section, where CO_2 is removed from the main syngas stream. The efficiency of this process is called CO_2 recovery or CO_2 absorption efficiency:

$$\eta_{CO_2} = \frac{\dot{m}_{CO_2\_Product\_CO_2}}{\dot{m}_{CO_2\_Shifted}} \tag{2-6}$$

Figure 2-7: Simplified process flow diagram of the capture unit (below-ambient temperature configuration)

Figure 2-8: Simplified process flow diagram of the capture unit (ambient temperature configuration)

To measure the efficiency of the entire capture unit the overall carbon removal (also called CO_2 capture rate) is used. It is calculated as the total mole flow of carbon in the CO_2 Product stream over the total carbon mole flow in the Untreated feed stream:

$$\eta_C = \frac{(\dot{n}_{CO_2} + \dot{n}_{CO} + \dot{n}_{COS} + \dot{n}_{CH_4})_{Product\_CO_2}}{(\dot{n}_{CO_2} + \dot{n}_{CO} + \dot{n}_{COS} + \dot{n}_{CH_4})_{Untreated}} \tag{2-7}$$

It should be noted that a fixed capture rate can be achieved with various combinations of CO_2 recovery and CO conversion. If the CO conversion is increased, the CO_2 recovery can be decreased and the opposite. An analytical explanation follows from Eq. (2-7). For a fixed CO_2 recovery $\dot{m}_{CO_2\_Product\_CO_2}$ is constant. If the CO conversion augments, more CO is shifted to CO_2, and the CO_2 flow rate in the Shifted Syngas ($\dot{m}_{CO_2\_Shifted}$) augments. Consequently, the CO_2 recovery decreases.

The energy consumption of the capture unit is significantly influenced by this trade-off. To increase the CO conversion typically more process water is added in order to augment the steam/CO ratio in front of the reactors. This augments the steam consumption in the Steam Heat Ex., and consequently the energy consumption of the water-gas shift section augments. On the other hand, if the CO conversion is increased the CO_2 recovery can be reduced. This can be achieved by changes in different process variables: decreasing the solvent/gas ratio in the CO_2 Absorber, increasing the temperature of the solvent, decreasing the number of stages in the CO_2 Absorber column, or lowering the extent of CO_2 desorption by varying the pressures in the CO_2 flash drums. All lead to a lower energy consumption of the absorption section [18]. The physical reason why the energy consumption is reduced is the following: if more CO is shifted to CO_2, the partial pressure of the CO_2 in the Shifted Syngas augments. A higher partial pressure is beneficial for the CO_2 absorption process, which consequently consumes less energy. The optimization of the entire capture unit will take into consideration this trade-off.

Chapter 3

Steady-State Modeling and Methodology

3-1 Modeling tools (Process software, thermodynamic model, optimization framework)

For the process modeling of the CO_2 capture unit the commercial software Aspen Plus Version 7.3 was chosen. The cost estimation and some optimization problems were also performed in Aspen. For the more complex optimizations the process simulator was interfaced with Matlab, and an available optimization algorithm was used.

Aspen Plus Aspen is a commercial software developed by AspenTech. It is a useful tool to model, optimize and monitor different processes, in particular chemical ones. Reaction kinetics, mass and energy balances, phase and chemical equilibrium are implemented in order to predict the process behaviour. The flowsheet is commonly solved in Sequential Modular (SM) mode. The outlet stream of each block is used as an inlet stream for the next block. If recycles are present, tear streams and process loops are identified, which are solved in an iterative manner. Therefore, for very complex flowsheets, as the case of the capture unit, the equation-oriented mode (EO) is more suitable. It solves all model equations simultaneously avoiding iterations and is computationally very efficient. Furthermore, in EO mode process optimizations can be performed. This functionality was used to optimize the overall capture unit. The drawback of the EO strategy is the complexity of the model development, because very good estimates for all the variables have to be given before solving the flowsheet [25]. This made the process development of the capture unit particularly difficult, since the model is very complex and has umpteen tear streams.

Aspen Plus also offers an integrated economic analyzer (Aspen Process Economic Analyzer), which can evaluate capital and operating costs. This enables the comparison of different process from an economic point of view. The cost estimation is performed after the flowsheet has

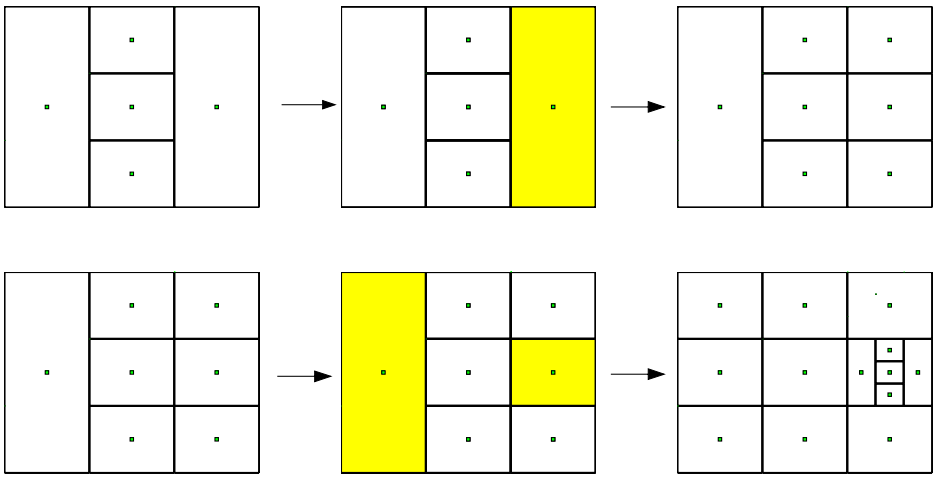

Figure 3-1: First two iterations of the DIRECT code on an objective function of two variables [26].

been solved, hence the cost estimation cannot be chosen as objective function for a process optimization.

Matlab For complex process optimization problems (e.g., large number of decision variables), the gradient-based internal optimization routine of Aspen has troubles to determine the solution. For these optimization cases, Aspen was interfaced with Matlab via a local COM Automation server. In Matlab an open-source optimization code, called Direct.m, was used in order to perform the optimization. This code was written by Dan Finkel and is described in his report from 2003 [26]. The code suits for for global optimization problems with bound constraints, were the objective function is the output of a simulation. The name 'DIRECT' comes from 'DIviding RECTangels' since the domain is divided into rectangles. In fact, the optimization algorithm initially transforms the domain of the objective function into a unit hyper-cube; namely,

$$\overline{\Omega} = x \in R^N : 0 \leq x_i \leq 1 \tag{3-1}$$

where $\overline{\Omega}$ represents the domain, R the set of real numbers and N the number of independent variables. Then, the hyper-cube is divided into more hyper-rectangles. The function is evaluated in the center of the hyper-cube and in each center of the hyper-rectangles. From the function evaluations potentially optimal hyper-rectangles are determined and further divided into smaller hyper-rectangles. The function is again evaluated in every hyper-rectangle and the procedure is repeated. Hereby, in every iteration the location of the optimum is restricted to a smaller fraction of the entire domain. The algorithm stops iterating, when the maximum number of iterations specified by the user is reached. An intuitive representation of how the code works is given in Figure 3-1. The two rows represent the first two iterations of the DIRECT code on a simple function of two variables. The column on the left shows the hyper-rectangles of the first iteration. The green dots show where the function is evaluated. From the first to the second column the potentially optimal hyper-rectangles are identified. In the figure, these optimal rectangles are highlighted in yellow. The optimal hyper rectangles are

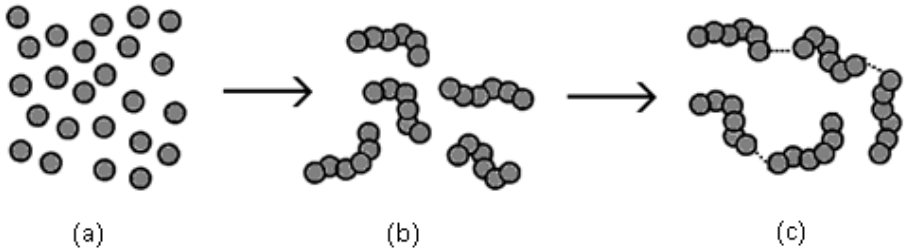

Figure 3-2: Components of the residual Helmholtz energy for SAFT EoS: (a): spherical segments; (b): molecule chains; (c): hydrogen bonding between chains [29].

then divided further, as shown in the third column. For a more detailed description the paper in Ref. [26] is recommended.

3-2 Perturbed Chain Statistical Associating Fluid theory (PC-SAFT) EoS

In order to model the capture plant, a sufficiently accurate estimation of the thermodynamic and transport properties of the substances involved is required. Especially a precise prediction of vapour/gas-liquid equilibria (VLE) is necessary. The fluid mixtures involved in the capture process are modeled with the Perturbed Chain Statistical Associating Fluid Theory (PC-SAFT) EoS. For its strong physical background it has the advantage to be robust, accurate and extrapolative [27]. The theory was developed by Gross and Sadowski and relies on the first order perturbation theory of Wertheim [28]. The PC-SAFT EoS is based on the calculation of the residual Helmholtz free energy (Helmholtz free energy minus the Helmholtz free energy of an ideal gas at the same temperature and pressure [28]) caused by different types of interaction between the molecules. Ilke Senol explained in his report of 2011 [29] the three considered contributes for the calculation of the residual Helmholtz free energy Figure 3-2, which are:

$$a_{res} = a_{seg} + a_{chain} + a_{assoc} \tag{3-2}$$

where a_{seg} is the Helmholtz energy of the equal-sized spherical segments, a_{chain} adds the energy of the molecule chain formation, and finally a_{assoc} represents the association energy by hydrogen bondings. In statistical dynamics, the Helmholtz free energy is often used to express EoS, since most thermochemical properties can be obtained by differentiation of the Helmholtz free energy. In order to calculate all the contributes of a_{res}, five parameters have to be estimated for each chemical component in consideration:

- two geometric parameters to describe the number of molecule segments (m) and their diameter (σ) ,
- three energy related parameters which indicate the dispersive interaction between segments (ϵ_i), the association energy between sites ($\epsilon^{A_iB_i}$) and the association volume ($\kappa^{A_iB_i}$).

To extend the EoS to mixtures, another parameter, called k_{ij}, has to be added for every possible binary pair of chemical components. This binary interaction parameter is necessary for the application of appropriate mixing and combining rules. In the PC-SAFT EoS the Wolbach and Sandler mixing rules shown in Eq. (3-3) and Eq. (3-4) were adopted:

$$\epsilon^{A_iB_j} = 0.5 \cdot (\epsilon^{A_iB_i} + \epsilon^{A_jB_j}) \tag{3-3}$$

$$\kappa^{A_iB_j} = \sqrt{\kappa^{A_iB_i} \cdot \kappa^{A_jB_j}} \left(\frac{\sqrt{\sigma_{ii} \cdot \sigma_{jj}}}{0.5(\sigma_{ii} + \sigma_{jj})} \right)^3 \tag{3-4}$$

All the aforementioned parameters were fitted with published and confidential VLE data from experiments. The data was provided by Clariant, which produces the DEPG-type solvent used in this work. Finally, the model was validated with the data from the Buggenum pilot plant.

The development of the PC-SAFT EoS is documented in Ref. [30]. Additional information about the PC-SAFT theory can be found in literature [28, 29, 31].

3-3 Model assumptions and development

Various models were developed in Aspen Plus Version 7.3. One is the steady-state model of the absorption and CO_2 compression section (AC model). This model was used in order to find out which is the more optimal configuration between the chilled and the unchilled absorption section. A second model comprises the entire capture unit and was used to answer the second research question. For both models the chilled and the unchilled configuration were developed. Another model was developed to simulate the H_2S absorption section when no CO_2 is captured. It was used together with the AC model during the analysis of the third research question. The modeling assumptions and simplifications are discussed in the following subsections. The last subsection contains information on the implementation of constraints in Aspen and on how the convergence of the models was achieved.

For all models, the Untreated Syngas feed stream to the H_2S Absorber was determined from previous studies within the same research work on the Magnum IGCC power plant. The stream composition, mass flow, temperature and pressure are summarized in Table 3-1. In addition to the chemical components reported in Table 3-1, also various other components could be present in minor fractions , e.g., NO_2, NO, S, SO_2, SO_3, Cl_2, HCl, CH_4, NH_3 and HCN [32], but were neglected for simplicity.

3-3-1 Absorption and CO_2 compression section model

In this subsection the model which comprises the absorption section and the CO_2 compression section will be described. This model does not contain the shifting section. Although the shifting section has an influence on the absorption section, it was assumed that a focus on

Table 3-1: Untreated Syngas feed stream to the capture unit

	Untreated Syngas
Temperature [°C]	40
Pressure [bar]	36
Mass flow [kg/s]	71.22
Composition [mol/mol]	
H_2O	0.003
CO_2	0.053
H_2S	0.003
COS	5 ppm
H_2	0.290
CO	0.565
N_2	0.085
Ar	900 ppm

the AC section is sufficient to answer the first and third research question. The idea is to fix the inlet streams to the absorption section, even if not all effects of the shifting section on the AC section can be neglected. The simplification shown in Figure 3-3 was made. The actual WGS section (see figure Figure 3-3 (a)) was split into an hypothetical sulphur-free water gas shift section and an hypothetical COS to H_2S Reactor (see figure Figure 3-3 (b)). The Unshifted Syngas coming from the H_2S Absorber was split into a Sulphur Free Unshifted Syngas stream and a stream containing the entire COS and H_2S. The Sulphur Free Unshifted Syngas was sent to the hypothetical sulphur free WGS section. The outlet stream of this unit was estimated by simulations for approximately 90 % of CO conversion for safe operating conditions for a fresh catalyst. The results are reported in Table 3-2. This stream was kept constant in the AC model, based on the assumption that the COS and H_2S would have a minor influence on the performance of the shift reactors. This hypothesis is valid, because the COS and H_2S content was varied only in a really small range (around 10 ppm of total sulphur content) and therefore the influences of a slightly varying COS and H_2S content on the shift reactors is negligible. The COS and H_2S were considered separately from the rest of the Unshifted Syngas, because one of the constraints is the maximum limit of sulphur content in the CO_2 Product stream. The sulphur content in the CO_2 Product stream depends mainly on: the sulphur content in the Lean Solvent downstream the H_2S Stripper, the pressure in the CO_2 Flash Drums, the slip of sulphur in the H_2S Absorber which passes the shifting section and is fed to the CO_2 Absorber, and if the sulphur in the Shifted Syngas is present as COS or H_2S. Hence, the influence of the shifting section on the sulphur content in the CO_2 Product stream cannot be neglected and the H_2S and COS cannot be kept constant in the Shifted Syngas stream. Furthermore, the reaction of sulphur from COS to H_2S in the shifting section has to be taken into account, because the absorption of sulphur in the CO_2 Absorber depends strongly on it. The solubility of hydrogen sulfide in DEPG is almost four times higher compared to the solubility of carbonyl sulfide [33]. The chemical reaction from COS to H_2S which takes place in the shift reactors is called COS hydrolysis [32] and is shown

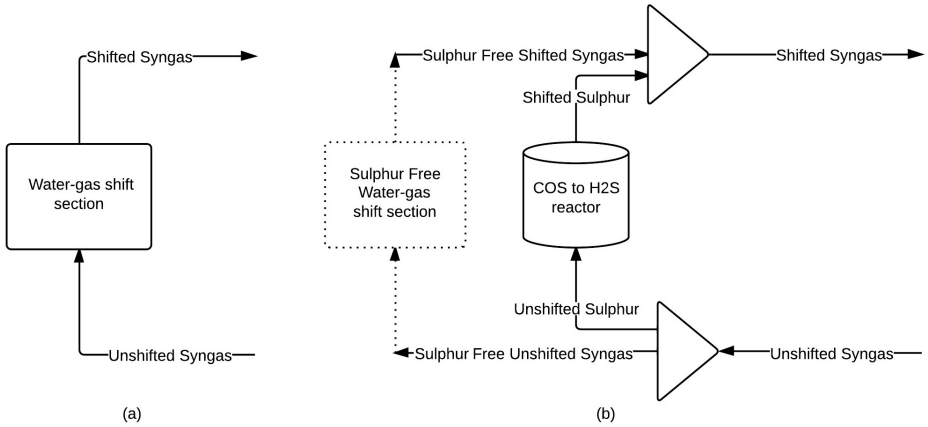

Figure 3-3: Process flow diagram of the real water-gas shift section (a) and process flow diagram of the simplified water-gas shift section for the AC model (b)

in the following equation:

$$COS + H_2O \rightleftharpoons CO_2 + H_2S \tag{3-5}$$

This reaction reaches equilibrium in the shift reactors and for simplicity it was assumed that 100% conversion is achieved. A stoichiometric reactor (RStoic) was used in Aspen Plus to simulate the COS hydrolysis taking place in the shift reactors (RStoic models reactions with a known reaction extent (conversion) [32]).

In the following two paragraphs the modeling process of both the absorption and CO_2 compression section of the AC model are described in more detail. The differences between the chilled and the unchilled absorption section are pointed out.

Absorption section The main components of the absorption section are the two absorption columns and the H_2S Stripper. These columns were modeled with the RadFrac model. The equilibrium based calculation mode was used. It does not require the specification of the diameter, height and type of packing of the column. For a more precise simulation, the rate-based calculation mode should be used. It is more accurate and simulates actual tray and packed columns, instead of idealized representations. It treats separations as as mass and heat transfer problems, rather than equilibrium processes [25]. However, the computational effort for a rate-based simulation is much higher, which makes this mode infeasible for the optimizations analyzed in this thesis. Furthermore, the column must already be designed when switching to the rate-base mode. In fact, AspenTech recommends designing the column in equilibrium-based mode, before running a rate-based calculation [25]. The switch to the rate-based calculation could represent an extension of the work done in this thesis.

For the CO_2 and H_2S Absorber, in addition to the number of equilibrium stages, only the pressure at the top of the column, the pressure drop and the feed stage number were specified (the feed stage number represents the stage at which the feed enters the column). No condenser and no reboiler were included in the RadFrac to model the absorber columns. Pressure drops in the columns were neglected. The H_2S Stripper is very similar to the above described

Table 3-2: Sulphur Free Shifted Syngas stream; for the H_2S and COS content see Shifted Sulphur stream

	Sulphur Free Shifted Syngas
Temperature [°C]	35
Pressure [bar]	36.5
Mass-flow [kg/s]	107.69
Composition [mol/mol]	
H_2O	0.002
CO_2	0.376
H_2S	/
COS	/
H_2	0.530
CO	0.035
N_2	0.056
Ar	593 ppm

absorbers. The only difference is that the bottom stage was represented by a reboiler with a specified heat duty. For this column a pressure drop of 0.2 bar was included. It was estimated in a previous analysis of Nuon [21]. The reason why the pressure drop in the absorber columns was neglected, but considered in the stripper, is that the operating pressure is notably different. The pressure in the stripper is around 2 bar, while the absorbers work at about 35 bar. Thus, the pressure drop in the stripper has a much higher influence. Its affect on the desorption process cannot be neglected.

The desorption of the CO_2 in the three CO_2 Flash Drums was modeled with two-outlet flash vessels. The pressure of the three vessels starting from the one at the highest pressure is around 16 bar, 5 bar and 1 bar, respectively. Note that these pressures were optimized in the later described optimization (see Sec. 3-7-1).

All the considered coolers are water coolers and have an outlet temperature of the hot stream of 35°C. A pressure drop of 0.3 bar for each cooler was considered. For the two solvent chillers of the chilled absorption section a pressure drop of 0.5 bar and a minimum outlet temperature of 4°C was used. Lower outlet temperatures were not considered, since otherwise the water in the solvent could crystallize to ice and damage the capture unit.
Table 3-3 shows a summary of the Aspen components used to model the main components of the absorption section. In the third column the most important input specification are given. The differences between the ATC (unchilled) and the BATC (chilled) are pointed out in Table 3-4.

CO_2 compression section The CO_2 compression section was modeled with the following Aspen Plus components: compressor, two-outlet flash vessel and cooler. The chosen compression ratio (β) for each stage is discussed in Sec. 3-7-1. Each stage is intercooled to 35°C

Table 3-3: Overview of component models and model parameters used for the absorption section model

Component	Aspen Plus model	Model parameters
CO_2 Absorber	RadFrac	Δp = 0 bar; p_{top} = 34.8 bar; $N°_{eq\_stages}$ = 13
H_2S Absorber	RadFrac	Δp = 0 bar; p_{top} = 35.4 bar; $N°_{eq\_stages}$ = 10
H_2S Stripper	RadFrac with reboiler	Δp = 0.2 bar; p_{top} = 1.8 bar; $N°_{eq\_stages}$ = 6; $\dot{Q}_{reboiler}$ = 6.5 MW
HP CO_2 Flash Drum	Two-outlet flash	p = 16 bar; $\dot{Q}$ = 0 W
MP CO_2 Flash Drum	Two-outlet flash	p = 5 bar; $\dot{Q}$ = 0 W
LP CO_2 Flash Drum	Two-outlet flash	p = 1.3 bar; $\dot{Q}$ = 0 W
Rich Solvent Flash Drum	Two-outlet flash	p = 10.5 bar; $\dot{Q}$ = 0 W

Table 3-4: Component models and model parameters for the ATC and BATC Aspen Plus model

Component (Aspen Plus model)	ATC: model parameters	BATC: model parameters
Lean Solvent Cooler/Chiller (Heater)	T_{out} = 35 °C; Δ p = 0.3 bar	T_{out} = 4 °C; Δ p = 0.5 bar
Semi-Lean Solvent Cooler/Chiller (Heater)	T_{out} = 35 °C; Δ p = 0.3 bar	T_{out} = 4 °C; Δ p = 0.5 bar
Heat Ex. 6 (Two-stream heat exchanger)	ΔT_{app} = 10 °C; Δ p = 0.5 bar	/
Heat Ex. 7 (Two-stream heat exchanger)	ΔT_{app} = 15 °C; Δ p = 0.5 bar	/

with a water-cooler. A pressure drop of 0.3 bar was used for each cooler. The outlet of the CO_2 compression section is fed to the transport pipelines in a critical state. This means that the temperature and pressure at the outlet are above the critical point of CO_2 (p_{cr} = 73.77 bar; T_{cr} = 30.98°C). The outlet stream of the last CO_2 compressor is cooled down to 40°C, which is the inlet temperature to the pipelines suggested by Kaufmann [11]. The outlet pressure of the CO_2 compression section is maintained at 110 bar, a typical pressure used in various studies, e.g. from the Newcastle University, UK [34].

3-3-2 Capture unit model

This model comprises the entire capture unit. The absorption section and CO_2 compression section are identical to the ones in the AC model, except of the simplification shown in Figure 3-3, which can be omitted. To complete the model only the shifting section is added. The next paragraph describes accurately the modeling of this section.

Shifting section The main components of the shifting section are the three water-gas shift reactors. The reactors were modeled as Gibbs reactors, called RGibbs in Aspen Plus. This kind of reactor does not require reaction stoichiometry and does not take into account the kinetics of the reaction. It calculates the chemical equilibrium minimizing the Gibbs free energy [25]. As possible products of the reaction CO, H_2, CO_2, H_2O, COS and H_2S were specified. N_2 and Ar were considered as inerts. To take into account that the chemical equilibrium will not be reached within the reactor, an approached temperature to equilibrium (ATE) of 10°C and 20°C, depending on the age of the catalyst, was used (for more detailed information see Sec. 3-7-2). A pressure drop of 0.4 bar for each reactor was considered. No catalyst has to be specified for the RGibbs. Instead, in a real reactor the type of catalyst influences significantly the performance, e.g., it influences the range of allowed operating temperatures. For the capture unit of the Magnum plant a sweet shift catalyst was used. The operating temperature of a typical sweet shift reactor suggested by Carbo is in between 350°C and 500°C [17]. Some estimations performed by Nuon showed that for the specific catalyst in consideration for the Magnum plant the maximum operating temperature of the reactors can be augmented to 520°C in respect to the operating conditions suggested by Carbo [21]. The lower limit of the operating temperature within the reactor depends on the catalyst activity and the reaction equilibrium and rate. As described in Subsection 3-7-2 different minimum inlet temperatures are compared in this thesis in order to point out the influence on the energy consumption.

Since the operating temperature of the WGS reactors is much higher than of the upstream H_2S Absorber and the downstream CO_2 Absorber, an effective heat exchanger train for the reactor feed/effluent streams can save steam in the Steam Heat Exchangers. For the heat exchangers in the shifting section a minimum pinch point temperature difference of 10 K was specified. The Heat Ex. 4 was treated differently, because its aim is to control the inlet temperatures for the first and third WGS reactor. For the Heat Ex. 1 and 3 the mentioned ΔT_{pinch} of 10 K was specified as temperature difference between the hot inlet and the cold outlet stream. This simplification was necessary, because in Aspen Plus it is not possible to specify a minimum ΔT_{pinch} within a heat exchanger. The same simplification cannot be made for the Heat Ex. 2. For this heat exchanger the pinch point is not at the inlet or outlet. The

Table 3-5: Overview of component models and model parameters used for the shifting section Aspen Plus model, based on CB&I Lummus

Component	Aspen Plus model	Model parameters
Booster compressor	Isoentropic compressor	Δp = 6.3 bar; $\eta_{iso} = 0.72$
Feed Splitting Vessel	Two-outlet Flash	Δp = 0 bar; $\dot{Q}$= 0 Watt
Shift Reactor	Gibbs Reactor	Δp = 0.4 bar; $\dot{Q}$= 0 W; ATE = 10/20°C; the possible products and inerts are specified
Rectifier	RadFrac	p_{top} = 35.8 bar; Δp = 0 bar
Rectifier Cooler	Heater	T_{out} = 35°C; Δp = 0.3 bar

reason is that the hot stream enters the heat exchanger as superheated vapor and is cooled down till it is partially condensed. The pinch point is situated where phase change starts. To solve this problem, the Heat Ex. 2 was split into two separate heat exchangers. One heat exchanger cools down the hot stream till saturated vapor ($x_{vap} = 1$), while the second heat exchanger is controlled by a ΔT of 10 K between the hot stream dew point and the cold stream outlet. For confirmation, after each simulation the heat exchange curves in the TQ diagram have been controlled in order to check if there are no points where a smaller ΔT than 10 K was reached - i.e., if the inlet/outlet is really the point of the heat exchanger with the lowest temperature difference.

During the development of the shifting section model, particular attention has been paid to the solvent slip in the H_2S Absorber column. Some simulations showed that the DEPG influences significantly the heat exchange properties of the syngas in the Aspen Plus model. Therefore, a component separator (called Sep in Aspen Plus) was used downstream the H_2S Absorber. It makes sure that the entrained DEPG is separated from the main syngas stream, to guarantee that no solvent enters the shifting section. Otherwise, the heat exchangers in the shifting section would not work properly. Separate the solvent is an approximation of reality; but the solvent content in the Unshifted Syngas is small (< 0.001 kg/hr), and would therefore have only a limited impact on the performance of the capture unit.
Table 3-5 shows a summary of the Aspen models used to model the main components of the shifting section. In the third column the most important model parameters are given.

A constant pressure drop of 0.3 bar for the coolers, 0.4 bar for the WGS reactors and 0.5 bar for the heat exchanger was specified.

3-3-3 Capture unit model without CO_2 capture

This model was developed to simulate the performance of the H_2S absorption section when no CO_2 is captured and is shown in Figure 3-4. The shifting and CO_2 absorption section are by-passed from the syngas. The Untreated Syngas passes through the H_2S Absorber and is then routed to the gas turbines. The configuration of the absorption section was adapted in

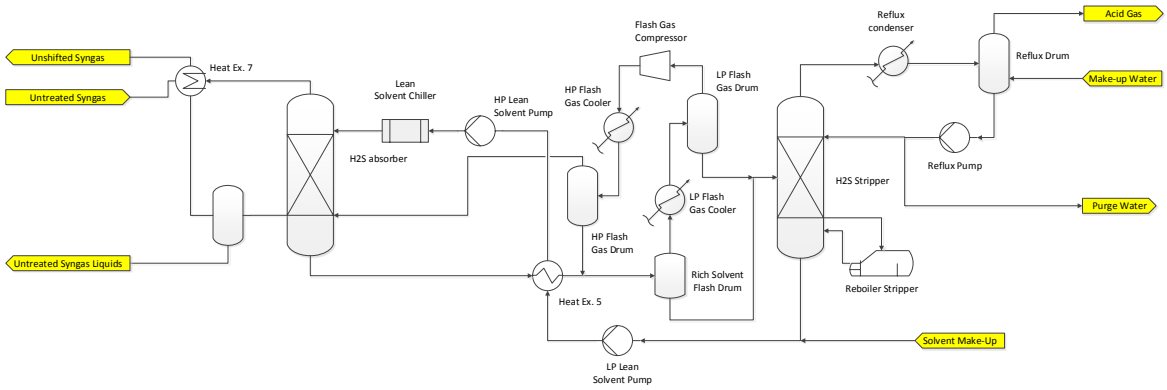

Figure 3-4: Capture unit model without CO_2 capture: used to simulate the H_2S absorption section when no CO_2 is captured.

the model, because in the reference configuration described in Chapter 2 the two absorption sections are integrated into each other. When no CO_2 is captured, no solvent circulates in the CO_2 absorption section, and hence no Semi-Lean Solvent flow would enter the H_2S Absorber. Therefore, the solvent downstream the Lean Solvent Chiller is directly routed to the H_2S Absorber. Except this, the model is equal to the chilled H_2S absorption section of the two above described models.

3-3-4 Convergence, Design specifications, Calculator blocks, Specification groups

The steady-state Aspen Plus models were first developed in SM mode including various design specifications ('design spec') and calculator blocks. Once good guesses for each stream were available, the switch to EO mode was done. The computational effort in SM mode would have been a major obstacle for the optimizations.

In SM mode, Design Specifications were used to respect the constraints of the optimization problems (for the constraints see Section 3-7). Design specifications set the value of a variable that is normally calculated from Aspen Plus. Hereby, e.g., the permissible amount of an impurity in an output stream (called specification) can be set by varying an input variable (called manipulated variable). This input variable could be, e.g., the purge rate to control the impurity. For a more complex regulation the specification can be a general Fortran expression, including more than one output variable. The drawback is that for every design specification Aspen Plus generates a loop that is solved iteratively. This augments the computational effort [25].

The process contains various recycles which makes model convergence more difficult. It is essential to provide good initial guesses which are close to the solution for the streams which are teared by the solution algorithm (in most cases the recycle streams). A good knowledge of the process has been very important; as well as the performance of several trial runs. Initially the model was divided into several submodels. A detailed analysis of each submodel was performed and the results were used to improve the initial guesses. In some cases the simulation

sequence of the SM mode has been specified manually in order to improve model convergence.

As soon as the model was solved in SM mode, the change to EO mode was done. When a simulation is run in EO mode, instead of design specifications, EO specification groups ('spec groups') are used. They are analogous, except that EO 'spec groups' cannot use a complex Fortran expression as specification. However, the same can be achieved by integrating a calculator block with a 'spec group'. In the calculator block the complex Fortran statement is solved. The result is saved in a newly created variable, which can be used as a specification in an EO 'spec group'. In this way any kind of 'design spec' can be written as a combination of a calculator block and a 'spec group'. For convenience some additional calculator blocks have been developed to simplify the analysis of the results. For example, different calculator blocks have been added to calculate the energy consumption of each section of the capture unit. How the energy consumption was calculated is described in Sec. 3-5.

3-4 Model validation

The two models have been validated with data provided by Nuon. The results show a good agreement with models already developed previously to this work, within the same research project. The largest difference was observed for the H_2S absorption section. In particular, the acid gas stream, which has an approximately 10% higher mass flow than predictions from previous models [21]. No further information can be provided for confidential reasons.

3-5 Power consumption estimation

The power consumption of the different sections of the capture unit was estimated in Aspen Plus. As reference case the IGCC plant without CO_2 capture and with a zero energy consumption for the H_2S absorption section was used. In case of CO_2 capture the power output of the IGCC power plant is reduced due to:

- auxiliary power consumption in the capture unit
- consumption of IP steam in the Steam Heat Exchangers
- consumption of LP steam in the Stripper Reboiler
- loss in syngas LHV due to water-gas shift reaction (the conversion from CO to CO_2 and H_2 reduces the LHV of the syngas)

The power consumption of the capture unit is therefore defined as the total power loss due to these four contributes. When no CO_2 is captured, the power consumption is given by the power consumption of LP steam in the Stripper Reboiler and the auxiliary power consumption of the H_2S removal section. In the following paragraphs the electrical power consumption is represented by $\dot{E}$, and the heat duty by $\dot{Q}$.

Pumps and compressors The electrical power consumption of pumps and compressors is directly estimated by Aspen Plus. Given an outlet pressure specification the program solves a system of linear equations to determine the power requirement, or the outlet pressure given a power specification.

Coolers The electrical power consumption of the water coolers was assumed to be equal to the power consumption of the coolant water circulating pump (note that the cooler is only a heat exchanger and does not consume any electrical power). The cooling duty $\dot{Q}$ is calculated from Aspen and was used as a starting point of the calculation. Known the specific heat for H_2O and assuming a fixed temperature increase of the water in the coolers, the mass flow of the coolant fluid is defined as

$$\dot{m}_{coolant} = \frac{\dot{Q}_{cooler}}{c_{p\_coolant}\Delta T_{coolant}} \tag{3-6}$$

where $c_{p\_coolant} = 4.186\frac{kJ}{kgK}$ and $\Delta T_{coolant} = 10°C$. $\Delta T_{coolant}$ was chosen in order to respect a minimum ΔT_{pinch} of 3-5°C for a feed cooling water at 20-22°C (note that the hot outlet temperature was set to 35°C). The power consumption of the coolant water circulating pump was then estimated from the mass flow of the coolant fluid and the pressure drop the pump has to overcome, which yields

$$\dot{E}_{cooler} = \dot{m}_{coolant} \cdot \frac{\nu_{coolant}\Delta p_{coolant}}{\eta_{pump}} \tag{3-7}$$

where $\Delta p_{coolant} = 2$ bar, $\nu_{coolant} = 1/\rho_{coolant} = 0.001\ m^3/kg$ is the specific volume of water and $\eta_{pump} = 0.7$ is the pump efficiency. The pressure drop is mainly given from pressure losses in the tubes and in the heat exchanger. A pressure drop of 2 bar was used as a first rough estimation. Note that a more accurate estimation of the pressure drop is dispensable, since the power consumption of the coolers has a limited impact on the total power consumption (below 2%). In conclusion, combining the two equations the power consumption for the coolers can be estimated as

$$\dot{E}_{cooler} = \frac{\dot{Q}_{cooler}}{c_{p\_coolant}\Delta T_{coolant}} \cdot \frac{\nu_{coolant}\Delta p_{coolant}}{\eta_{pump}} \tag{3-8}$$

Chillers The chillers were implemented as coolers in Aspen Plus and thus Aspen Plus delivers the necessary cooling duty, but not the electrical power consumption. The electrical power consumption of the chillers was then calculated from the energy efficiency ratio (EER). The EER is the ratio of the cooling capacity to the electrical input of the chiller. The nominal EER ratio depends on the type of machine and is given from the manufacturer for specified nominal conditions. In other conditions the EER can vary significantly, for example if the condensing temperature varies. Furthermore, manufacturers deliver data for standard machines for water or air chilling. Machines for DEPG chilling have to be produced specifically, and therefore no specific data is available. Chillers using water as a secondary fluid were chosen for the capture unit of the Magnum plant. In a first approximation they were compared to water-water chillers. The $EER_{nominal}$ for water-water chillers of about the same chilling duty have an EER of 4 or higher [35]. For the DEPG chillers a more conservative value of 3.5 was chosen

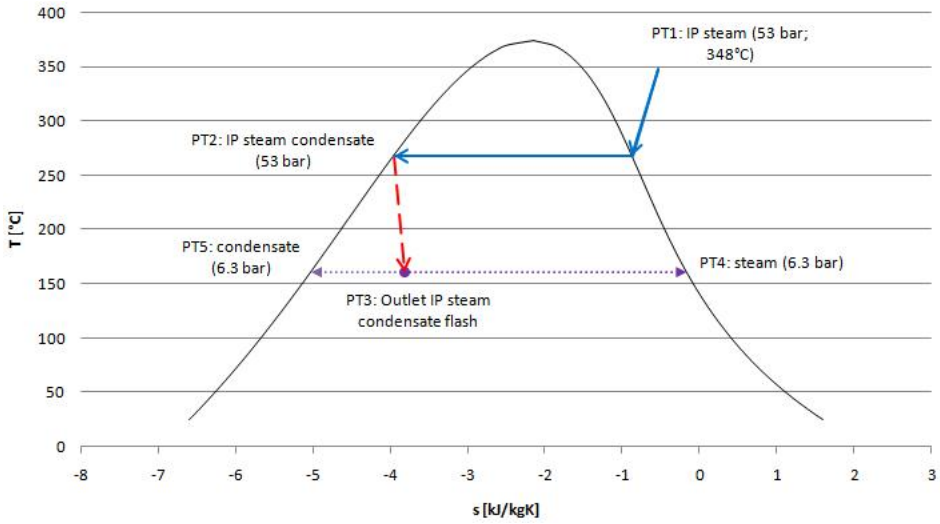

Figure 3-5: IP steam cooled down in the Steam Heat Exchangers (bold line), IP steam condensate flashed down to 6.3 bar (dash line) and vapor/liquid separation in the flash vessel (dotted line)

for the following reasons: firstly, the chiller is not always working at reference conditions; secondly, the chillers of the capture unit are not water-water machines, which could influence negatively the performance; finally, to take into account the power consumption of the cooling water pump, which is not included in the EER.
The power consumption of the chillers can then be estimated by:

$$\dot{E}_{chiller} = \frac{\dot{Q}_{chiller}}{EER} \tag{3-9}$$

LHV loss The power consumption due to the LHV loss in the Magnum IGCC power plant was estimated from Nuon previously to this work. Considering the LHV flow rate entering ($\dot{H}_{in\_WGS}$) and exiting ($\dot{H}_{out\_WGS}$) the shifting section unit, the LHV power loss can be expressed as

$$\dot{E}_{LHV} = (\dot{H}_{in\_WGS} - \dot{H}_{out\_WGS}) \cdot f_{LHV} \tag{3-10}$$

where $f_{LHV} = 0.575$ MW/MW is the estimated LHV power loss factor from Nuon. For the LHV flow rate, only the LHV values of H_2 and CO were taken into account, because the mass flow of the only other burnable components COS and H_2S is neglectable (remember that the total sulphur mole fraction in the shifting section was set to below 10 ppm (dry)). With this simplification the LHV flow rate was calculated as

$$\dot{H} = \dot{m}_{CO} LHV_{CO} + \dot{m}_{H_2} LHV_{H_2} \tag{3-11}$$

where $LHV_{CO} = 10.16\ MJ/kg$ and $LHV_{H_2} = 120.09\ MJ/kg$ are taken from Ref. [36] at approximately 15.6°C.

IP steam loss The water vapor used in the Steam Heat Ex. of the shifting section (called intermediate pressure (IP) is withdrawn at a pressure of 53 bar and a temperature of 348°C

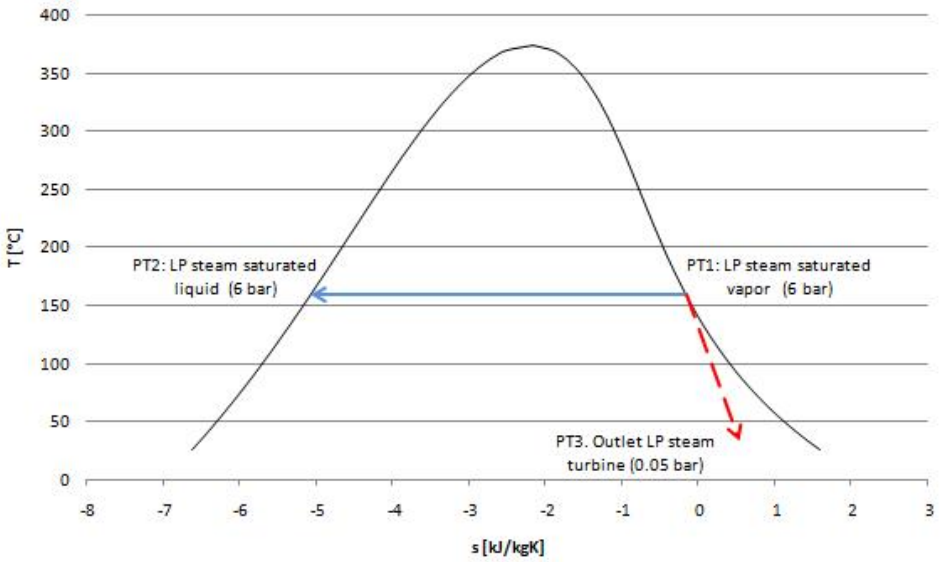

Figure 3-6: LP steam cooled down in the Solvent Reboiler (solid line) and LP steam expanded in LP steam turbine (dash line)

from the gasification island. Consequently, the flow rate of IP steam from the gasification island to the HRSG decreases and less steam is expanded in the steam turbine. Therefore, the steam power consumption is a virtual loss due to the unused steam for expansion in the steam turbine. The magnitude of this loss was estimated by Nuon. The following equation was proposed [21]:

$$\dot{E}_{IP\_steam} = \dot{Q}_{SteamHeatEx.} \cdot f_{IP\_steam} \tag{3-12}$$

where $\dot{Q}_{SteamHeatEx.}$ is the heat duty for the Steam Heat Ex. and $f_{IP\_steam} = 0.41453$ MW/MW is the power loss factor. Eq. (3-12) expresses the power loss as a function of $\dot{Q}_{SteamHeatEx.}$. This is of practical use in Aspen Plus, since a simple heater instead of a heat exchanger can be used to simulate the Steam Heat Exchangers - i.e., the mass flow of IP steam is not calculated. For the calculation of the conversion factor f_{steam} it was assumed that the IP is condensed without pressure losses to saturated liquid. Then it is flashed to 6.3 bar in order to produce steam which can be expanded in the LP steam turbine (the LP steam at the inlet of the steam turbine is at 6 bar). Figure 3-5 shows this process.

LP steam loss The lost power due to the steam consumption in the Solvent Reboiler was estimated assuming that saturated vapor at 6 bar (LP steam) is used to heat up the solvent in the reboiler of the H_2S Stripper [21]. The steam is withdrawn at the inlet of the LP steam turbine. Hence, less steam is expanded in the steam turbines, which causes a power loss. In the reboiler the LP steam is cooled down to saturated liquid. The temperature of this stream is about 159°C and some heat could be recovered to preheat other streams, e.g., the syngas in the shifting section. This is not considered in the present work.

FluidProp was used to estimate the thermodynamic properties of water (FluidProp is a software developed by the Delft University of Technology to calculate thermodynamic and transport properties for a series of fluids and mixtures [37]). Two steps were considered to calculate

the power loss (see Figure 3-6). First, the flow rate of steam to the Solvent Reboiler was estimated as

$$\dot{m}_{LP\_steam\_reboiler} = \frac{\dot{Q}_{Reboiler}}{\Delta h_{lv}(p = 6\ bar)} = \frac{\dot{Q}_{Reboiler}}{h_1 - h_2} \tag{3-13}$$

where $\Delta h_{lv}(6\ bar) = 2{,}116.87$ kJ/kg was calculated with FluidProp. The solid line in Figure 3-6 shows the condensation process of the LP steam. In a second step, the power loss connected to the $\dot{m}_{LP\_steam\_reboiler}$ was calculated. It was assumed that this flow rate of LP steam would be expanded in the LP steam turbine when no CO_2 is captured (see dash line Figure 3-6). The specific work produced from this expansion was estimated for an isoentropic turbine efficiency of 70% and a condensing pressure of 0.05 bar; this results in

$$\Delta h_{LP\_steam\_turbine} = [h_{sv}(p = 6bar) - h_{is}(p = 0.05\ bar)] \cdot \eta_{is} = h_1 - h_3 \tag{3-14}$$

Combining Eq. (3-13) and Eq. (3-14) the power loss due to the LP steam consumption in the reboiler can be expressed as

$$\dot{E}_{LP\_steam} = \frac{\dot{Q}_{Reboiler}}{h_1 - h_2} \cdot (h_1 - h_3) \tag{3-15}$$

In analogy to the power consumption of the IP steam, the power loss factor of the LP steam can be calculated from Eq. (3-15) and is equal to 0.233. This means that 0.233 MW of electrical power are lost for each 1 MW of reboiler duty.

For some of the performed optimizations, the total power consumption of the capture unit was divided into 5 major consumption sections: CO_2 absorption section, H_2S absorption section, CO_2 compression section, shifting section and LHV loss. The LHV loss is mainly attributable to the shifting section, nevertheless it was considered as a single virtual section in order to point out its contribution. The power consumption of the shifting section includes the power consumption of the Booster Compressor, the Rectifier Cooler, the two Steam Heat Exchangers and the three pumps of the unit. The power consumption of the CO_2 compression section comprises the power requirement of the five CO_2 compressors and the respective CO_2 coolers. For the absorption section no unique choice can be made on how the power consumption is split between the CO_2 absorption section and the H_2S absorption section. The dubious components are the Lean Solvent Pumps, the Semi-Lean Solvent Pump, the Lean Solvent Chiller and the Semi-Lean Solvent Chiller. It was decided to attribute the power consumption of the LP and HP Lean Solvent Pump to the H_2S removal unit. The power consumption of the Semi-Lean Solvent Chiller and the Semi-Lean Solvent Pump was attributed to the CO_2 removal unit. Instead, the power consumption of the Lean Solvent Chiller (LSC) was divided, based on the solvent inlet temperature of the H_2S Absorber (SA) and CO_2 Absorber (CA):

$$\dot{E}_{LSC \rightarrow H2S\_abs} = \dot{E}_{LSC} \cdot \frac{T_{in\_LSC} - T_{in\_SA}}{T_{in\_LSC} - T_{out\_LSC}} \tag{3-16}$$

$$\dot{E}_{LSC \rightarrow CO2\_abs} = \dot{E}_{LSC} \cdot \frac{T_{in\_SA} - T_{out\_LSC}}{T_{in\_LSC} - T_{out\_LSC}} \tag{3-17}$$

With this approach the power consumption of the H_2S removal unit is calculated approximately as if there would not be any CO_2 removal unit.

3-6 Investment cost

For the comparison of the chilled and unchilled design of the absorption section also the investment costs were compared. An equipment cost estimation and a Net Present Value (NPV) calculation were performed for the AC model.
The investment cost estimation was performed using the Aspen Economic Analyzer Version 7.3. The software was used to estimate the equipment cost of the process units. The bare equipment cost for each process unit was considered; not the total direct cost, which includes all material and labor costs connected with the unit [38]. Other CAPital EXpenditure (CAPEX) costs, as the initial investment for the solvent, were not taken into account. The cost calculations were performed following the Aspen Process Economic Analyzer V 7.0 user guide [38]. The 'European Metric' Template from Aspen Plus was used. The start of the basic engineering was set together with the plant startup to the 01.01.2014. For all the components, except of the chillers, the cost functions provided directly from Aspen Plus were used. For the absorber columns and the stripper the cost functions for packed towers were used (note that the Economic Analyzer uses trayed columns as default). Cost functions for water coolers are not implemented in the Aspen Process Economic Analyzer. In a first approximation the cost was calculated for air coolers. Therefore, the equipment costs of the water coolers were overestimated; but this overestimation was in part compensated, because the equipment cost for the water circulating pumps was not taken into account. Furthermore, the equipment cost of all the coolers together is below 3% of the total equipment cost of the AC section (see Chapter 4), and therefore the overestimation of the cooler costs will not significantly affect the comparison between the two absorption section configurations. The cost of the chillers was not estimated with the Aspen Economic Analyzer. The chillers were simulated with simple coolers, and therefore the Aspen Process Economic Analyzer would have evaluated the wrong costs. A cost of 125 € for each kW of chilling duty was considered. This estimation was done based on data from the Florida Power & Light Company [39] and Aermec S.p.A. [35].

The calculation of the NPV was limited to the AC section. Only the equipment cost and the cost of the consumed energy (see Sec. 3-5) were considered. The following assumptions were made:

- life cycle of 30 years (typical for IGCC plants) [40]
- 6,000 equivalent hours per year (typical for IGCC plants) [41]
- price for consumed electricity in the capture unit: 0.06 €/kWh
- interest rate = 5.5%
- inflation rate = 2.5 %
- investment is considered as overnight cost
- straight-line depreciation over 10 years for a residual asset value of 0€

3-7 Process analysis and optimization

The design and optimization of the capture unit is based on steady-state simulations in Aspen Plus. All the necessary mass and energy balances are directly solved within the program. The process analysis and optimization for each research question will be analyzed in the following three subsections.

3-7-1 Comparison between the ATC and the BATC

The first of the three research questions focuses on the comparison between the chilled and the unchilled absorption section configuration. As described in Sec. 3-3-1 an AC model for each of the two configurations was developed. The advantage of the chilled configuration is that the absorption process is favoured at lower temperatures; therefore, a lower solvent mass flow is necessary to achieve the same CO_2 recovery efficiency. The energy consumption of all major auxiliaries of the absorption section decreases. Furthermore, also the equipment costs decrease, because the equipment size is proportional to the circulating mass flow. Despite the advantages of the chilled configuration, it cannot be concluded a priori that it is the more favourable configuration. In fact, the equipment cost of the chillers is significantly higher than the cost of simple coolers, and the energy consumption for chilling is much higher than for cooling.

Given these facts, the comparison of the two configurations has to consider the energy consumption and the equipment cost. Given the two objectives, a multi-objective optimization could be used. A range of non-dominated solutions which form the so called Pareto-front could be found. These would represent the best solutions for both objectives. Nevertheless, for the comparison in this thesis a simpler approach was used. Both configurations were optimized by using a single-objective optimization based on the energy consumption of the absorption and CO_2 compression section. Various decision variables were included in the optimization. Initially the same number of equilibrium stages in the absorber and stripper columns were used: 13 for the CO_2 Absorber, 10 for the H_2S Absorber and 6 for the H_2S Stripper. Then, the optimization was repeated for different choices of equilibrium stages in the absorber and stripper columns, in order to guarantee an equal comparison between the two configurations. In fact, the ideal number of equilibrium stages could vary between the two configurations and is a trade-off between CAPEX ('CAPital EXpenditure') and OPEX ('OPerational EXpenditure') costs. A higher number of equilibrium stages augments the equipment cost of the towers, but the solvent flow rate can be reduced and the energy consumption together with the equipment cost of the rest of the unit decrease. Given the results of the energy based optimization, the total equipment cost of all the optimized designs was evaluated. The designs were compared for energy consumption and equipment cost. This simpler approach, compared to a multi-objective optimization, was chosen because some preliminary analyses showed that the total investment cost of the AC section is small in respect to the overall life cycle costs of the consumed energy (for detailed results see Chapter 4). Therefore, as the overall objective is to maximize the NPV (Net Present Value) a multi-objective optimization would not bring significant advantages compared to a single-objective optimization based on the energy consumption [42].

For the optimization the DIRECT algorithm described in Sec. 3-1 was used. The following decision variables were included in the optimization:

- pressure of the MP CO_2 Flash Drum
- pressure of the LP CO_2 Flash Drum
- pressure of the H_2S Stripper
- pressure of the Rich Solvent Flash Drum
- H_2S Stripper Reboiler boil-up ratio
- water content in the solvent
- outlet temperature chillers
- flow rate Semi-Lean Solvent stream
- flow rate Lean Solvent stream

The pressure of the high pressure (HP) CO_2 Flash Drum was not included in the optimization. This pressure influences the amount of CO and H_2 which is recycled back to the CO_2 Absorber. If the pressure increases, less CO and H_2 are recycled and the LHV flow rate of the syngas decreases. Less electrical power is produced by the combined cycle. More CO and H_2 end up in the CO_2 Product stream, where their maximum content is limited [43]. Therefore, for simplicity it was decided to fix the pressure of the HP CO_2 Flash Drum.

For the compression section the following assumptions were made. The outlet pressure of the first compression stage was chosen such that the stream at the outlet of the first CO_2 Cooler was at the same pressure as the MP CO_2 Flash Drum. In the model this is ensured by an EO connection which sets both pressures (outlet first CO_2 Cooler and MP CO_2 Flash Drum) equal. For the other compression stages is was assumed that enthalpy increase (Δh) is kept constant; but considering that in the CO_2 compression section the mass flow is almost constant, keeping the Δh constant corresponds to keep the compression power constant. Accordingly, an equal power consumption for the last four compression stages was assumed. This was achieved by a calculator and a connection block. Note that in Aspen Plus each compression stage is represented by a single compressor.

The following constraints have been respected in the optimization:

- H_2S content in the acid gas stream of 25 mole%
  A minimum H_2S content in the acid gas stream is necessary to ensure a proper operation of the Claus plant [44]. To control the H_2S content in the acid gas stream the pressure in the Rich Solvent Flash Drum was manipulated. If the pressure decreases the H_2S content augments. The drawback is that the pressure ratio of the Flash Gas compressor increases and consequently its energy consumption. Therefore, the minimum energy consumption was expected to be found for exactly 25% and a equality constraint was used.

- maximum solvent temperature in the H_2S Stripper Reboiler of 146°C
  The maximum solvent temperature in the H_2S Stripper Reboiler was chosen in order to respect approximately a ΔT_{pinch} of 13 K between the solvent and the LP steam temperature.
- minimum chiller outlet temperature of 4°C
  A constraint on the minimum outlet temperature of the chillers had to be fixed in order to avoid the water in the solvent to freeze.
- minimum pressure in the H_2S Stripper of 1.8 bar
  The minimum pressure of 1.8 bar is necessary to overcome all the pressure drops of the acid gas stream which is routed to the Claus plant.
- total mole sulphur fraction in the CO_2 Product stream of 10 ppm (dry)
  The limit on the maximum sulphur content in the CO_2 Product stream was set in accordance with Ref. [11] to 10 ppm (dry). To control the sulphur fraction in the CO_2 Product stream, the Lean Solvent mass flow was manipulated. The latter determines the L/G ratio in the H_2S Absorber and is therefore crucial to determine how much H_2S is removed from the syngas. On the other hand, the L/G ratio influences significantly the energy consumption in the H_2S removal unit, and therefore the minimum energy consumption was expected to be found for the lower limit of 10 ppm. The inequality constraint was converted into an equality constraint.
- maximum water content in the solvent of 6 wt% [18]
- fixed CO_2 recovery of 92.5%
  For the comparison of the BATC and ATC a constant CO_2 recovery of 92.5% was chosen, which is in accordance with estimations for the Magnum power plant.

In Aspen Plus the equality constraints were implemented as 'spec groups'. Their use reduces the computational effort compared to the use of inequality constraints, for which the lower or upper variable bound was set in EO mode. A rigorous sensitivity study was performed, before the optimization was executed. The aim was to find out if any inequality constraint can be transformed in an equality constraint or if any independent variable hits its upper or lower bound and can be removed from the set of decision variables.

3-7-2 Overall capture unit optimization

In the first part of the overall capture unit optimization a framework for the optimization was developed. It was analyzed how the power consumption and the most important process variables vary with the CO_2 capture rate. In the second part, different operating conditions of the WGS reactors have been compared.

The main process variables which define the performance of the entire capture unit are the CO conversion of the water-gas shift section and the CO_2 recovery efficiency of the absorption section. There is a trade-off between both variables in order to reach a given total CO_2 capture rate: a defined capture rate can be achieved by a low CO conversion and a high CO_2 recovery or by a high CO conversion and a low CO_2 recovery. Hence, both variables should be

optimized in order to find the optimal combination in terms of overall energy consumption for a given capture rate. The following paragraph describes in detail the optimization framework of the performed capture unit optimization.

For the optimization the chilled absorption section configuration was used, which also turned out to be more optimal than the unchilled design as a result of the techno-economic comparison presented in Sec. 3-7-1. The entire capture unit was optimized, such that the energy consumption is minimized. Equipment costs were not included in the objective function. The optimization was performed for all the capture ratios from 75 to 91% in order to point out how the power consumption and the optimal operating conditions vary for different capture ratios. The following decision variables were used:

- flow rate of the Semi-Lean Solvent (absorption section)
- flow rate of the Lean Solvent (absorption section)
- flow rate of the Process Water (shifting section)
- temperature of the Feed Splitting Vessel quench stream (shifting section)
- pressure of the Rich Solvent Flash Drum (absorption section)

The respected constraints for each optimization are:

- A fixed CO_2 capture rate
  The optimization was repeated for each percentage of capture ratio between 75 and 91%. To achieve a fixed capture ratio the trade-off between CO conversion and CO_2 recovery was taken into account. To control the CO conversion and the CO_2 recovery, the flow rate of the process water and the Semi-Lean Solvent mass flow were manipulated in Aspen Plus. The process water determines the steam/CO ratios in front of the reactor, and hence the CO conversion. The Semi-Lean Solvent mass flow manipulates the L/G ratio in the CO_2 Absorber and consequently the CO_2 recovery.
- A minimum steam/CO ratio at the inlet of each WGS reactor of 2.65 mol/mol
  A minimum steam/CO ratio at the inlet of the shift reactors of 2.65 mol/mol has to be respected in order to avoid coke formation [18]. In Aspen Plus the CO conversion was controlled by manipulating the overall steam/CO ratio in the syngas. To achieve a lower CO conversion the overall steam/CO ratio was decreased. Hence, the limit of the minimum steam/CO ratio is particularly restrictive for low CO conversions. If the minimum was reached, a part of the syngas was withdrawn downstream the H_2S Absorber. It by-passed the entire shifting and CO_2 removal unit, and downstream the CO_2 Absorber it was routed back to the main syngas stream.
- A inlet temperature for each WGS reactors of 340°C
  As the minimum steam/CO ratio, the minimum inlet temperature to the shift reactors is normally given from the catalyst manufacturer. This is chosen in order to guarantee a minimum reaction velocity and is furthermore a trade-off between the cost of the reactor and the operating costs (see Sec. 2-1). For simplicity, the inlet temperature of each WGS reactor was set to its minimum of 340°C.

- A maximal outlet temperature of each WGS reactor of 520°C
  The maximum outlet temperature of 520°C for the here considered catalyst was estimated by Nuon. For higher outlet temperatures the catalyst would irreversibly deactivate due to sintering [23].
- minimum H_2S content in the acid gas stream of 25%
  (for more details see Sec. 3-7-1)
- maximum total mole sulphur fraction in the CO_2 Product stream of 10 ppm (dry)
  (for more details see Sec. 3-7-1)

In Aspen Plus the equality constraints have been implemented as 'spec groups', while for the inequality constraints a lower or upper variable bound was set in EO mode. The optimization was performed with the gradient-based internal optimizer of Aspen Plus.

In the second part of the capture unit optimization, the developed framework for the capture unit optimization was used to compare the impact on the power consumption of different minimum steam/CO ratios and minimum inlet temperatures to the WGS reactors. The optimization was repeated for different limits for these constraints. Three cases were defined. The first and the second case were defined for a fresh catalyst, and were therefore called Start of Run (SOR). The third case was defined at the end of the life cycle of the catalyst, and was therefore called End of Run (EOR). During the life cycle of the catalyst the minimum inlet temperature and the minimum steam/CO ratio for the reactors have to be adapted. With increasing number of operating hours the catalyst deactivates, and thus the reaction front tends to move out of the reactor. To compensate this effect, the inlet temperature of the reactors has to be increased. Furthermore, also the steam/CO ratio has to be increased, because this compensates the higher risk of carbide formation for older catalysts. Table 3-6 shows the three cases which have been defined and compared from 75% to 91% of carbon removal.

The first case, called SOR conservative case, represents safe conditions for a fresh catalyst. These conditions have been used as constraints for the optimization described above. The SOR conservative case was chosen as a reference case. The second case is called SOR limit case, representing the most optimal conditions. In fact, from the outcome of the pilot plant's test runs and from an apposite reactor model, which was developed from Nuon, it was concluded that the S/CO ratio and inlet temperature can be lowered. It was estimated that the minimum steam/CO ratio can be reduced from 2.65 to 1.5 mol/mol. However, for a better comparison two different limits were studied: 1.5 and 2.0 mol/mol. It was also concluded that the minimum inlet temperature for reactor one and two can be reduced from 340°C to 315°C - without moving the reaction front out of the reactor [21]. The reactor model predicted that for the planned reactors of the Magnum IGCC power plant the operation can be maintained for 1.3 years at this temperature; only after that, the minimum inlet temperature for reactor one and two has to be increased [21]. For reactor three the inlet temperature was kept equal to the SOR conservative case, as this reactor being the last one hardly deactivates throughout its lifetime. For all SOR cases an ATE of 10 K was used in order to take into account that the chemical equilibrium will not be reached within the reactors. The EOR case refers to a catalyst after four years of operation. The reactor model predicted that the temperature in EOR conditions has to be increased to about 365°C for reactor one and two. Furthermore,

Table 3-6: Comparison of the constraints on the minimum steam/CO ratio, inlet temperature of the WGS reactors and ATE for all three analyzed cases of the capture unit optimization

		SOR conservative	SOR limit	EOR
T_{min} [°C]	1° reactor	340	315	365
	2° reactor	340	315	365
	3° reactor	340	340	340
ATE [K]	1° reactor	10	10	20
	2° reactor	10	10	20
	3° reactor	10	10	10
$(\frac{steam}{CO})_{min}$ $[mol/mol]$	1° reactor	2.65	1.5 & 2	2.65
	2° reactor	2.65	1.5 & 2	2.65
	3° reactor	2.65	1.5 & 2	2.65

the ATE was increased to 20 K. The inlet temperature and the ATE for reactor three were maintained as for case one and two. A minimum steam/CO ratio of 2.65 mol/mol was considered.

Finally, a last case study was performed. An additional case with an inlet temperature to the third reactor of 315°C was defined. Except this, the case is equal to the SOR limit case with a minimum steam/CO ratio of 1.5 mol/mol. In all three aforementioned cases, the inlet temperature of the third reactor was kept at 340°C. This temperature can be lowered if the dimension of the reactor is increased. This leads to higher investment costs. Nevertheless, a lower inlet temperature could save a significant amount of energy.

3-7-3 Performance H_2S removal section when no CO_2 is captured

As mentioned in Sec. 1-4 a sweet-shift configuration was chosen, as for this configuration the CO_2 capture can easily be by-passed. A by-pass is useful if the CO_2 price of the market is not adequate to justify the additional costs connected to the power requirement of the capture unit. When no CO_2 is captured, the shifting and CO_2 absorption section are by-passed by the syngas. In contrast, the H_2S absorption section is not by-passed, as the sulphur content of the Untreated Syngas has to be reduced in order to guarantee a proper operation of the downstream gas turbines. The model described in Sec. 3-3-3 was used. For this model, the solvent downstream the Lean Solvent Chiller is directly routed to the H_2S Absorber. This solvent stream has a different composition of the Semi-Lean Solvent which usually enters the H_2S Absorber, and hence the performance of the entire H_2S absorption section could change. The aim of this study is to point out these differences. Therefore, the performance of the H_2S absorption section when CO_2 is captured was compared to the case when no CO_2 is captured. The chilled AC model and the capture unit model without CO_2 capture were used, respectively. For the latter, the outlet temperature of the Lean Solvent Chiller was set equal to the temperature of the Semi-Lean Solvent stream entering the H_2S Absorber in the AC model (7.32°C). 13 equilibrium stages in the CO_2 Absorber, 10 in the H_2S Absorber and 6

in the H_2S Stripper were used for both models together with the corresponding optimized operating conditions found during the analysis of the first research question. The same constraints as described in Sec. 3-7-1 were respected, except the constraint on the total mole sulphur fraction in the CO_2 Product stream. Instead of this limit, a constraint on the total mole sulphur content in the Unshifted Syngas stream of 5.5 ppm was set. It corresponds approximately to a total mole sulphur fraction in the CO_2 Product stream of 10 ppm (dry), and was controlled with a 'spec group' by manipulating the Lean Solvent flow rate. It was chosen to use the same constraint on the maximum sulphur content in the Unshifted Syngas stream for both models in order to point out the influence of the syngas composition at the inlet of the H_2S Absorber. Note that when no CO_2 is captured, the limit of the maximum sulphur content could be increased, as the maximum mole sulphur fraction in the syngas at the inlet of the gas turbines is 20 ppm [21].

Chapter 4

Results and discussion

This chapter presents the results and discussion of the three research questions defined in Chapter 1: the comparison between the ATC and the BATC, the optimization of the entire capture unit, and the analysis of by-passing the CO_2 absorption section. Finally recommendations about how future studies could make use of the present work are treated in the concluding section.

4-1 Comparison between the ATC and the BATC

4-1-1 Thermodynamic optimization

Before performing the optimization of the AC model described in Chapter 3, a rigorous sensitivity analysis was performed. The Aspen Plus EO Sensitivity tool was used for this purpose. It was observed, that for the optimized operating conditions, some of the decision variables would reach their upper or lower bound. In particular, the pressure in the H_2S Stripper would hit its lower limit of 1.8 bar, and the outlet temperature of the chillers would hit its lower limit of 4°C. These variables were removed from the set of decision variables and were set to their respective lower bound. A similar observation was made for the water content in the solvent. Even if no specific constraint on the minimum water content in the solvent was defined, the minimum water content is indirectly limited by the maximum solvent temperature of 146°C in the H_2S Stripper Reboiler. This temperature is mainly affected by two variables: the water content in the solvent, and the reboiler duty, whereby the reboiler duty has a limited impact in the typical operating conditions of the stripper. Therefore, the water content in the solvent was set to 40 mole%, which corresponds to an approximately constant temperature in the H_2S Stripper Reboiler of 146°C. Like the pressure in the H_2S Stripper and the outlet temperature of the chillers, the water content was removed from the set of decision variables.

As second step, the optimization of the AC section targeting the power consumption was performed. The optimization was done using different numbers of equilibrium stages in the

absorber and stripper columns for both the ATC and the BATC. The reference number of equilibrium stages was estimated in a previous study to 13 stages for the CO_2 Absorber, 10 stages for the H_2S Absorber, and 6 stages for the H_2S Stripper. Although different combinations of number of equilibrium stages exist, only two additional cases were defined: one with a lower number of equilibrium stages, and one with a higher number of equilibrium stages. The number of stages in each column was varied by the same percentage. The aim was to give a general idea about how the number of equilibrium stages influences the performance.

Based on experience of multiple preliminary optimization tests the number of iterations for the DIRECT algorithm was set to 1500. The performance results and other relevant system parameters are reported in Table 4-1. The results show that the optimized operating conditions are different for the analyzed cases. In a first approximation, it can be assumed that the number of equilibrium stages in the CO_2 Absorber influences only the CO_2 removal unit, while the number of equilibrium stages in the H_2S Absorber and Stripper influence only the H_2S removal unit. Hence, the change in the optimal pressures in the CO_2 Flash Drums is attributed to the different number of stages in the CO_2 Absorber, while the change in the optimal reboiler duty and pressure of the Rich Solvent Flash Drum is attributed to the different number of stages in the H_2S Absorber and Stripper.

The optimal pressures in the two CO_2 Flash Drums increase with the number of equilibrium stages and are higher for the BATC than for the ATC. The pressure in the LP Flash Drum (p_{LP_FD}) is a trade-off between the power consumption of the first CO_2 Compressor and the power requirement of the CO_2 removal unit (note that each stage of CO_2 compression was modeled with an individual CO_2 compressor in Aspen Plus). For a higher p_{LP_FD} the energy consumption of the first CO_2 Compressor decreases, while the energy consumption of the CO_2 removal unit increases for increased solvent flow. Consequently, the optimal p_{LP_FD} depends on the solvent mass flow in the CO_2 absorption section (see Table 4-1). The solvent mass flow decreases, as the number of equilibrium stages augments, and is lower for the BATC than for the ATC, because the column can operate at a lower L/G ratio. As a result, for a higher number of equilibrium stages and/or for a lower temperature in the CO_2 Absorber, the optimal p_{LP_FD} increases. The pressure in the MP Flash Drum (p_{MP_FD}) adapts to the higher p_{LP_FD}. As the p_{MP_FD} increases for a fixed p_{LP_FD}, more CO_2 is stripped off at the last CO_2 Flash Drum, and less at the MP CO_2 Flash Drum. Accordingly, the power consumption of the first CO_2 Compressor increases, while the power consumption of the last four CO_2 compressors decreases. Hence, for each p_{LP_FD} there is an optimal p_{MP_FD} depending on the power consumption of the CO_2 compression unit. Note that for a given p_{LP_FD} the optimal p_{MP_FD} could be different for the ATC and BATC. In fact, the operating temperature of the CO_2 Flash Drums is different and this influences the amount of entrained gases in the off-gas of the flash vessels.
The optimal boil-up ratio is mainly influenced by the number of equilibrium stages in the H_2S Stripper. As the number of equilibrium stages increases, the G/L ratio in the stripper can be reduced and less vapor has to be produced. In addition to the boil-up ratio, the optimal reboiler duty is reported in Table 4-1, as it influences directly the power requirement. It decreases with the boil-up ratio, but depends also on the solvent mass flow which is heated up in the H_2S Stripper Reboiler. As mentioned before, the latter decreases for a higher number of equilibrium stages and lower operating temperatures in the absorber. As a result, the reboiler duty decreases as the number of equilibrium stages augments and is lower for the BATC than

Table 4-1: Comparison of performance and other relevant system parameters of the ATC and BATC for different numbers of equilibrium stages (N) in the CO_2 Absorber (CA), H_2S Absorber (SA) and H_2S Stripper (SS) for a CO_2 recovery of 92.5%.

Design ($\mathbf{N}_{CA}/\mathbf{N}_{SA}/\mathbf{N}_{SS}$) [1]	$\mathbf{p}_{MP\_FD}$ [bar]	$\mathbf{p}_{LP\_FD}$ [bar]	$\dot{\mathbf{Q}}_{reb}$ [MW]	**boil-up ratio** [/]	$\mathbf{p}_{RS\_FD}$ [bar]	$\dot{\mathbf{E}}$ [MW]
ATC (10/8/5)	1.09	4.59	21.00	0.16	4.25	41.16
ATC (13/10/6)	1.20	4.78	13.52	0.14	5.50	37.56
ATC (17/13/8)	1.25	4.96	9.26	0.12	6.63	35.61
ATC (21/16/10)	1.33	5.09	7.71	0.11	7.45	34.65
BATC (10/8/5)	1.18	4.76	9.31	0.18	8.21	34.62
BATC (13/10/6)	1.26	4.96	6.45	0.15	10.20	32.93
BATC (21/16/10)	1.36	5.25	4.26	0.13	15.51	31.35

[1] The design is distinguished by the type of configuration (BATC, ATC) and the number of equilibrium stages in the CO_2 Absorber, H_2S Absorber and H_2S Stripper, called CA, CS and SS, respectively;

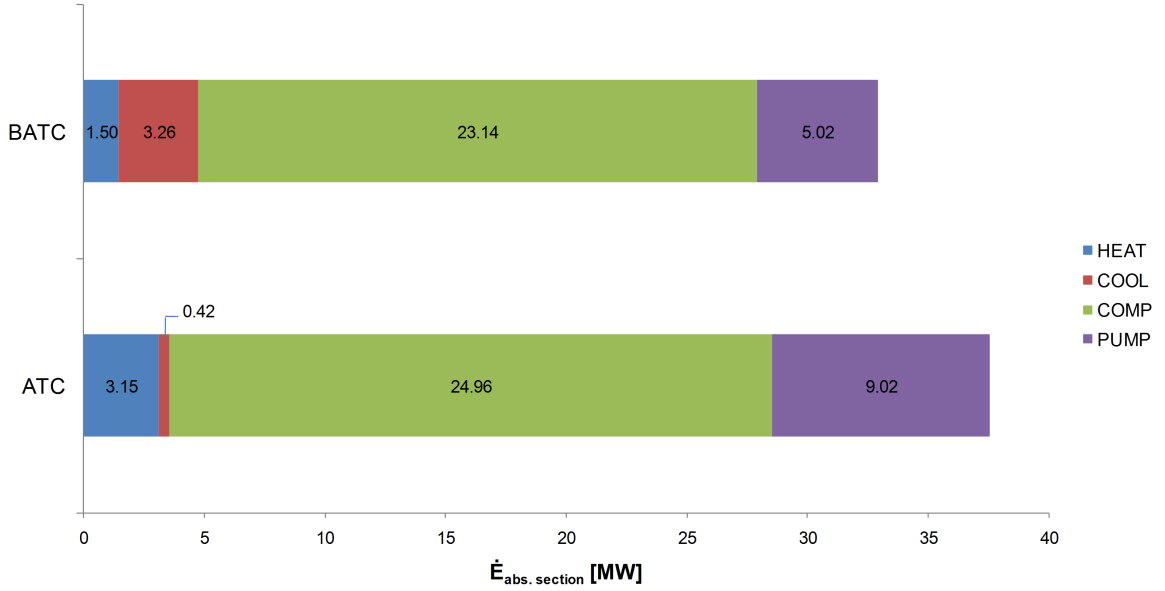

Figure 4-1: Power consumption due to heating, cooling, compressors and pumps of the ATC and the BATC, with $N_{CA} = 13$, $N_{SA} = 10$ and $N_{SS} = 6$

for the ATC.
The optimal pressure in the Rich Solvent Flash Drum is directly determined from a 'spec group' in order to achieve a 25 mole% H_2S content in the Acid Gas stream. As the flow rate of the Acid Gas stream is almost equal for all the cases, this pressure depends on the flow rate of CO_2 in front of the Rich Solvent Flash Drum: the higher the flow rate is, the lower the pressure will be. In a first approximation the flow rate of CO_2 is proportional to the Lean-Solvent flow rate. Therefore, the pressure in the Rich Solvent Flash Drum is higher for the BATC than for the ATC, and increases with the number of equilibrium stages. Note that for a more accurate comparison also the mole fraction of CO_2 in front of the Rich Solvent Flash Drum should be considered.

Table 4-1 shows that the power requirement in all analyzed cases is higher for the ATC than for the BATC - i.e., chilling instead of cooling the solvent in the absorption section saves energy. Figure 4-1 displays in more detail the power requirement for the ATC and BATC. The bar diagrams represent the design with $N_{CA} = 13$, $N_{SA} = 10$ and $N_{SS} = 6$. The power consumption for cooling/chilling of the BATC is 2.84 MW higher compared to the ATC. Nevertheless, the total power consumption of the BATC is lower, because of a lower power consumption for heating the solvent in the Stripper Reboiler and the lower power consumption of pumps and compressors. This is attributable to the lower solvent flow rate of the BATC. Note that the same phenomenon can be also observed for the other combinations of number of equilibrium stages.

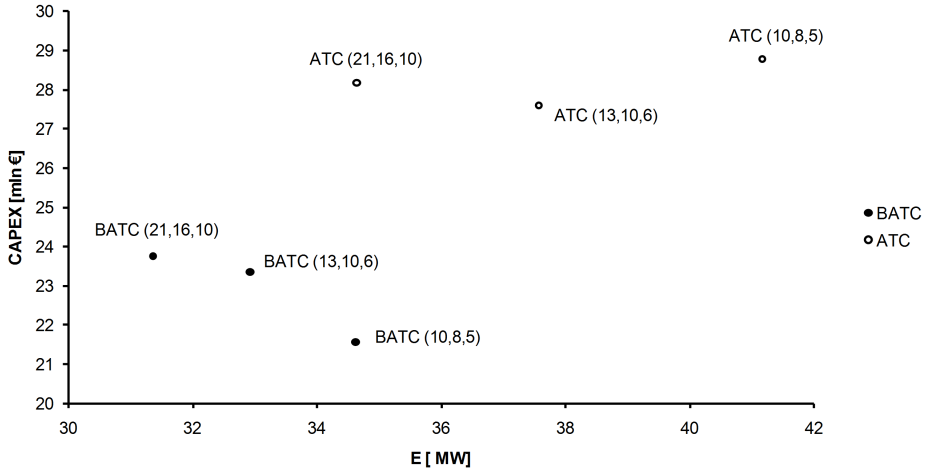

Figure 4-2: Equipment cost and power consumption of the ATC and BATC for different numbers of equilibrium stages in the CO_2 Absorber, H_2S Absorber, and H_2S Stripper, respectively (indicated in brackets)

4-1-2 Evaluation equipment cost

The equipment cost of the components of the AC section was evaluated for all the optimized designs. Figure 4-2 shows a comparison of the energy consumption and equipment cost. For all the analyzed cases, the BATC consumes less energy and has a lower equipment cost than the ATC. Hence, for the analyzed cases the BATC is thermodynamically and economically more beneficial than the ATC. For a rigorous comparison, more cases should be analyzed or a multi-objective optimization should be done in order to find the Pareto Front. Only such a rigorous comparison can prove that for all possible choices of equilibrium stages the BATC is techo-economically more advantageous than the ATC. From the performed analysis it can not be concluded if the evaluated designs are Pareto optimal. However, the investigated designs allow a rough comparison of the chilled and unchilled configuration. For sure, the point of the ATC with the lowest number of equilibrium stages is not Pareto optimal. In fact, it has a higher power consumption and a higher equipment cost than the ATC with 13, 10 and 6 equilibrium stages. This is attributable to the high solvent mass flow which increases the size of the components. Another difference to the Pareto Front is that for a high number of equilibrium stages a vertical asymptote should limit the minimum energy consumption - i.e., adding a stage increases the equipment cost of the column, but the energy consumption will not decrease anymore. It is expected, that the number of equilibrium stages for the BATC and the ATC should be increased above $N_{CA} = 13$, $N_{SA} = 10$ and $N_{SS} = 6$ in order to observe this phenomenon.

A simplified calculation of the NPV was performed for both the BATC and the ATC for $N_{CA} = 13$, $N_{SA} = 10$ and $N_{SS} = 6$. As mentioned in the previous chapter, only the cost of electricity and the equipment cost were taken into account. The equipment cost was assumed as CAPEX expenditure, while the electricity consumption defines the OPEX costs. As only the costs were included, the NPV is negative. The results are reported in Figure 4-3. As expected, the power consumption of the AC section contributes significantly more to

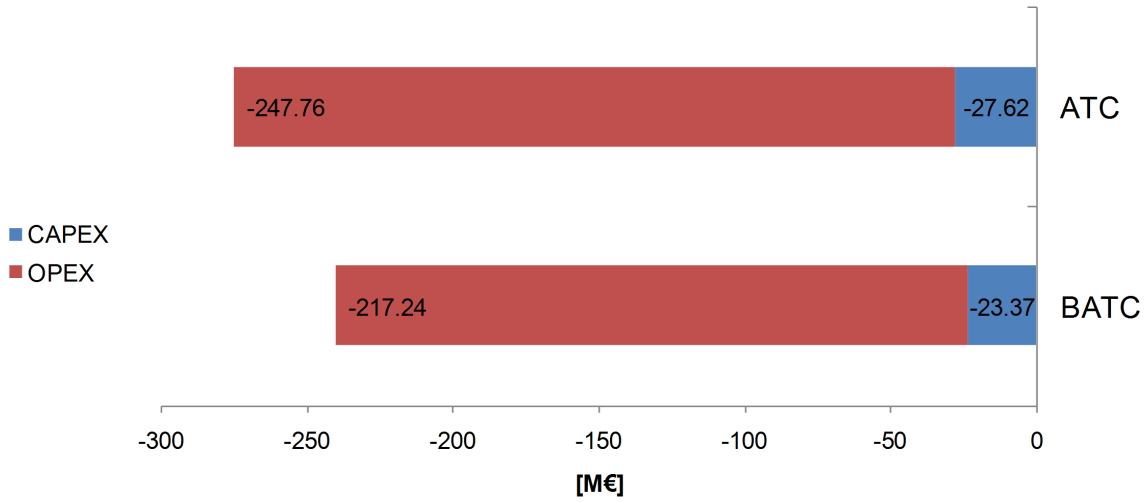

Figure 4-3: NPV for the BATC and the ATC with $N_{CA} = 13$, $N_{SA} = 10$ and $N_{SS} = 6$

the NPV than the equipment cost. This justifies that an optimization only considering the energy consumption and not the cost provides a reasonable preliminary estimation. The same observation can be made for the other analyzed number of equilibrium stages. However, note that this analysis is a first rough estimation of the equipment cost. Further analyses should take into consideration the total direct cost of the unit instead of the equipment cost. This could influence the share of the CAPEX costs on the NPV.

4-2 Overall capture unit optimization of the BATC

Before performing the optimization of the capture unit described in Chapter 3, a rigorous sensitivity analysis was done. It was observed that the ΔT_{pinch} of 10°C in the Heat Ex. 3 limits the highest achievable quench temperature. As the quench temperature is optimized, a fixed ΔT_{pinch} could affect the optimal operating conditions of the shifting section. Nevertheless, the ΔT_{pinch} was not included in the set of decision variables, because an analysis showed that the ΔT_{pinch} does not influence the power requirement. Therefore, it was decided to remove the Heat Ex. 3 from the flowsheet. The power consumption is not influenced, because the ΔT_{pinch} in the Heat Ex. 3 does not affect the hot stream outlet temperature of the Heat Ex. 1, and hence the same amount of heat is recovered from the hot reactor effluent. Furthermore, the analysis showed that the IP steam consumption of the Steam Heat Ex. 1 and 2 change, but the total required amount of IP steam does not vary, and hence the reduction of the electrical power output of the IGCC power plant due the Steam Heat Exchangers is constant. Note that future studies should take into account also the equipment costs of the shifting section. The Heat Ex. 3 could not be removed anymore, because it could influence the area of the heat exchangers. Furthermore, note that future studies could consider using steam at a different temperature and pressure for the two Steam Heat Exchangers. The Heat Ex. 3 could not be removed anymore, as the power consumption of the Steam Heat Exchangers would be influenced.

Table 4-2: Comparison of performance and other relevant system parameters of the optimized capture unit for different CO_2 capture rates

η_C [/]	$\dot{m}_{lean}$ $[kg/s]$	$\dot{m}_{semilean}$ $[kg/s]$	$\frac{steam}{CO}_{overall}$ $[kg/kg]$	$\dot{E_{tot}}$ $[MW]$
0.75	133.82	728.52	1.38	83.89
0.77	133.75	751.79	1.38	86.01
0.79	133.69	775.06	1.38	88.12
0.81	133.62	798.33	1.38	90.23
0.83	133.56	821.59	1.38	92.35
0.85	133.51	884.84	1.38	94.46
0.87	133.21	921.48	1.37	96.53
0.89	132.50	957.12	1.63	104.91
0.91	131.75	1019.93	2.15	121.18

In the previous section it was pointed out that for all analyzed cases the BATC consumes less energy and costs less than the ATC. Accordingly, it was decided to perform the thermodynamic optimization of the entire capture unit with the chilled absorption section. For the CO_2 Absorber, H_2S Absorber and H_2S Stripper, 13, 10 and 6 equilibrium stages were used, respectively. Some of the respective optimized operating conditions found in the previous section were used as constraints in the optimization: the pressure of the MP CO_2 Flash Drum, the pressure of the LP CO_2 Flash Drum, the pressure of the H_2S Stripper, the outlet temperature of the chillers, the H_2S Stripper boil-up ratio and the water content in the solvent.

4-2-1 Optimization capture unit

The thermodynamic optimization was performed following the approach described in Figure 4-12. Performance results and relevant system parameters are summarized in Table 4-2.

For capture rates above 87%, the CO conversion is controlled by manipulating the flow rate of the Process water, and hence the overall steam/CO ratio. For capture rates below 87%, the lower limit of the steam/CO ratio in front of reactor two, which is 2.65 mol/mol, is reached. To achieve lower capture rates, the process water cannot be further reduced without any adaptations. The steam/CO ratio in front of the second WGS reactor would decrease below 2.65 mol/mol, and catalyst coking could occur. Therefore, a by-pass of the shifting and absorption section for a part of the Unshifted Syngas was used. Hereby, the CO fed to the shifting section decreases, and consequently the flow rate of process water can be reduced by maintaining a constant steam/CO ratio. In fact, the optimized overall steam/CO ratio for capture rates below 87% was found to be constant at 1.38 kg/kg (see Table 4-2). Initially, two alternatives to the described by-pass were considered in order to guarantee a minimum steam/CO ratio: by-passing only the third WGS reactor, and increasing the inlet temperature of the reactors. Both strategies lead to the desired increase of the steam/CO ratio in front of the second WGS reactor for a fixed CO_2 capture rate, but they were found to be less efficient and were excluded from further analyses.

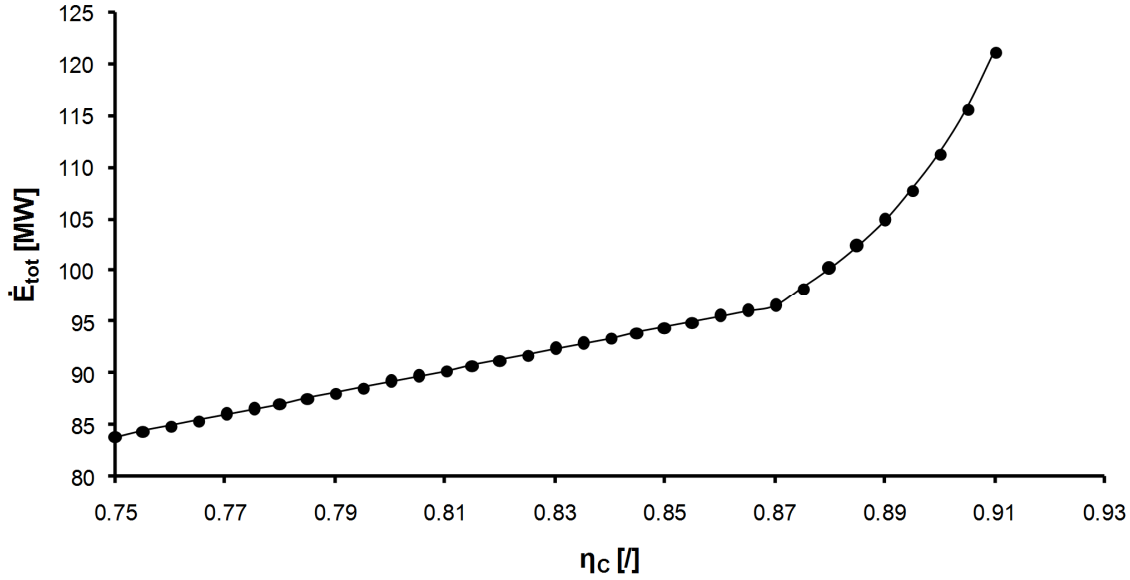

(a)

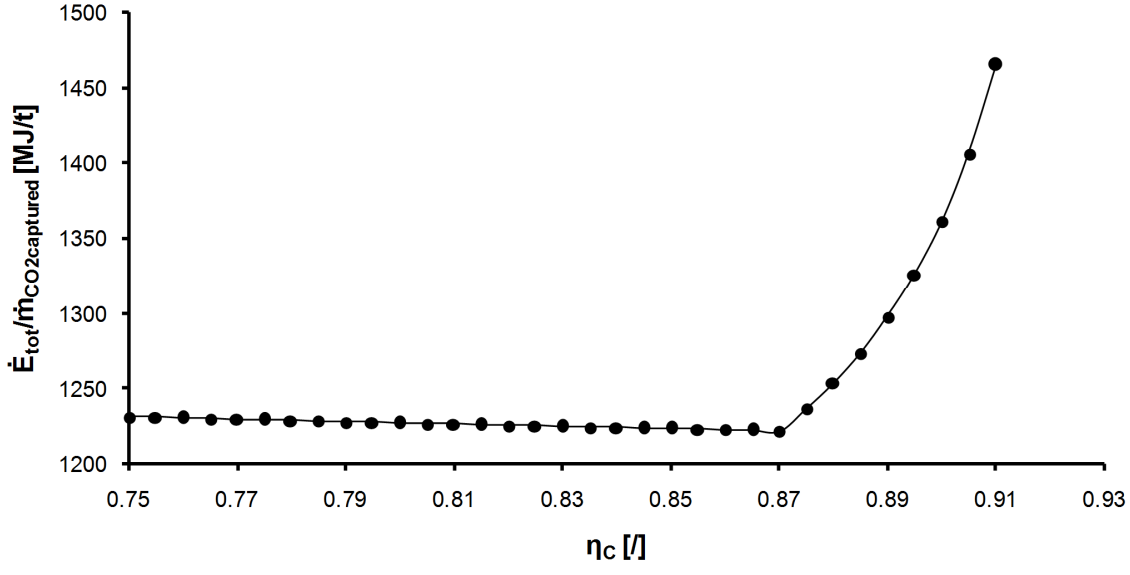

(b)

Figure 4-4: Total power consumption (a) and specific energy requirement (b) of the capture unit as a function of the CO_2 capture rate

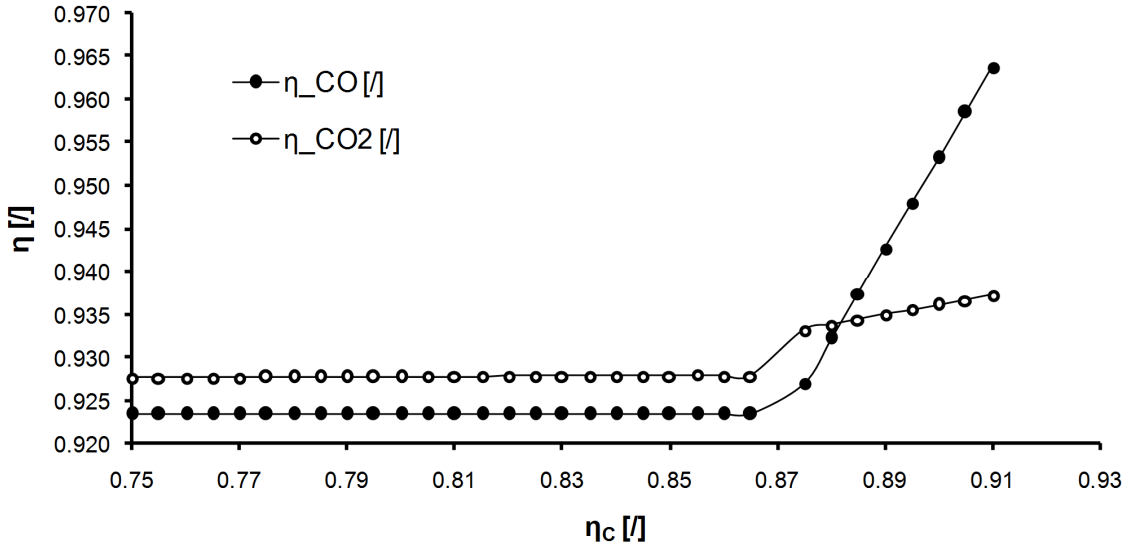

Figure 4-5: The CO conversion and CO_2 recovery as a function of the CO_2 capture rate

Figure 4-4 indicates the total power requirement and the specific energy consumption of the capture unit. The total power consumption increases almost linearly until 87% of capture rate, while for higher capture rates it augments significantly. The specific energy consumption per ton of CO_2 captured has a minimum of 1221 MJ/kg for a capture rate of 87%. Like the total power consumption, also the specific energy consumption increases for high capture rates: from about 1220 MJ/t for 87% of carbon removal to 1470 MJ/t for 91% of carbon removal. For capture rates below 87%, the specific energy consumption is almost constant. This is due to the by-pass. The optimized operating conditions of the shifting and absorption section remain almost constant, only the mass flows in the units decrease. For a better understanding of the phenomena connected to the power requirement and the trend of the specific energy consumption Figure 4-5 and Figure 4-6 are reported.

Figure 4-5 shows the optimal combination of the CO conversion and CO_2 recovery for different capture rates. 91% of capture rate is approximately the highest achievable for the analyzed capture unit. Both the CO conversion and the CO_2 recovery are pushed to their upper limit. Even if the solvent mass flow in the absorption section and the steam/CO ratio in the shifting section would be further increased, the capture rate would not augment anymore. To achieve lower capture rates, the optimal CO conversion decreases significantly, while the CO_2 recovery decreases less. The latter varies from approximately 93.7% to 92.8%, while the CO conversion decreases from 96.4% to 92.3%. For capture rates below 87%, both the CO conversion and the CO_2 recovery are almost constant. This is related to the fact that a part of the Unshifted Syngas is by-passed, and hence the optimum operating conditions in terms of CO conversion and CO_2 remain constant. Note that the CO conversion and CO_2 recovery are calculated on the effective amount of syngas entering the unit (the flow rate of the by-passed Unshifted Syngas is not considered). The by-pass explains also the abrupt change in the slope of the CO conversion and CO_2 recovery at 87%.

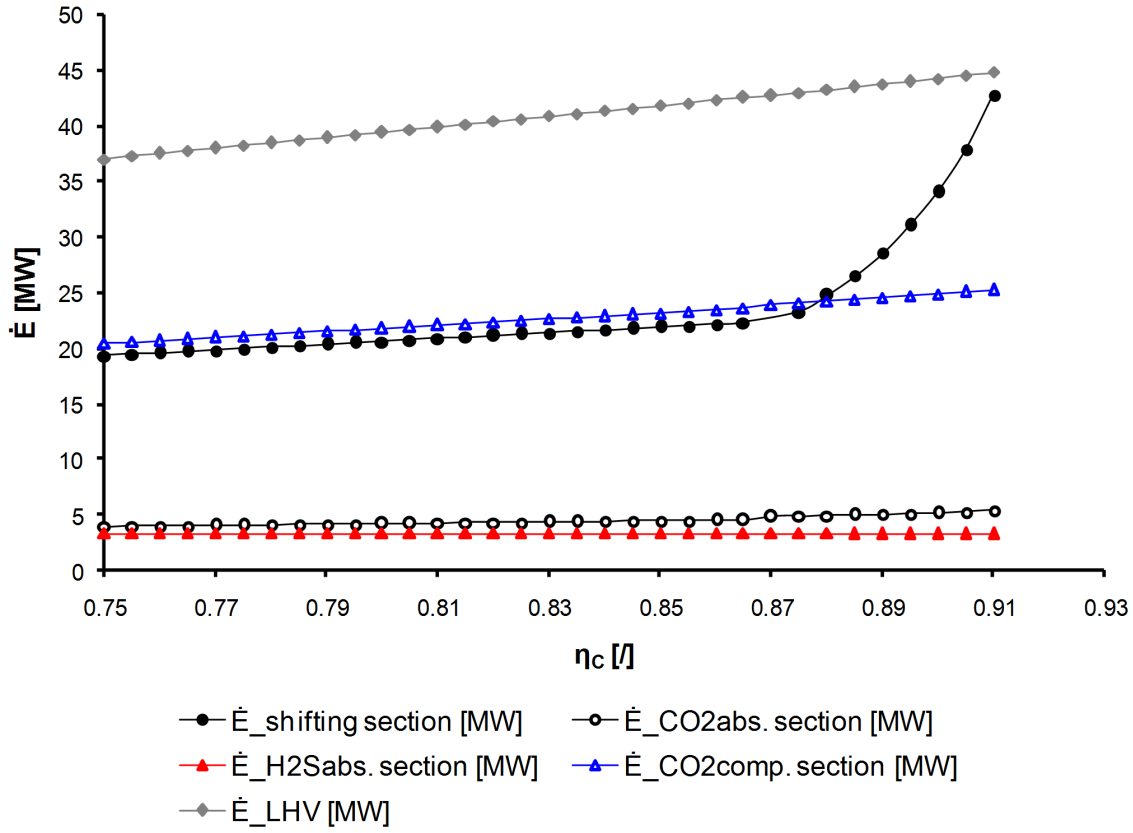

Figure 4-6: The power consumption in each section of the capture unit as a function of the CO_2 capture rate

Figure 4-6 shows the power consumption in each section of the capture unit. The LHV loss is considered as a hypothetical section. Its power consumption is around 40 MW and is higher than the consumption of any other section. It decreases for lower capture rates, because less CO is shifted to CO_2 (see Figure 4-5 and note that once the by-pass is opened less CO is shifted to CO_2 as the less syngas enters the shifting section). The power consumption in the shifting section is mainly given by the IP steam consumption of the two Steam Heat Exchangers. For high CO conversions the power consumption increases significantly, as the stoichiometric excess of steam is increased in order to push the equilibrium of the WGS reaction to the products. The mass flow of the shifting section increases, and consequently also the power requirement. For low capture rates, the shifting section consumes about 20 MW. The CO_2 compression section has a similar power requirement. Its power consumption is proportional to the captured amount of CO_2. The total power consumption in the absorption section varies from 7.61 MW to 8.73 MW and is herewith considerably lower than the power consumption in the other sections. It was split into two parts: the power consumption in the CO_2 removal section and the power consumption in the H_2S removal section. Analogous to the power consumption in all the other units, the CO_2 removal unit increases its power demand for higher capture rates. In contrast, the power consumption in the H_2S removal unit decreases. This is attributable to the amount of sulphur which has to be removed from the Untreated Syngas. As the capture rate increases, the flow rate of the Product CO_2 stream augments, but the amount of sulphur which has to be removed in the H_2S removal section decreases, because the mole fraction of sulphur in CO_2 Product stream is constant at 10 ppm. Consequently, the Lean Solvent mass flow and the power consumption of the H_2S removal unit decrease for higher capture rates. This explains also the slight increase of the specific energy consumption for capture rates below 87% (see Figure 4-4).

4-2-2 Performance comparison for different operating conditions of the WGS reactors

Design third reactor for inlet temperature of 340°C

In the second part of the capture unit optimization, the SOR limit, SOR conservative, and EOR cases defined in Sec. 3-7-2 were analyzed and compared. Figure 4-7 displays the optimized specific energy consumption as a function of the capture rate. For each case, the specific energy consumption has a minimum. It increases significantly for high capture rates, while it flattens out at low capture rates. The differences for high and low capture rates are pointed out in the following two paragraphs.

For capture rates above 87%, all cases have optimized steam/CO ratios greater than 2.65 mol/mol. This means that the three cases differ only by the inlet temperature of the reactors and in the ATE. There is only a small difference in the specific energy consumption between the cases and the curves are almost parallel. The EOR case has the highest power consumption, followed by the SOR conservative case, and finally by the SOR limit cases. The two SOR limit subcases coincide. The latter has a 15 MJ/t lower specific energy consumption than the EOR case (decrease of less than 1.5%), and a 6.5 MJ/t lower specific energy consumption than the SOR conservative case (decrease of less than 1%). For a fixed capture rate, the EOR and the SOR conservative case have a higher power consumption than the SOR limit case,

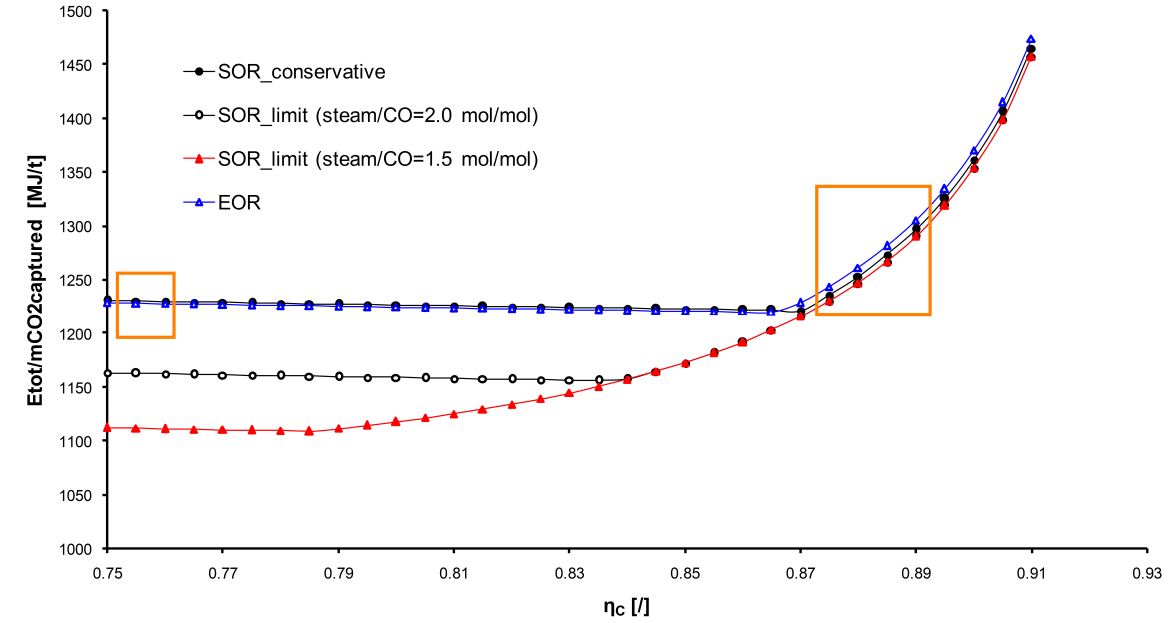

(a)

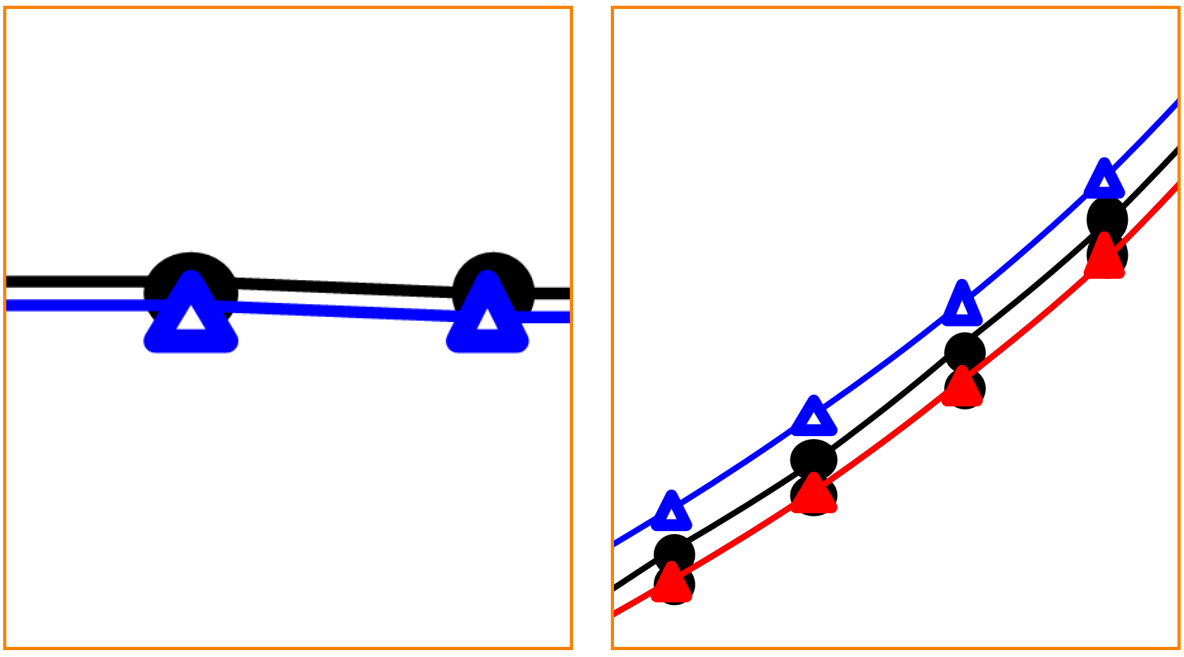

(b)

Figure 4-7: Specific energy consumption for SOR conservative, SOR limit and EOR conditions (a) with magnifications at 75.5% and 88% of carbon removal, respectively (b)

because they operate at higher inlet temperatures of the first and second reactor. Higher inlet temperatures are less favourable for the thermodynamic equilibrium of the WGS reaction, and thus the CO conversion decreases. This negative effect can be balanced by two strategies: increasing the steam/CO ratio in the shifting section, or increasing the CO_2 recovery. Both increase the power requirement and hence the specific energy consumption. The results of the optimization show that it is more beneficial to increase the steam/CO ratio. In fact, at high capture rates the optimized CO conversion and CO_2 recovery are almost coincident for all the cases for each capture rate (the maximum absolute difference is less than 0.06% for the CO_2 recovery at 87% of carbon removal). For the EOR case, the higher power consumption compared to the SOR limit case is further amplified, because the ATE is higher. The effect is the same as for higher inlet temperatures of the reactors: the CO conversion tends to decrease and is compensated by a higher steam/CO ratio, which augments the power requirement. Nevertheless, the difference in the specific energy consumption compared to the SOR limit and SOR conservative case is limited to below 1.5%, because there is a good heat integration for the first and second WGS reactor.

For capture rates below 87%, the EOR case and the SOR conservative case require almost the same specific energy, which differs by less than 2.5 MJ/t (0.02%). Both reach their lower limit of the steam/CO ratio at around 87% of carbon removal for the second reactor. To achieve lower capture rates, a part of the Unshifted Syngas is by-passed and a minimum steam/CO ratio of 2.65 mol/mol is maintained in front of the second reactor. The EOR case and the SOR conservative case differ only by the inlet temperatures to the first and second reactor, which is 365°C for the EOR case and 340°C for the SOR conservative case. This difference causes the slightly different specific energy consumption. A sensitivity analysis was done in order to understand the phenomenon. Although the higher reactor inlet temperatures of the EOR case are disadvantageous for the WGS reaction, this effect is overcompensated by another one: once the minimum steam/CO ratio in front of reactor two is reached, the higher inlet temperature of the second reactor reduces the necessary overall steam/CO ratio. In fact, the higher inlet temperature to the second reactor of the EOR case is achieved by a lower quench flow rate (note that this effect is partially reduced by the higher inlet temperature to the first reactor, which also augments the outlet temperature of the first reactor). The quench stream has a low steam/CO ratio, and hence a lower quench flow rate augments the inlet steam/CO ratio in front of the second reactor (note that in the Feed Splitting Vessel most of the water rests in the liquid bottom stream). The overall steam/CO ratio can be reduced until the steam/CO ratio in front of the second reactor reaches again its lower limit of 2.65 mol/mol. In fact, the overall steam/CO ratio is about 1.37 kg/kg for the EOR case and 1.38 kg/kg for the SOR conservative case and this leads to the lower specific energy consumption of the EOR case. Like for the SOR conservative and the EOR case, the specific energy consumption of the two SOR limit cases flattens out for low capture rates. This happens once the limit of the minimum steam/CO ratio is reached, and the by-pass of the Unshifted Syngas is opened. There is a gap in the specific energy consumption up to 119 MJ/t between the SOR limit cases and the other cases. This gap is mainly related to the different minimum steam/CO ratios in front of the reactors. The inlet temperatures and the ATE of the first and second WGS reactors play a minor role, as the EOR and SOR conservative case prove. As described above, the lower limit of the minimum steam/CO ratio for the SOR conservative case and the EOR case is already reached at 87% of capture rate. The by-pass is opened, the

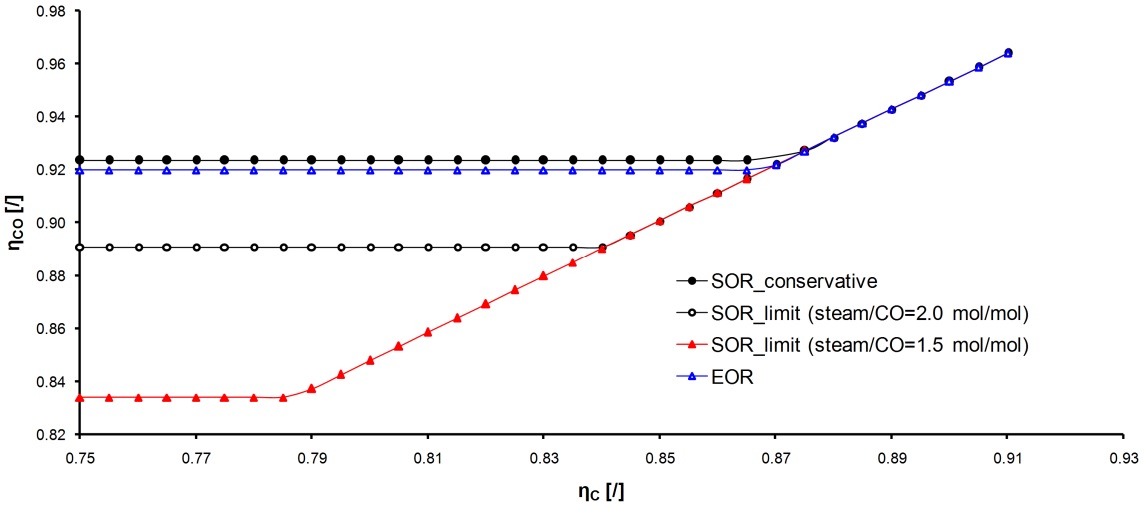

(a)

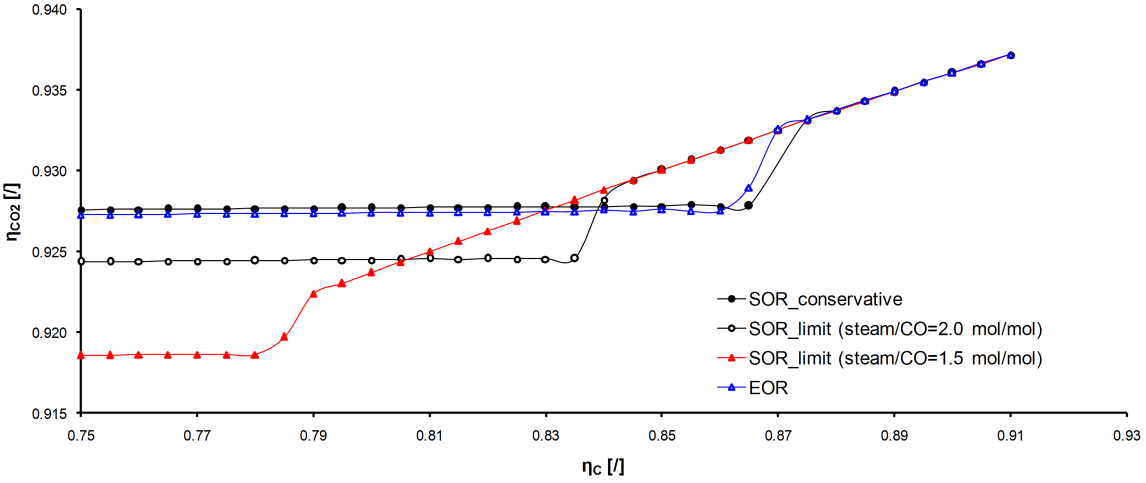

(b)

Figure 4-8: Optimized CO conversion (a) and CO_2 recovery (b) for SOR convservative, SOR limit and EOR as a function of the capture rate

steam/CO ratio rests at its lower limit, and the specific energy requirement is constant. In contrast, for the SOR limit cases, in order to achieve lower capture rates, instead of opening the by-pass, the steam/CO ratio can be further reduced. A higher amount of syngas passes through the shifting and absorption section and less syngas is by-passed. Consequently, to capture the same amount of CO_2, a lower CO conversion and/or lower CO_2 recovery is necessary (remember that the CO conversion and the CO_2 recovery are defined for the syngas which passes in the respective section). Accordingly, the stoichiometric excess of steam in the shifting section and/or the solvent flow in the CO_2 absorption section can be reduced, and therefore the specific energy consumption decreases. Figure 4-8 confirms the phenomenon.

The comparison between the three cases shows that the specific energy consumption varies significantly between high and low capture rates. For high capture rates, the minimum steam/CO ratio is irrelevant. Lower inlet temperatures to the first and second reactor are beneficial and reduce the specific energy consumption up to 15 MJ/t. Once the limit of the minimum steam/CO ratio is reached, the specific energy consumption is approximately constant. Both the steam/CO ratio and the inlet temperature of the first and second reactor influence this constant value. Lower limits for the minimum steam/CO ratio are beneficial, while lower inlet temperatures to the first and second have a limited impact. Operating the shifting section at SOR limit conditions with a lower limit of the steam/CO ratio of 1.5 mol/mol is advantageous compared to operating the shifting section at SOR conservative conditions. For capture rates above 87% a reduction in the specific energy consumption of about 5-8 MJ/kg is observed, while at lower capture rates savings up to 120 MJ/kg are possible. For partially deactivated catalysts represented by the EOR case, at high capture rates, the specific energy consumption is 7-9 MJ/t higher than for the SOR conservative case, and 13-16 MJ/t higher than for the SOR limit case. This means that after few years of operation the power consumption of the capture unit increases due to the deactivation of the catalyst. For low capture rates, the EOR case has almost the same specific energy consumption as the SOR conservative case. Note that for all cases increasing the inlet temperature of the second reactor would reduce the specific energy consumption at low capture rates.

Design third reactor for inlet temperature of 315°C

In the above described study the inlet temperature of the third reactor was maintained for all the cases at 340°C. The following analysis shows how much energy can be gained if the inlet temperature of this reactor is decreased to 315°C. As described in Sec. 3-7-2, the optimization of the capture unit was performed for an additional case which was defined for this aim. Figure 4-9 shows a comparison of this case to the SOR conservative and SOR limit case with a minimum steam on CO ratio of 1.5 mol/mol. Compared to the latter one, only the inlet temperature of the third reactor is reduced. The lower inlet temperature reduces the specific energy consumption of over 100 MJ/t for a capture rate of 91%, but the gain decreases for lower CO_2 capture rates. As it has already been observed, lower inlet temperatures favour the thermodynamic equilibrium of the WGS reaction and the specific energy consumption is reduced. This effect is particularly large if the inlet temperature of the third reactor is reduced. In fact, the first and second WGS reactors convert only the bulk of CO, while the third reactor ensures the deep removal. Therefore, some authors as Carbo suggest to use a low temperature catalyst for the third reactor with minimum inlet temperature down to

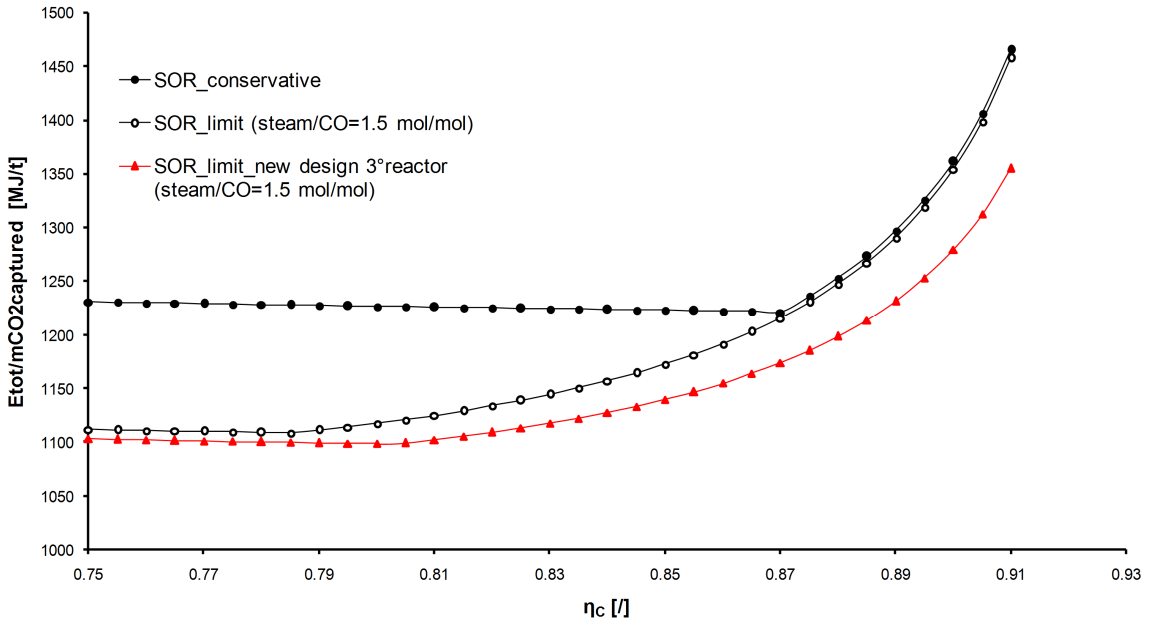

Figure 4-9: Specific energy consumption for the SOR limit case with a new design of the third reactor compared to SOR conservative and SOR limit conditions

185°C [17]. At low capture rates, the gain in the specific energy consumption for the fresh design of the third WGS reactor is reduced. Compared to the SOR limit case with steam/CO = 1.5 mol/mol, about 10 MJ/t can be saved. The gain is lower, because at low capture rates the CO conversion is lower - i.e., most of the CO is already converted in the first and second WGS reactor, while in the last WGS reactor almost no conversion takes place. Therefore, lowering the inlet temperature of the third reactor is less relevant.

It can be concluded, that the lower inlet temperature of the third reactor leads to a lower specific energy consumption in all the range of analyzed capture rates, especially at high ones. Nevertheless, the decrease of the inlet temperature of the third reactor increases the reactor size and the equipment cost (see Sec. 3-7-2). Future analyses should be made to compare the additional reactor costs to the lower OPEX costs related to the reduced power consumption.

4-3 Performance H_2S removal section when no CO_2 is captured

The aim of the third research question is to compare the performance of the H_2S absorption section with and without CO_2 capture. Table 4-3 summarizes main performance results and other relevant system parameters. The power requirement of the H_2S absorption section is 3.37 MW when CO_2 is captured, while it increases of almost 10% to 3.70 MW when no CO_2 is captured. The difference is due to the fact, that the solvent at the inlet of the H_2S Absorber has a different composition. When CO_2 is captured, the solvent is pre-loaded with CO_2. As Breckenridge et al. [45] described in 2000, this minimizes the temperature rise across the H_2S Absorber and prevents the additional CO_2 pickup from the syngas passing through the H_2S

Table 4-3: Comparison of performance and other relevant system parameters of the chilled H_2S absorption section with and without CO_2 capture

	Without CO_2 capture	**With CO_2 capture**
$\dot{m}_{rich\_solvent}$ $[kg/s]$	146.43	137.88
$\dot{m}_{lean\_solvent}$ $[kg/s]$	143.92	135.45
$x_{CO2\_rich\_solvent}$ $[mol/mol]$	0.0488	0.0495
$x_{CO2\_lean\_solvent}$ $[mol/mol]$	27ppb	29 ppb
$\dot{m}_{CO2\_rich\_solvent}$ $[kg/s]$	1.82	1.74
$x_{H2S\_rich\_solvent}$ $[mol/mol]$	0.0132	0.0138
$x_{H2S\_lean\_solvent}$ $[mol/mol]$	8.4 ppm	9.2 ppm
p_{RS_FD} $[bar]$	9.61	10.14
$\dot{m}_{flash\_gas}$ $[kg/s]$	1.20	1.08
$\dot{E}$ $[MW]$	3.70	3.37

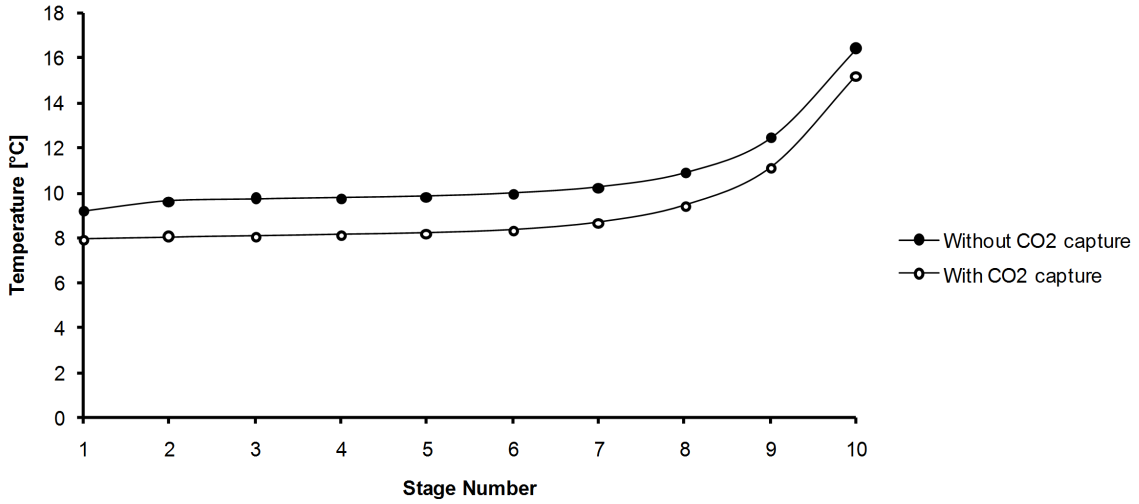

Figure 4-10: Operating temperature across the H_2S Absorber with and without CO_2 capture

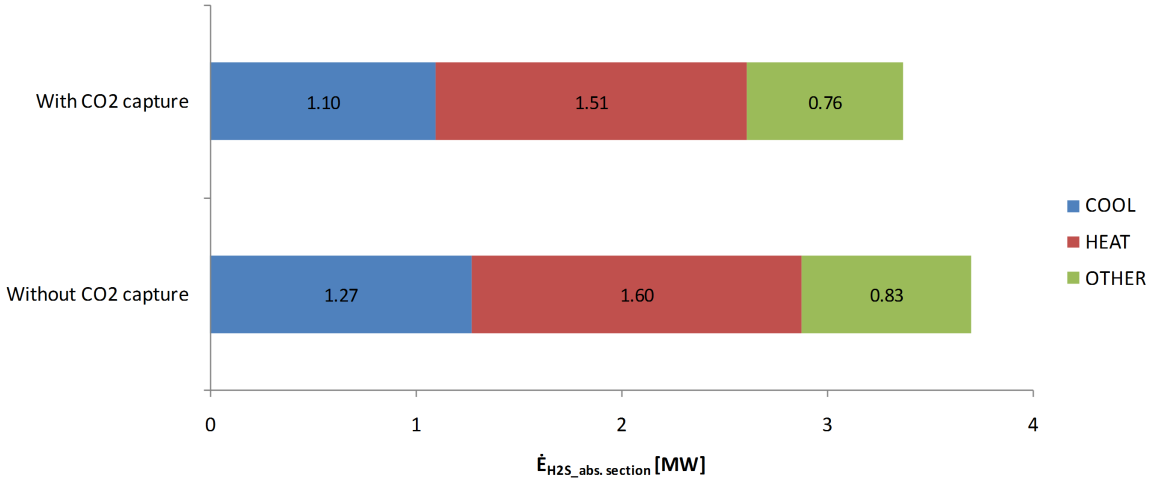

Figure 4-11: Power consumption of the H_2S absorption section with and without CO_2 capture

Absorber. The selectivity of the solvent and the H_2S capacity augment (the H_2S capacity, also called maximum loading or saturation capacity, describes the maximum concentration of solute that a solvent can contain under specified conditions) [45]. Consequently, a lower Lean Solvent flow rate is necessary to remove the same amount of sulphur. Furthermore, even if the $\dot{x}_{CO2\_rich\_solvent}$ is higher, the flow rate of CO_2 in the Rich Solvent is lower. Therefore, the pressure in the Rich Solvent Flash Drum can be increased, and the flow rate of the Flash Gas is lower. The power consumption of the Flash Gas Compressor decreases, because the compression ratio and the Flash Gas flow rate are lower. The Flash Gas is then cooled and enters the H_2S Absorber at a higher temperature than the operating temperature of the tower. Hence, the lower the flow rate of the Flash Gas is, the lower the operating temperature of the tower will be. This effect is proved in Figure 4-10. The operating temperature of the H_2S Absorber is lower across the entire tower when CO_2 is captured. This favours the absorption process and further reduces the power requirement. A detailed comparison of the power consumption is shown Figure 4-11. Especially the power consumption for cooling and chilling, given mainly by the power consumption of the Lean Solvent Chiller, augments when no CO_2 is captured. This is because the inlet temperature to the Lean Solvent Chiller augments, due to the higher outlet temperature of the H_2S Absorber. The increase in the power consumption for heating is given by the LP steam consumption in the H_2S Stripper and increases due to the higher solvent mass flow which is heated up in the Solvent Reboiler (the boil-up ratio was maintained constant for both cases). The remaining power consumption is given by the power requirement of the pumps and compressors. It increases because of the higher solvent mass flow, but also due to the higher power consumption of the Flash Gas Compressor (see above).

In this analysis, the solvent inlet temperature to the H_2S Absorber was maintained constant, in order to point out the different temperature profile in the tower caused by the solvent CO_2 loading. In future studies, it could be considered to reduce the solvent inlet temperature of the H_2S Absorber. Furthermore, the mole sulphur fraction in the Unshifted Syngas was limited to 5.5 ppm for both cases; the maximum mole sulphur content could be increased to 20 ppm

[21] in case no CO_2 is captured. This could significantly reduce the power requirement of the H_2S absorption section. In fact, a first estimation showed that the power requirement could be reduced to 2.77 MW, when the outlet temperature of the Lean Solvent Chiller is reduced to 4°C and the mole sulphur fraction in the Unshifted Syngas is set to 20 ppm.

4-4 Future improvement and recommendations

Process configuration changes Any process configuration changes were beyond the scope of the present work. Nevertheless, for further studies some changes are proposed. In order to avoid integer variables in the optimization, the proposed changes should be analyzed by means of case studies. Two process configuration changes are proposed: including Solvent Expanders in the absorption section and using an H_2S Concentrator.

Two hydraulic turbines, called Solvent Expanders, could be included in the absorption section. One downstream the CO_2 Absorber, and one downstream the H_2S Absorber. The liquid at the outlet of these absorbers has a pressure of around 35 bar. The downstream HP CO_2 Flash Drum and Rich Solvent Flash Drum have an operating pressure of around 5-20 bar, and hence the solvent expanders could recuperate power from the absorber effluent streams. First rough estimations for the BATC with a capture rate of 85% show that the total electrical output of the turbines would be around 1.8 MW: 1.5 MW for the turbine downstream the CO_2 Absorber, and 0.3 MW for the turbine downstream the H_2S Absorber. For a sour shift pre-combustion CO_2 capture unit hydraulic turbines have already been proposed by Padurean et al. [46]. Although there should not be substantial changes for a sweet shift configuration, a study should estimate the vapor fraction at the outlet of the turbines and verify that it is acceptable for the turbine blades. If it is too high, the outlet pressure of the turbines has to be adapted. Furthermore, the performance of the Heat Ex. 5 is influenced by the additional turbines. The increased vapor fraction could increase the area of the heat exchanger and/or could influence the choice of the ΔT_{pinch}. Finally, the technical feasibility of the Solvent Expanders has to be demonstrated and the investment cost of these turbines has to be estimated in order to show if their power production justifies the additional investment cost.

Instead of using the Rich Solvent Flash Drum in order to ensure a minimum H_2S content in the Acid Gas stream, a H_2S Concentrator could be used. This component is explained in detail in Ref. [47]. It is a stripper using N_2 coming from the air separation unit as stripping gas. The advantage is that the operating pressure of the H_2S Concentrator can be significantly higher compared to the pressure in the Rich Solvent Flash Drum, ensuring the same H_2S content in the Acid Gas stream. Consequently, the power consumption of the Flash Gas Compressor is reduced. The advantage of a H_2S Concentrator was already demonstrated from Bhattacharyya et al. [18] for a sour shift configuration. A study should be performed to analyze the techno-economic influence of a H_2S Concentrator on the sweet shift capture unit in consideration.

Entire capture unit optimization approach For the optimization of the entire capture unit, also the pressures of the CO_2 Flash Drums and the boil-up ratio can be included as decision

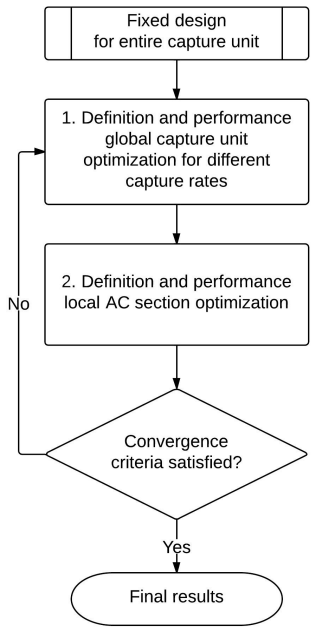

Figure 4-12: Top-down capture unit optimization approach

variables. A two-step top-down optimization hierarchy is proposed (see Figure 4-12) for this purpose. The idea is to optimize the operating conditions of the AC section separately from the global optimization problem. In the first step, the capture unit optimization described in Sec. 3-7-2 is performed in the range 75% to 91% of capture rate. The model of the entire capture unit can be used. From the results the mean CO_2 recovery (note that it is almost constant) and the mean mass flow and composition of the Shifted Syngas stream are calculated. In the second step, they are used as constraints and the operating parameters of the absorption section are optimized. They are optimized for the fixed CO_2 recovery, independently from the shifting section. The AC model can be used for this optimization. As shown in Figure 4-12, the first and second step of the top-down optimization approach should then be iteratively repeated till the convergence criteria are satisfied. The convergence criteria should be based on an absolute or relative difference between the expected and the actual mean CO_2 recovery, mass flow and composition of the Shifted Syngas stream.

It is proposed to perform the optimization of the pressures of the CO_2 Flash Drums and the boil-up ratio independently from the shifting section, because the optimized operating conditions of the absorption section do not depend significantly on the shifting section. Furthermore, they can be optimized independently from the capture rate, because of two reasons. First, the optimized pressures of the two flash vessels are expected to vary in a small range in the analyzed range of catpure rates. As described in Sec. 4-1 their optimized pressure depends mainly on the trade-off between the power requirement of the CO_2 compression section and the power consumption of the CO_2 absorption section, which in a first approximation is determined by the ratio between the flow rate of the CO_2 Product Stream and the total solvent flow rate ($\dot{m}_{CO2\_product}/\dot{m}_{solvent\_tot}$). The results of the optimizations described in Sec. 4-2 show that this ratio varies of less than 10% (it is within 0.072 and 0.079) for all

the analyzed cases. Second, the H_2S removal unit is influenced only in a minor way by the capture rate, and therefore also the optimal boil-up ratio. In fact, the results show that the power consumption of the H_2S removal unit is almost constant for different capture rates. These simplifications could lead to a significant reduction in the computational effort for the optimization of the entire capture unit.

Chapter 5

Conclusion

In this work an analysis and optimization of the pre-combustion CO_2 capture unit of the Magnum IGCC power plant was performed. The study was performed in collaboration with Nuon, the Delft University of Technology, and the Energy Research Centre of the Netherlands within a larger research project aimed at developing pre-combustion CO_2 capture technology. The process configuration and other relevant information on the CO_2 capture process were delivered by Nuon, which operates a pilot plant at the Buggenum IGCC power station. The analyzed capture unit of the Magnum IGCC power plant comprises an integrated CO_2 and H_2S removal unit, a sweet water-gas shift (WGS) unit, and a five-stage intercooled CO_2 compression. The entire capture unit was modeled in Aspen Plus Version 7.3 using the PC-SAFT EoS for the estimation of the thermodynamic and transfer properties of the substances involved. The thesis focused on three research questions.

The first research question aimed to compare the chilled and unchilled absorption section. The comparison was performed for three different combinations of number of equilibrium stages in the CO_2 Absorber, H_2S Absorber and H_2S Stripper. It considered the power consumption and the equipment cost of the absorption section. For all three combinations of number of equilibrium stages, the chilled absorption section consumes less energy and has a lower equipment cost. Therefore, the chilled absorption section is in a first approximation thermodynamically and economically the more convenient configuration. Nevertheless, future studies should investigate a wider range of number of equilibrium stages in order to find the Pareto Front for both configurations.

The second research question focused on the optimization of the entire capture unit for CO_2 capture rates in the range 75% to 91%. Different operating conditions for fresh and partially deactivated WGS catalysts were compared. The objective function was limited to the minimization of the power consumption, which includes the auxiliaries, the LHV loss and the LP and IP steam usage. It was observed, that the specific energy consumption (per captured amount of CO_2) has a minimum within the analyzed range of CO_2 capture rates. The minimum depends mainly on the minimum steam/CO ratio in front of the WGS reactors and is

reached once this limit is hit. The specific energy consumption increases slightly for lower capture rates, while the increase is significant for higher capture rates. In fact, in order to achieve higher capture rates, the steam/CO ratio in the shifting section and the solvent mass flow in the absorption section are increased considerably.

For fresh catalysts, a reference case with a minimum steam/CO ratio of 2.65 mol/mol and a WGS reactor inlet temperature of 340°C was defined (SOR conservative case); but some test runs in the Buggenum IGCC pilot plant showed that these operating conditions are too conservative. It was estimated that the minimum steam/CO ratio can be reduced from 2.65 mol/mol to 1.5 mol/mol and the minimum inlet temperature of the reactors can be reduced from 340°C to 315°C. Operating the WGS reactors at lower inlet temperatures to the WGS reactors is beneficial as long as the minimum steam/CO ratio is not reached. Decreasing the inlet temperature of the first and second WGS reactor from 340°C to 315°C reduces the specific energy consumption up to 8 MJ/kg (a reduction of 0.5%). If also the inlet temperature of the third reactor is reduced to 315°C, savings of almost 110 MJ/kg (a reduction of 7%) are achieved. For partially deactivated WGS catalysts, the inlet temperature of the first and second WGS reactor have to be increased to 365°C. The power consumption increases of 8-9 MJ/kg compared to the SOR conservative case. When the minimum steam/CO ratio is hit, a partial by-pass of the Unshifted Syngas of the shifting and CO_2 absorption section was opened in order to achieve lower capture rates. For this lower range of capture rates, the power consumption does not vary significantly when the catalyst deactivates. Decreasing the inlet temperature of the third WGS reactor is, like for higher capture rates, beneficial. However, in this range of capture rates, the specific energy consumption is mainly influenced by the minimum steam/CO ratio. When the minimum steam/CO ratio is reduced from 2.65 mol/mol to 1.5 mol/mol, a benefit in terms of the specific energy consumption of almost 130 MJ/kg (reduction of 10%) was observed compared to the SOR conservative case.

To answer the third research question, a comparison of the performance of the H_2S absorption section with and without CO_2 capture was performed. This is important, because the H_2S absorption section has to be sized adequately to guarantee an effective operation also when the IGCC power plant operates without CO_2 capture. The solvent inlet temperature to the H_2S absorber was maintained constant at 7.32°C. Furthermore, the sulphur content in the Unshifted Syngas stream was maintained constant at 5.5 ppm. The power requirement of the H_2S absorption section when no CO_2 is captured is 3.70 MW. Instead, when CO_2 is captured, it decreases to 3.37 MW, because the solvent at the inlet of the H_2S absorber is preloaded with CO_2. This augments the H_2S capacity and the selectivity of the solvent. The solvent mass flow in the H_2S absorption section decreases. Note that it makes no sense to preload the solvent artificially with CO_2 when no CO_2 is captured, as the CO_2 tends to be stripped off together with the H_2S in the H_2S Stripper. This demonstrates that the integration of the CO_2 and H_2S absorption section positively affects the power consumption of the absorption section. Furthermore, the H_2S absorption section has to be sized for the case without CO_2 capture in order to handle also the higher solvent mass flows when no CO_2 is captured. Nevertheless, note that when no CO_2 is captured, the IGCC power plant could be operated with a solvent inlet temperature to the H_2S absorber of 4°C and the sulphur content in the Unshifted Syngas stream could be augmented to 20 ppm. First estimations show that the power requirement could be reduced to 2.77 MW and the solvent mass flow would decrease. The H_2S absorption section could be sized for the case with CO_2 capture, as it would represent the case with the

higher power consumption and solvent mass flow.

Appendix A

Matlab code

A-1 Matlab code - optimization absorption and CO_2 compression section

For the optimization of the AC section the open source Direct.m file was used. The required objective function of the Direct code is defined in the 'Optimization function'. This function creates a local COM Automation server to interface Matlab with Aspen Plus, runs the Aspen Plus file, verifies that all the constraints of the optimization are respected, and checks if errors or warnings were issued during the simulation. The bounds of the optimization and the maximum number of iterations of the Direct.m optimization code are defined in the 'Optimization script'.

A-1-1 Optimization script

```
1  Aspen_file='D:\timonthomaser\Desktop\abs.apw';
2  x_L=[4.8;1.2;6400000]
3  x_U=[5.2;1.4;7000000]
4
5  global Aspen AspenEngine Aspen_file
6  Aspen=actxserver('Apwn.Archive')
7  AspenEngine=Aspen.Application.Engine
8  Aspen_file = Aspen_file;
9  InitFromArchive2(Aspen,Aspen_file,0);
10
11 Aspen.Visible=1
12 Run2(AspenEngine)
13 pause(1);
14
15 global gl_EEtot gl_pMP gl_i gl_counter gl_pLP gl_reboilerduty
       gl_errorconstraints
16 gl_i=0;
```

```
gl_counter=0;
gl_errorconstraints=0;

    x_L=x_L;
    x_U=x_U;

    bounds(:,1) = x_L;
    bounds(:,2) = x_U;

        opts.maxevals = 1500;
        opts.maxits = 1500;

        Problem.f = 'optimizationfunctiondirect';

        [fmin,x,history] = Direct(Problem,bounds,opts)
        Result.x_k = x;
        Result.f_k = fmin;
        Result.history = history;


results=[gl_pMP; gl_pLP; gl_reboilerduty; gl_EEtot]

%Shows the number of total errors in the constraints
gl_errorconstraints
```

A-1-2 Optimization function

```
function [ EEtot] = optimizationfunctiondirect (variables)
path = 'D:\Desktop\';

global Aspen AspenEngine gl_i gl_EEtot gl_pMP gl_counter Aspen_file
    gl_pLP gl_reboilerduty gl_errorconstraints
gl_counter=gl_counter+1
gl_i=gl_i+1

pMP = Aspen.Application.Tree.FindNode('\Data\EO Configuration\EO Input\
    Input\IVVALUE\#3');
SetValueAndUnit(pMP, variables(1) , 0)

pLP = Aspen.Application.Tree.FindNode('\Data\EO Configuration\EO Input\
    Input\IVVALUE\#4');
SetValueAndUnit(pLP, variables(2) , 0)

reboilerduty = Aspen.Application.Tree.FindNode('\Data\EO Configuration\EO
     Input\Input\IVVALUE\#5');
SetValueAndUnit(reboilerduty, variables(3) , 0)

%run
Run2(AspenEngine)

while (get(AspenEngine, 'IsRunning'))==1
    pause(1)
end
```

```
23
24 pause(1);
25
26              k=0;
27              while k<=1
28
29                      % Open .txt file to check for Aspen Errors
30                      while (get(AspenEngine, 'IsRunning'))==1
31                           pause(1)
32                      end
33                          pause(2);
34
35                          path = path;
36                      name = Aspen.Application.Tree.FindNode('\Data\Results
                            Summary\Run-Status\Output\RUNID').Value;
37                      string = char(strcat(path,name,'.atslv'));
38                      fid = fopen(string,'r');
39                      Data = textscan(fid, '%s', 'delimiter', '\n', '
                           whitespace', '');
40              fclose('all');
41              CStr = Data{1};
42              SearchedString = 'Iteration status    =>  Error';
43              IndexC = strfind(CStr, SearchedString);
44                      Index = find(~cellfun('isempty', IndexC), 1);
45
46
47
48              error_check = Aspen.Application.Tree.FindNode('\Data\Results
                    Summary\Run-Status\Output\UOSSTAT2').Value;
49
50              if  (error_check == 3) || (isempty(Index) == 0) || (
                    gl_counter == 10)
51                   disp('Error')
52                   gl_counter = 0;
53                   k=k+1
54
55              Aspen.Close;
56              Aspen.delete;
57              Aspen = actxserver('Apwn.Archive');
58              AspenEngine = Aspen.Application.Engine;
59              InitFromArchive2(Aspen,Aspen_file,0);
60              Aspen.Visible=1;
61
62              pMP = Aspen.Application.Tree.FindNode('\Data\EO Configuration
                    \EO Input\Input\IVVALUE\#3');
63              SetValueAndUnit(pMP, variables(1) , 0)
64
65              pLP = Aspen.Application.Tree.FindNode('\Data\EO Configuration
                    \EO Input\Input\IVVALUE\#4');
66              SetValueAndUnit(pLP, variables(2) , 0)
67
68              reboilerduty = Aspen.Application.Tree.FindNode('\Data\EO
                    Configuration\EO Input\Input\IVVALUE\#5');
```

```
69              SetValueAndUnit(reboilerduty, variables(3) , 0)
70
71              Run2(AspenEngine);
72                  while (get(AspenEngine, 'IsRunning'))==1
73                   pause(1)
74                  end
75                  pause(1);
76              else
77              break
78              end
79
80              end
81
82 %Retrieve results
83 if (k==0)  || (k == 1)
84 EEtot = Aspen.Application.Tree.FindNode('\Data\Flowsheeting Options\
       Calculator\EE-TOT\Output\WRITE_VAL\2').value;
85
86 gl_EEtot(gl_i)=EEtot;
87 gl_pMP(gl_i)=variables(1);
88 gl_pLP(gl_i)=variables(2);
89 gl_reboilerduty(gl_i)=variables(3);
90
91 else
92     disp ('ERROR AFTER RECONCILIATION')
93
94 end
95
96     %CHECK CONSTRAINTS
97     maxtempsolvent = Aspen.Application.Tree.FindNode('\Data\Streams\205\
           Output\TEMP_OUT\MIXED').value;
98     watercontentsolvent = Aspen.Application.Tree.FindNode('\Data\Streams\
           FEED\Output\MOLEFRAC\MIXED\H2O').value;
99     Scontentco2streamdry = Aspen.Application.Tree.FindNode('\Data\
           Flowsheeting Options\Calculator\H2SCOS\Output\WRITE_VAL\6').value;
100    CO2eff=Aspen.Application.Tree.FindNode('\Data\Flowsheeting Options\
           Calculator\CO2EFF\Output\WRITE_VAL\3').value;
101
102    if (CO2eff < 0.924) || (CO2eff > 0.926) || (maxtempsolvent>150)  || (
           watercontentsolvent > 0.41) || (watercontentsolvent < 0.39)|| (
           Scontentco2streamdry > 0.000011) || (Scontentco2streamdry <
           0.000009)
103
104    disp (strcat('ERROR IN CONSTRAINTS in global interation number: ',
           num2str(gl_i)))
105    gl_errorconstraints=gl_errorconstraints+1
106
107    end
108
109 end
```

A-2 Matlab code - overall capture unit optimization

The overall optimization of the capture unit was performed with the gradient-based internal optimization routine of Aspen Plus. A Matlab script was developed in order to run the optimization through a local COM Automation server in all the range of 75 to 91% of capture rate and to copy the results automatically in Excel. Furthermore, the Matlab script checked if all the constraints of the optimization were respected and eventual adaptations were directly done in Matlab through the local COM server.

```
steamoncolimit=1.5;
exelsheetnumber=1;

global Aspen AspenEngine Aspen_file
Aspen=actxserver('Apwn.Archive');
AspenEngine=Aspen.Application.Engine;
Aspen_file = 'D:\Desktop\test.apw';
InitFromArchive2(Aspen,Aspen_file,0);
Aspen.Visible=1;
Run2(AspenEngine)
pause(5);

%Set S/CO limit
sco_ratio = Aspen.Application.Tree.FindNode('\Data\EO Configuration\EO
    Input\Input\IVVALUE\#11');
SetValueAndUnit(sco_ratio, steamoncolimit , 0)
i=0;
step=0.005;
CO2start=0.91;
CO2end=0.75;
iter=(CO2start-CO2end)*100*1/(step*100);
while i<=iter
    ov_capt = Aspen.Application.Tree.FindNode('\Data\EO Configuration\EO
        Input\Input\IVVALUE\#6');
    SetValueAndUnit(ov_capt, CO2start-i*step , 0)
    CO2capt = CO2start-i*step

    Run2(AspenEngine)

while (get(AspenEngine, 'IsRunning'))==1
    pause(1)
end

pause(1);

numberlimittempoutreac1=0;
numberlimitsteamonco=0;

%Check if outlet temperature of the first WGS reactor is below 520řC
tempoutreac1 = Aspen.Application.Tree.FindNode('\Data\Streams\S36\Output\
    TEMP_OUT\MIXED').value;
if tempoutreac1>520
    if numberlimittempoutreac1==0
```

```
41      Msg = 'Reactor 1 Temp at limit'
42      tout=Aspen.Application.Tree.FindNode('\Data\EO Configuration\Spec
            Groups\Input\ENABLED\TOUREAC1');
43      SetValueAndUnit(tout,'YES', 0)
44      Qe9005=Aspen.Application.Tree.FindNode('\Data\EO Configuration\Spec
            Groups\Input\ENABLED\QE9005');
45      SetValueAndUnit(Qe9005,'NO', 0)
46
47      qe9005eoinput=Aspen.Application.Tree.FindNode('\Data\EO Configuration
            \EO Input\Input\IVENABLED\#8');
48      SetValueAndUnit(qe9005eoinput,'NO', 0)
49      touteoinput=Aspen.Application.Tree.FindNode('\Data\EO Configuration\
            EO Input\Input\IVENABLED\#5');
50      SetValueAndUnit(touteoinput,'YES', 0)
51
52                      Aspen.Application.Tree.FindNode('\Data\Setup\Sim-
                            Options\Input\RESTART');
53                      Run2(AspenEngine)
54                      while (get(AspenEngine, 'IsRunning'))==1
55                          pause(1)
56                      end
57                      pause(1);
58       end
59
60  numberlimittempoutreac1=1;
61  end
62
63  % Check if steam/CO ratio is within the limit
64  h2oco2=Aspen.Application.Tree.FindNode('\Data\Flowsheeting Options\
        Calculator\2H2O:CO\Output\WRITE_VAL\3').value;
65  h2oco2
66  if (h2oco2+0.001)<steamoncolimit
67      if numberlimitsteamonco==0
68      Msg = 'Steam/CO ratio at limit'
69      sco2=Aspen.Application.Tree.FindNode('\Data\EO Configuration\Spec
            Groups\Input\ENABLED\SCONEW');
70      SetValueAndUnit(sco2,'YES', 0)
71
72      scoeoinput=Aspen.Application.Tree.FindNode('\Data\EO Configuration\EO
             Input\Input\IVENABLED\#11');
73      SetValueAndUnit(scoeoinput,'YES', 0)
74
75      %Calculate one point below and then go back to the original point
            again
76      ov_capt = Aspen.Application.Tree.FindNode('\Data\EO Configuration\EO
            Input\Input\IVVALUE\#6');
77      SetValueAndUnit(ov_capt, CO2start-i*step-0.005 , 0)
78
79                      Aspen.Application.Tree.FindNode('\Data\Setup\Sim-
                            Options\Input\RESTART');
80                      Run2(AspenEngine)
81                      while (get(AspenEngine, 'IsRunning'))==1
82                      pause(1)
```

```
83                      end
84                      pause(1);
85
86      ov_capt = Aspen.Application.Tree.FindNode('\Data\EO Configuration\EO
            Input\Input\IVVALUE\#6');
87      SetValueAndUnit(ov_capt, CO2start-i*step , 0)
88
89                      Aspen.Application.Tree.FindNode('\Data\Setup\Sim-
                            Options\Input\RESTART');
90                      Run2(AspenEngine)
91                      while (get(AspenEngine, 'IsRunning'))==1
92                      pause(1)
93                      end
94                      pause(1);
95      %End step down and up
96      end
97  numberlimitsteamonco=1;
98
99  end
100
101
102
103
104 overall_capture=Aspen.Application.Tree.FindNode('\Data\Flowsheeting
        Options\Calculator\CAPTURE\Output\WRITE_VAL\7').value;
105 coconversion=Aspen.Application.Tree.FindNode('\Data\Flowsheeting Options\
        Calculator\COCONVER\Output\WRITE_VAL\3').value;
106 co2recovery=Aspen.Application.Tree.FindNode('\Data\Flowsheeting Options\
        Calculator\CO2EFF\Output\WRITE_VAL\3').value;
107 EEtot = (Aspen.Application.Tree.FindNode('\Data\Flowsheeting Options\
        Calculator\EE-TOT\Output\WRITE_VAL\2').value)/1000000;
108 mco2=(Aspen.Application.Tree.FindNode('\Data\Streams\91\Output\MASSFLOW\
        MIXED\CO2').value)/3600/1000;
109 EEtot_mco2=EEtot/mco2;
110 EEshift=(Aspen.Application.Tree.FindNode('\Data\Flowsheeting Options\
        Calculator\EE-SEC\Output\WRITE_VAL\1').value)/1000000;
111 EEco2=(Aspen.Application.Tree.FindNode('\Data\Flowsheeting Options\
        Calculator\EE-SEC\Output\WRITE_VAL\2').value)/1000000;
112 EEh2s=(Aspen.Application.Tree.FindNode('\Data\Flowsheeting Options\
        Calculator\EE-SEC\Output\WRITE_VAL\3').value)/1000000;
113 EEcomp=(Aspen.Application.Tree.FindNode('\Data\Flowsheeting Options\
        Calculator\EE-SEC\Output\WRITE_VAL\12').value)/1000000;
114 EElhv=(Aspen.Application.Tree.FindNode('\Data\Flowsheeting Options\
        Calculator\EE-SEC\Output\WRITE_VAL\16').value)/1000000;
115 h2oco1=Aspen.Application.Tree.FindNode('\Data\Flowsheeting Options\
        Calculator\1H2O:CO\Output\WRITE_VAL\3').value;
116 h2oco2=Aspen.Application.Tree.FindNode('\Data\Flowsheeting Options\
        Calculator\2H2O:CO\Output\WRITE_VAL\3').value;
117 h2oco3=Aspen.Application.Tree.FindNode('\Data\Flowsheeting Options\
        Calculator\3H2O:CO\Output\WRITE_VAL\3').value;
118 tempoutreac1 = Aspen.Application.Tree.FindNode('\Data\Streams\S36\Output\
        TEMP_OUT\MIXED').value;
```

```
119 tempoutreac2 = Aspen.Application.Tree.FindNode('\Data\Streams\S40\Output\
    TEMP_OUT\MIXED').value;
120 tempoutreac3 = Aspen.Application.Tree.FindNode('\Data\Streams\S43\Output\
    TEMP_OUT\MIXED').value;
121 tinreac1=Aspen.Application.Tree.FindNode('\Data\Streams\S32\Output\
    TEMP_OUT\MIXED').value;
122 tinreac2=Aspen.Application.Tree.FindNode('\Data\Streams\S38\Output\
    TEMP_OUT\MIXED').value;
123 tinreac3=Aspen.Application.Tree.FindNode('\Data\Streams\S42\Output\
    TEMP_OUT\MIXED').value;
124 tquench=Aspen.Application.Tree.FindNode('\Data\Streams\S19\Output\
    TEMP_OUT\MIXED').value;
125 qe9003=(Aspen.Application.Tree.FindNode('\Data\Blocks\E9003AB\Output\
    QCALC').value)/1000000;
126 qe9005=(Aspen.Application.Tree.FindNode('\Data\Blocks\E9005\Output\QCALC'
    ).value)/1000000;
127 steamco=Aspen.Application.Tree.FindNode('\Data\Flowsheeting Options\
    Calculator\SONCO\Output\WRITE_VAL\3').value;
128 lean=Aspen.Application.Tree.FindNode('\Data\Streams\40\Output\MASSFLMX\
    MIXED').value;
129 semilean=Aspen.Application.Tree.FindNode('\Data\Streams\22\Output\
    MASSFLMX\MIXED').value;
130 mshiftingtot=Aspen.Application.Tree.FindNode('\Data\Streams\S42\Output\
    MASSFLMX\MIXED').value;
131 mbypass=Aspen.Application.Tree.FindNode('\Data\Streams\BYPASS\Output\
    MASSFLMX\MIXED').value;
132
133 xl=strcat('A',num2str(40-i));
134 filename = 'Results overall optimization automatic.xlsx';
135 A = {overall_capture,coconversion,co2recovery,EEtot,EEtot_mco2,EEshift,
    EEco2,EEh2s,EEcomp,EElhv,h2oco1,h2oco2,h2oco3,tempoutreac1,
    tempoutreac2,tempoutreac3,tinreac1,tinreac2,tinreac3,tquench,qe9003,
    qe9005,steamco,lean,semilean,mshiftingtot,mco2,mbypass};
136 sheet = 1;
137 xlRange = xl;
138 xlswrite(filename,A,sheet,xlRange)
139
140
141 i=i+1;
142 end
143
144 Msg ='Finished'
145
146 Aspen.Close;
147 Aspen.delete;
```

Glossary

List of Acronyms

GHG	Greenhouse Gases
CPS	Current Policies Scenario
NPS	New Policies Scenario
450	450 Scenario
IEA	International Energy Agency
IGCC	Integrated Gasification Combined Cycle
WGS	Water-gas shift
GE	General Electrics
EOR	End of Run
ATC	Ambient temperature configuration
BATC	Below-ambient temperature configuration
AC	Absorption and CO_2 compression
EER	Energy efficiency ratio
LP	Low pressure
MP	Medium pressure
IP	Intermediate pressure
HP	High pressure
NPV	Net present value
LSC	Lean Solvent Chiller
EoS	Equation of state
PC − SAFT	Perturbed Chain Statistical Associating Fluid theory
ppm	Parts per million
ppb	Parts per billion
CAPEX	CAPital EXpenditure
OPEX	OPerational EXpenditure
DEPG	Dimethyl-ether of poly-ethylene-glycol

List of Symbols

$\dot{\mathbf{Q}}$	Heat/Cooling duty
$\dot{\mathbf{W}}$	Power
$\dot{\mathbf{E}}$	Electrical power
$\dot{\mathbf{m}}$	Mass flow rate
$\mathbf{T}$	Temperature
$\mathbf{p}$	Pressure
$\mathbf{s}$	Entropy
$\mathbf{x}$	Mole fraction
c_p	Heat capacity
N	Number of equilibrium stages

Subscripts

vl	vapor liquid
sv	saturated vapor
sl	saturated liquid
is	isoentropic
app	approached
reb	H_2S Stripper Reboiler
MP_FD	Medium Pressure CO_2 Flash Drum
LP_FD	Low Pressure CO_2 Flash Drum
RS_FD	Rich Solvent Flash Drum
CA	CO_2 Absorber
SA	H_2S Absorber
SS	H_2S Stripper
tot	total
C	carbon removal
CO_2	CO_2 recovery
CO	CO conversion
$pinch$	pinch point
LSC	Lean Solvent Chiller
in	inlet
out	outlet

Greek letters

ρ	Density
β	Compression ratio
η	Efficiency

Bibliography

[1] United States Environmental Protection Agency. Climate Change: Basic Information. http://www.epa.gov/climatechange/basics/, 2013. [Online; accessed 1-July-2013].

[2] World Bank. Climate Change Overview. http://www.worldbank.org/en/topic/climatechange/overview, 2013. [Online; accessed 1-October-2013].

[3] Jochen Oexmann, Alfons Kather, Sebastian Linnenberg, and Ulrich Liebenthal. Post-combustion CO_2 capture: chemical absorption processes in coal-fired steam power plants. *Greenhouse Gases: Science and Technology*, 2(2):80–98, 2012.

[4] International Energy Agency. World Energy Outlook 2012. Technical report, International Energy Agency, 2012.

[5] International Energy Agency. IEA - Energy Technology Perspectives 2012. Technical report, International Energy Agency, 2012.

[6] Matthias Finkenrath. Cost and Performance of Carbon Dioxide Capture from Power Generation. Technical report, International Energy Agency, 2011.

[7] International Energy Agency. Technological Roadmap Carbon Capture and Storage. Technical report, International Energy Agency, 2009.

[8] S. A. Rackley. *Carbon Capture and Storage*. Elsevier, 2010.

[9] International Energy Agency. Capturing CO_2 . Technical report, International Energy Agency, 2007.

[10] International Energy Agency. Carbon Capture and Storage: Progress and Next Steps. Technical report, International Energy Agency, 2010.

[11] Klaus Dieter Kaufmann. Carbon Dioxide Transport in Pipelines - Under Special Consideration of Safety-Related Aspects. 2008.

[12] International Energy Agency. CO_2 Capture and Storage: A key carbon abatement option. Technical report, International Energy Agency, 2008.

[13] Y. Huang, S. Rezvani, D. McIlveen-Wright, A. Minchener, and N. Hewitt. Techno-economic study of CO_2 capture and storage in coal fired oxygen fed entrained flow IGCC power plants. *Fuel Processing Technology*, 89(9):916 – 925, 2008.

[14] U.S. Department Of Energy. Gasifipedia - CO_2: CO_2 Capture: Impacts on IGCC Plant Designs. http://www.netl.doe.gov/technologies/coalpower/gasification/gasifipedia/impacts.html, n.d. [Online; accessed 24-September-2013].

[15] Emanuele Martelli, Thomas Kreutz, Michiel Carbo, Stefano Consonni, and Daniel Jansen. Shell coal IGCCS with carbon capture: Conventional gas quench vs. innovative configurations. *Applied Energy*, 88(11):3978 – 3989, 2011.

[16] Christian Kunze, Karsten Riedl, and Hartmut Spliethoff. Structured exergy analysis of an integrated gasification combined cycle (IGCC) plant with carbon capture. *Energy*, 36(3):1480 – 1487, 2011.

[17] M.C. Carbo, J. Boon, D. Jansen, H.A.J. van Dijk, J.W. Dijkstra, R.W. van den Brink, and A.H.M. Verkooijen. Steam demand reduction of water-gas shift reaction in IGCC power plants with pre-combustion CO_2 capture. *International Journal of Greenhouse Gas Control*, 3(6):712 – 719, 2009.

[18] Debangsu Bhattacharyya, Richard Turton, and Stephen E. Zitney. Steady-State Simulation and Optimization of an Integrated Gasification Combined Cycle Power Plant with CO_2 Capture. *Industrial & Engineering Chemistry Research*, 50(3):1674–1690, 2011.

[19] F. Casella and P. Colonna. Dynamic modeling of IGCC power plants. *Applied Thermal Engineering*, 35(0):91 – 111, 2012.

[20] Vattenfall. Nuon Magnum. http://www.vattenfall.com/en/ccs/magnum.htm, 2012. [Online; accessed 1-October-2013].

[21] Nuon Vattenfall. Private communication, 2013.

[22] Anon. Nuon Magnum IGCC power Plant, Netherlands. http://www.power-technology.com/projects/nuonmagnum-igcc/, n.d. [Online; accessed 1-October-2013].

[23] M. C. Carbo, D. Jansen, J. W. Dijkstra, R.W. van den Brink, and A. H. M. Verkooijen. Pre-combustion decarbonisation in IGCC: Abatement of both steam requirement and CO_2 emissions. 2007.

[24] P. Perrot. *A to Z of Thermodynamics*. Oxford University Press, Incorporated, 1998.

[25] Aspen Technology, Inc. Aspen Plus User Guide Version 10.2, 2000.

[26] Daniel Finkel. DIRECT optimization algorithm user guide. *Center for Research in Scientific Computation, North Carolina State University*, 2, 2003.

[27] Kay Damen, Radoslaw Gnutek, Joost Kaptein, Nawin Ryan Nannan, Bernardo Oyarzun, Carsten Trapp, Piero Colonna, Eric van Dijk, Joachim Gross, and AndrÃľ Bardow. Developments in the pre-combustion CO_2 capture pilot plant at the Buggenum IGCC. *Energy Procedia*, 4(0):1214 – 1221, 2011.

[28] Nikolaos I. Diamantonis and Ioannis G. Economou. Modeling the phase equilibria of a H_2O - CO_2 mixture with PC-SAFT and tPC-PSAFT equations of state. *Molecular Physics*, 110(11-12):1205–1212, 2012.

[29] Ilke Senol. Perturbed-Chain Statistical Association Fluid Theory (PC-SAFT) Parameters for Propane, Ethylene, and Hydrogen under Supercritical Conditions. 2011.

[30] N.R. Nannan and T.P. van der Stelt and P. Colonna and A. Bardow. Modeling the Thermodynamic Properties of the selexol^{TM} Solvent Using PC-SAFT, 2012. unpublished.

[31] Nikolaos I. Diamantonis, Georgios C. Boulougouris, Erum Mansoor, Dimitrios M. Tsangaris, and Ioannis G. Economou. Evaluation of Cubic, SAFT, and PC-SAFT Equations of State for the Vapor-Liquid Equilibrium Modeling of CO_2 Mixtures with Other Gases. *Industrial & Engineering Chemistry Research*, 52(10):3933–3942, 2013.

[32] F. Emun, M. Gadalla, T. Majozi, and D. Boer. Integrated gasification combined cycle (IGCC) process simulation and optimization. 2009.

[33] B. Burr and L. Lyddon. A comparison of physical solvents for acid gas removal. n.d.

[34] P. Seevam, J. Race, and M. Downie. Carbon dioxide impurities adn their effects on CO_2 pipelines. http://pipeliner.com.au/news/carbon_dioxide_impurities_adn_their_effects_on_co2_pipelines/011846/, 2008. [Online; accessed 11-October-2013].

[35] Aermec S.p.A. Private communication, 2013.

[36] Anon. Fuel gases - heating values. http://www.engineeringtoolbox.com/heating-values-fuel-gases-d_823.html, n.d. [Online; accessed 11-October-2013].

[37] Anon. FluidProp - Software for the calculation of thermophysical properties of fluids. http://www.fluidprop.com/, n.d. [Online; accessed 11-October-2013].

[38] Aspen Technology, Inc. Aspen Process Economic Analyzer 7.0, 2008.

[39] Florida Power & Light Company. Water-Cooled Chillers. n.d.

[40] National Energy Technology Laboratory. Life Cycle Analysis: Integrated Gasification Combined Cycle (IGCC) Power Plant. 2010.

[41] Fondazione Politecnico di Milano. Reliability of the Electric energy Supply in a Competitive Market. n.d.

[42] O.L. De Weck. Multiobjective optimization: history an promise. 2004.

[43] Erika de Visser, Chris Hendriks, Maria Barrio, Mona J. Mølnvik, Gelein de Koeijer, Stefan Liljemark, and Yann Le Gallo. Dynamis CO_2 quality recommendations. *International Journal of Greenhouse Gas Control*, 2(4):478 – 484, 2008.

[44] Ralph H. Weiland. Acid gas enrichment - maximizing selectivity. 2008.

[45] William Breckenridge, Allan Holiday, James OY Ong, and Curtis Sharp. Use of SELEXOL® process in coke gasification to ammonia project. In *Proceedings of the Laurance Reid Gas Conditioning Conference*, pages 397–418, 2000.

[46] Anamaria Padurean, Calin-Cristian Cormos, and Paul-Serban Agachi. Pre-combustion carbon dioxide capture by gas-liquid absorption for Integrated Gasification Combined Cycle power plants. *International Journal of Greenhouse Gas Control*, 7(0):1 – 11, 2012.

[47] David M. Nicholas and William P. Hegarty. Hydrogen Sulfide concentrator for acid gas removal systems, 1980.